

Theoretical Biology



Rob J. de Boer & Kirsten ten Tusscher

Theoretical Biology & Bioinformatics

Utrecht University

© Utrecht University, 2015

Ebook publically available at: <http://theory.bio.uu.nl/rdb/books/>

Contents

1	Introduction	1
1.1	The simplest possible model	1
1.2	Exponential growth and decay	3
1.3	Summary	4
1.4	Exercises	5
2	Population growth: replication	9
2.1	Density dependent death	10
2.2	Density dependent birth	11
2.3	Logistic growth	12
2.4	Stability and return time	12
2.5	Summary	14
2.6	Exercises	14
3	Lotka Volterra model	19
3.1	Summary	22
3.2	Exercises	22
4	The predator functional response	25
4.1	Summary	28
4.2	Exercises	29
5	Competitive exclusion	33
5.1	Exercises	34
6	Alternative Model Formalisms	37
6.1	Cellular Automata	37
6.2	Individual Based Models	38
6.3	Summary	40
6.4	Exercises	41
7	Gene regulation	43
7.1	Models	43
7.2	Separation of time scales	44
7.3	Lac-operon	45
7.4	Gene networks	48
7.5	Summary	48
7.6	Exercises	48
8	Chronic viral infections and immune control	53
8.1	Immune response	53
8.2	Separation of time scales	55

8.3	Summary	57
8.4	Exercises	57
9	The Hodgkin-Huxley model	61
9.1	Introduction	61
9.2	Background	61
9.3	The Model	64
9.4	Putting the model together	67
9.5	The Fitzhugh-Nagumo model	69
9.6	Exercises	71
10	Introduction in Spatial Patterns	75
10.1	Introduction	75
10.2	Including space in models: PDEs and Diffusion	76
10.3	Inherently spatial models: CAs and IBMs	78
10.4	Exercises	81
11	Dynamic Patterns: Excitable Media	83
11.1	Introduction	83
11.2	Wave patterns	84
11.3	Cardiac tissue and Arrhythmias	86
11.4	Other excitable media	88
11.5	Exercises	88
12	GRIND	91
12.1	Lotka Volterra model	91
12.2	Exercises	93
13	Examples of exam questions	99
14	Glossary	101
15	Answers to the exercises	103

Chapter 1

Introduction

This course is an introduction into Theoretical Biology for biology students. We will teach you how to read mathematical models, and how to analyze them, with the ultimate aim that you can critically judge the assumptions and the contributions of such models whenever you encounter them in your future biological research. Mathematical models are used in all areas of biology. Most models in this course are formulated in ordinary differential equations (ODEs). These will be analyzed by computing steady states, sketching nullclines and determining the vectorfield, to determine the long term behavior of the system. We will develop the differential equations by ourselves following a simple graphical procedure, depicting each biological process separately. Experience with an approach for writing models will help you to evaluate models proposed by others.

This first chapter introduces some basic concepts underlying modeling with differential equations. To keep models general they typically have free parameters, i.e., parameters are letters instead of numbers. You will become familiar with the notion of a “solution”, “steady state”, “half life”, and the “expected life span”. Concepts like solution and steady state are important because a differential equation describes the *change* of the population size, rather than its *actual size*. We will start with simple models that are convenient to introduce these concepts. The models used later on in the course are more challenging and much more interesting.

1.1 The simplest possible model

A truly simple mathematical model is the following

$$\frac{dM}{dt} = k , \tag{1.1}$$

which says that the variable M increases at a rate k per time unit. For instance, this could describe the amount of pesticide in your body when you eat the same amount of fruit sprayed with pesticide every day. Another example is to say that M is the amount of money in your bank account, and that k is the amount of Euros that are deposited in this account on a daily basis. In the latter case the “dimension” of the parameter k is “Euros per day”. The ODE formalism assumes that the changes in your bank account are continuous. Although this is evidently wrong, because money is typically deposited on a monthly basis, this makes little difference when one considers time scales longer than one month.

This equation is so simple that one can derive its *solution*

$$M(t) = M(0) + kt , \quad (1.2)$$

where $M(0)$ is the initial value (e.g., the amount of money that was deposited when the account was opened). Plotting $M(t)$ in time therefore gives a straight line with slope k intersecting the vertical axis at $M(0)$. The slope of this line is k , which is the derivative defined by Eq. (1.1). Thus, the differential equation Eq. (1.1) gives the “rate of change” and the solution of Eq. (1.2) gives the “population size at time t ”. Typically, differential equations are too complicated for solving them explicitly, and their solutions are not available. In this course we will not consider the integration methods required for obtaining those solutions. However, having a solution, one can easily check it by taking the derivative with respect to time. For example, the derivative of Eq. (1.2) with respect to time is $\partial_t[M(0) + kt] = k$, which is indeed the right hand side of Eq. (1.1). Summarizing, the solution in Eq. (1.2) gives the amount of money at time t , and Eq. (1.1) gives the daily rate of change.

As yet, the model assumes that you spend no money from the account. Suppose now that you on average spend s Euros per day. The model then becomes $dM/dt = k - s$ Euros per day. Mathematically this remains the same as Eq. (1.1), and one obtains exactly the same results as above by just replacing k with $k - s$. If $k < s$, i.e., if you spend more than you receive, the bank account will decrease and ultimately become negative. The time to bankruptcy can be solved from the solution of Eq. (1.2): from $0 = M(0) + (k - s)t$ one obtains $t = -M(0)/(k - s)$. Although our model has free parameters, i.e., although we do not know the value of k or s , it is perfectly possible to do these calculations.

This all becomes a little less trivial when one makes the more realistic assumption that your spending is proportional to the amount of money you have. Suppose that you spend a fixed fraction, d , of your money per day. The model now becomes

$$\frac{dM}{dt} = k - dM , \quad (1.3)$$

where the parameter d is a “rate” and here has the dimension “per day”. This can be checked from the whole term dM , which should have the same dimension as k , i.e., “Euros per day”. Biological examples of Eq. (1.3) are red blood cells produced by bone marrow, shrimps being washed onto a beach, daily intake of vitamins, and so on. The k parameter then defines the inflow, or production, and the d parameter is a death rate. Although this seems a very simple extension of Eq. (1.1), it is much more difficult to obtain the solution

$$M(t) = \frac{k}{d} (1 - e^{-dt}) + M(0)e^{-dt} , \quad (1.4)$$

which is depicted in Fig. 1.1a. The term on the right gives the exponential loss of the initial value of the bank account. The term on the left is more complicated, but when evaluated at long time scales, e.g., for $t \rightarrow \infty$, the term $(1 - e^{-dt})$ will approach one, and one obtains the “steady state” $\bar{M} = k/d$. We conclude that the solution of Eq. (1.4) ultimately approaches the steady state $M = k/d$, which is the ratio of your daily income and daily spending. Note that this is true for any value of the initial condition $M(0)$.

Fortunately, we do not always need a solution to understand the behavior of a model. The same steady state can also directly be obtained from the differential equation. Since a steady state means that the rate of change of the population is zero we set

$$\frac{dM}{dt} = k - dM = 0 \quad \text{to obtain} \quad \bar{M} = \frac{k}{d} , \quad (1.5)$$

which is the same value as obtained above from the solution for $t \rightarrow \infty$. Note that a steady state also gives the population size. This steady state provides some insight in the behavior of the model, and therefore in the way people spend their money. Suppose that rich people spend the same *fraction* of their money as poor people do, and that rich people just have a higher daily income k . This means that both rich and poor people approach a steady state where their spending balances their income. Basically, this model says that people with a 2-fold higher income spend 2-fold more money, and have 2-fold more money in the bank. This is not completely trivial: if you were asked what would happen with your bank account if both your income and spending increases n -fold you might have given a different answer.

1.2 Exponential growth and decay

Consider the unfortunate case that your daily income dries up, i.e., having a certain amount of money $M(0)$ at time zero, one sets $k = 0$ and is left with $dM/dt = -dM$. This is the famous equation for exponential decay of radioactive particles, with the almost equally famous solution $M(t) = M(0)e^{-dt}$. Ultimately, i.e., for $t \rightarrow \infty$, the population size will approach zero. Plotting the natural logarithm of $M(t)$ as a function of time would give a straight line with slope $-d$ per day. This equation allows us to introduce two important concepts: the half life and the expected life span. The half life is defined as the time it takes to lose half of the population size, and is found from the solution of the ODE. From

$$\frac{M(0)}{2} = M(0)e^{-dt} \quad \text{one obtains} \quad \ln \frac{1}{2} = -dt \quad \text{or} \quad t = \frac{\ln 2}{d}. \quad (1.6)$$

Since $\ln 2 \simeq 0.69$ the half life is approximately $0.69/d$ days. Note that the dimension is correct: a half life indeed has dimension time because we have argued above that d is a rate with dimension day^{-1} . The other concept is expected life span: if radioactive particles or biological individuals have a probability d to die per unit of time, their expected life span is $1/d$ time units. This is like throwing a die. If the probability to throw a four is $1/6$, the expected waiting time to get a four is six trials. Finally, note that this model has only one steady state, $\bar{M} = 0$, and that this state is stable because it is approached at infinite time. A steady state with a population size of zero is often called a “trivial” steady state.

The opposite of exponential decay is exponential growth

$$\frac{dN}{dt} = rN \quad \text{with the solution} \quad N(t) = N(0)e^{rt}, \quad (1.7)$$

where the parameter r is known as the “natural rate of increase”. The solution can easily be checked: the derivative of $N(0)e^{rt}$ with respect to t is $rN(0)e^{rt} = rN(t)$. Biological examples of this equation are the growth of mankind, the exponential growth of a pathogen in a host, the growth of a tumor, and so on. Similar to the half life defined above, one can define a doubling time for populations that are growing exponentially:

$$2N(0) = N(0)e^{rt} \quad \text{gives} \quad \ln 2 = rt \quad \text{or} \quad t = \ln[2]/r. \quad (1.8)$$

This model also has only one steady state, $\bar{N} = 0$, which is unstable because any small perturbation above $N = 0$ will initiate unlimited growth of the population. To obtain a non-trivial (or non-zero) steady state population size in populations maintaining themselves by reproduction one needs density dependent birth or death rates. This is the subject of the next chapter.

In biological populations, this natural rate of increase of $dN/dt = rN$ should obviously be a composite of birth and death rates. A more natural model for a biological population that grows exponentially therefore is

$$\frac{dN}{dt} = (b - d)N \quad \text{with solution} \quad N(t) = N(0)e^{(b-d)t}, \quad (1.9)$$

where b is a birth rate with dimension t^{-1} , and d is the death rate with the same dimension. Writing the model with explicit birth and death rates has the advantage that the parameters of the model are strictly positive (which will be true for all parameters in this course). Moreover, one now knows that the “generation time” or “expected life span” is $1/d$ time units. Since every individual has a birth rate of b new individuals per unit of time, and has an expected life span of $1/d$ time units, the expected number of offspring of an individual over its entire life-span is $R_0 = b/d$. We will use this R_0 as the maximum “fitness” of an individual, i.e., the life-time number of offspring expected under the best possible circumstances. In epidemiology the R_0 is used for predicting the spread of an infectious disease: whenever $R_0 < 1$ a disease will not be able to spread in a population because a single infected host is expected to be replaced by less than one newly infected host (Anderson and May, 1991).

Biological examples of Eq. (1.9) are mankind, the exponential growth of algae in a lake, and so on. Similarly, the natural rate of increase $r = b - d$ yields a “doubling time” solved from $2N(0) = N(0)e^{rt}$ giving $t = \ln[2]/r$ time units. A famous example of the latter is the data from Malthus (1798) who investigated the birth records of a parish in the United Kingdom and found that the local population had a doubling time of 30 years. Solving the natural rate of increase r per year from $30 = \ln[2]/r$ yields $r = \ln[2]/30 = 0.0231$ per year, which is sometimes expressed as a growth rate of 2.31% per year. More than 200 years later the global human growth rate is still approximately 2% per year. Simple exponential growth therefore seems a fairly realistic model to describe the growth of the quite complicated human population over a period of several centuries.

In this book we will give solutions of differential equations whenever they are known, but for most interesting models the solution is not known. We will not explain how these solutions are obtained. The textbook by Adler (1997) gives an overview of methods of integration. You can also use software like Mathematica to find the explicit solution of some of the differential equations used here. Solutions are typically difficult to obtain, but much more easy to check. For instance the solution of $N(t) = N(0)e^{(b-d)t}$ of $dN/dt = (b - d)N$, can easily be checked: using the chain rule, the derivative of $N(0)e^{(b-d)t}$ with respect to t is $N(0)(b - d)e^{(b-d)t} = (b - d)N(t)$.

1.3 Summary

An ordinary differential equation (ODE) describes the rate of change of a population. The actual population size is given by the solution of the ODE, which is generally not available. To find the population size one can compute the steady state(s) of the model (the ODE), and/or solve the ODEs numerically on a computer, which gives the model behavior. Steady states are derived by setting the rate of change to zero, and solving for the actual population size. Doubling times and half-lives are solved from the solution of the exponential growth (or decay) equation $N(t) = N(0)e^{rt}$. The fitness, R_0 , of a population is the expected number of offspring of one individual over one generation, under the best possible circumstances.

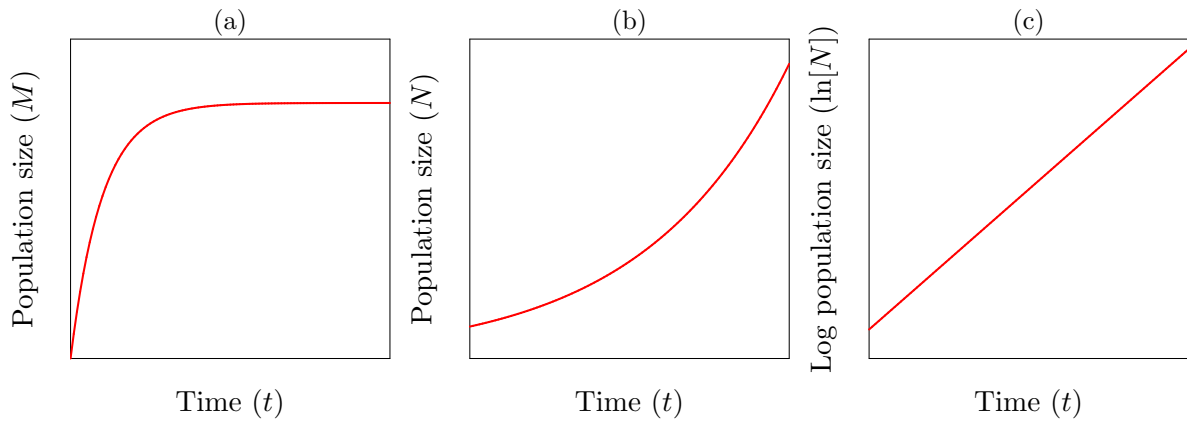


Figure 1.1: Population growth. Panel (a) depicts the solution of Eq. (1.4). Panels (b) and (c) depict exponential growth on a linear and a logarithmic vertical axis, respectively. A differential equation describes the slope of the solution for each value of the variable(s): dN/dt is the slope of the $N(t) = N(0)e^{rt}$ curve for each value of $N(t)$.

1.4 Exercises

Question 1.0. Read the chapter

- What is the difference between a parameter and a variable?
- What is the difference between the solution of an ODE and its steady state?
- Why is the ODE dx/dt not telling you how much x there is at time t ?
- What is the dimension of d in $dx/dt = -dx$?
- What is a half-life and a doubling time?
- What is the difference between a half-life and an expected life span?
- What is a steady state? When is a steady state called ‘trivial’?

Question 1.1. Red blood cells

Red blood cells are produced in the bone marrow at a rate of m cells per day. They have a density independent death rate of d per day.

- Which differential equation from this chapter would be a correct model for the population dynamics of red blood cells?
- Suppose you donate blood. Sketch your red blood cell count predicted by this model in a time plot.
- Suppose a sportsman increases his red blood cell count by receiving blood. Sketch a time plot of his red blood cell count.

Question 1.2. Pesticide on apples

During their growth season apples are frequently sprayed with pesticide to prevent damage by insects. By eating apples you accumulate this pesticide in your body. An important factor determining the concentration of pesticide is their half life in the human body. An appropriate mathematical model is

$$\frac{dP}{dt} = \sigma - \delta P,$$

where σ is the daily intake of pesticide, i.e., $\sigma = \alpha A$ where A is the number of apples that you eat per day and α is the amount of pesticide per apple, and δ is the daily rate at which the pesticide decays in human tissues.

- Sketch the amount of pesticide in your body, $P(t)$, as a function of your age, assuming you

eat the same number of apples throughout your life.

- b. How much pesticide do you ultimately accumulate after eating apples for decades?
- c. Suppose you have been eating apples for decades and stop because you are concerned about the unhealthy effects of the pesticide. How long does it take to reduce your pesticide level by 50%?
- d. Suppose you start eating two apples per day instead of just one. How will that change the model, and what is the new steady state? How long will it now take to reduce pesticide levels by 50% if you stop eating apples?
- e. What is the decay rate if the half-life is 50 days?

Question 1.3. Bacterial growth

Every time you brush your teeth, bacteria enter your blood circulation. Since this is a nutritious environment for them they immediately start to grow exponentially. Fortunately, we have neutrophils in our blood that readily kill bacteria upon encountering them. A simple model would be:

$$\frac{dB}{dt} = rB - kNB ,$$

where B and N are the number of bacteria and neutrophils per ml of blood, r is the growth rate of the bacteria (per hour), and k is the rate at which bacteria are killed by neutrophils.

- a. What is the doubling time of the bacteria in the absence of neutrophils?
- b. Neutrophils are short-lived cells produced in the bone marrow, and chemotherapy can markedly reduce the neutrophil counts in the peripheral blood. What is the critical number of neutrophils that is required to prevent rampant bacterial infections after chemotherapy?
- c. What is the dimension of the parameters r and k ?
- d. The kBN term is called a mass-action term because it is proportional to both the bacterial and the neutrophil densities. A disadvantage of such a term is that each neutrophil is assumed to kill an infinite number of bacteria per hour if the bacterial density $B \rightarrow \infty$ (please check this). Later in the course we will use saturation functions to allow for maximum killing rates per killer cell. An example of such a model would be $dB/dt = rB - kNB/(h + B)$ where the total number of bacteria killed per hour approaches kN when $B \rightarrow \infty$ (please check this). What is now the dimension of k ?
- e. What is now the critical number of neutrophils that is required to prevent bacterial infections after chemotherapy? Can you sketch this?
- f. What is the dimension of h , and how would you interpret that parameter?

Question 1.4. Injecting anesthesia

Before you undergo a minor operation a certain amount of anesthesia is injected in the muscle of your upper arm. From there it slowly flows into the blood where it exerts its sedating effect. From the blood it is picked up by the liver, where it is ultimately degraded. We write the following model for the amount of anesthesia in the muscle M , blood B and liver L :

$$\frac{dM}{dt} = -eM , \quad \frac{dB}{dt} = eM - cB \quad \text{and} \quad \frac{dL}{dt} = cB - \delta L ,$$

where the parameter e is the efflux from the muscle, c is the clearance from the blood, and δ is the degradation in the liver. All parameters are rates per hour. We assume that the degradation in the muscle and blood is negligible. The initial amount of anesthesia injected is $M(0)$: the amount in the muscle at time zero.

- a. Sketch the amounts of anesthesia in the muscle, $M(t)$, in the blood, $B(t)$, and in the liver, $L(t)$, as a function of time.
- b. How long does it take before half of the injected amount has flown from the muscle to the blood?
- c. Is this the right time to do the operation?

- d. Suppose the degradation rate is slow, i.e., let $\delta \rightarrow 0$, how much anesthesia will ultimately end up in the liver?

Question 1.5. SARS

Consider a deadly infectious disease, e.g., SARS, and write the following model for the spread of the disease:

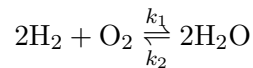
$$\frac{dI}{dt} = \beta I - \delta I ,$$

where I is the number of human individuals infected with SARS, β is the number of new cases each infected individual causes per day, and $1/\delta$ is the number of days an infected individual survives before he/she dies of SARS. Epidemiologists define the R_0 of a disease as the maximum number of new cases expected per infected individual. Since an infected individual here is expected to live for $1/\delta$ days, and is expected to cause β new cases per day, the R_0 of this disease is β/δ .

- It has been estimated that on average a SARS patient causes $R_0 = 3$ new cases, during a typical disease period of two weeks (Lipsitch et al., 2003). Most patients die at the end of these two weeks. How long does it take with these parameters to reach the point where 3×10^9 individuals (i.e., half of the world population) are infected? Note that at this time point the healthy uninfected pool is less than half of the world population because many people will have died (i.e., your simple estimate is a worst case estimate).
- Alternatively, estimate the time point at which half of the world population is still uninfected.
- Do you think this is a realistic estimate? How would you extend the model to make it more realistic?

Question 1.6. Chemical reactions

Chemical reaction schemes can directly be translated into differential equations. For instance the ODE for water in the reaction

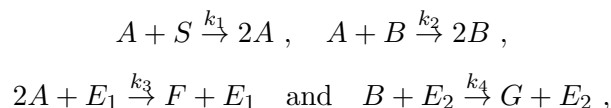


is uniquely translated into

$$\frac{dz}{dt} = 2k_1x^2y - 2k_2z^2 ,$$

where x, y , and z are the $[\text{H}_2]$, $[\text{O}_2]$ and $[\text{H}_2\text{O}]$ concentrations. Two hydrogen molecules x have to meet one oxygen molecule y , and will form two water molecules z with reaction speed k_1 . Similarly two water molecules can dissociate into one oxygen molecule and two hydrogen molecules at rate k_2 . Note that the speed of the reaction is proportional to the product of the concentrations x^2y of all the molecules involved. This is called the “law of mass action”.

Now consider the reaction scheme



where S , E_1 , and E_2 remain constant. Translate this into two differential equations for A and B .

Question 1.7. Physics (Extra exercise for cool students)

The linear ODEs used in this chapter should be familiar to those of you who studied the famous equations for velocity and acceleration. One typically writes:

$$\frac{dx}{dt} = v \quad \text{and} \quad \frac{dv}{dt} = a ,$$

where x is the total distance covered, v is the velocity, and a is the time derivative of the velocity, which is defined as the “acceleration”. Integrating dv/dt gives $v(t) = at + v(0)$, where the integration constant $v(0)$ is the velocity at time zero, and integrating $dx/dt = at + v(0)$ gives $x(t) = \frac{1}{2}at^2 + v(0)t$.

- a. Check the dimensions of v and a .
- b. Check these solutions.

Chapter 2

Population growth: replication

Populations change by migration, birth and death processes. In Chapter 1 we saw that one can write simple differential equations for populations that maintain themselves by immigration, and by replication (i.e., birth). We will here study similar models with explicit birth and death processes, and will add functions to describe how these processes may depend on the population size. There are always many different models for each particular situation, and rather than taking well-known equations for granted, we will introduce an approach for “how to develop a mathematical model”. Models will be analyzed by computing steady states, and by sketching nullclines. It is important to realize that all models introduced here require a number of “unrealistic assumptions”: (1) all individuals are equal, (2) the population is well-mixed, (3) the population size N is large, and (4) the parameters are constants. Nevertheless such “unrealistic” models will help us to think clearly about the biology described by the model (May, 2004).

We have seen in Chapter 1 that a non-replicating population which is maintained by an external influx, and has a density independent death rate, e.g., Eq. (1.3), will ultimately approach a steady state where the influx balances the death. This is not the case for a model with density independent *per capita* birth and death rates: the only equilibrium of Eq. (1.9) is $N = 0$. If $b > d$, i.e., if the fitness $R_0 > 1$, this equilibrium is unstable because introducing the smallest number of individuals into the $N = 0$ state leads to exponential growth. If $R_0 < 1$ this equilibrium is stable because every population will ultimately go extinct (i.e., for $t \rightarrow \infty$ the solution $N(0)e^{(b-d)t} \rightarrow 0$ when $d > b$). Note that one could argue that Eq. (1.9) also has a steady state when $b = d$. However, this is a rare and strange condition because the birth rate and the death rate would have to be exactly the same over long time scales.

Birth and death rates are typically not fixed because the processes of birth and death can depend on the population size. Due to competition at high population densities birth rates may become lower and death rates higher when the population size increases (see Fig. 2.1). This is called density dependence. We here wish to develop models that are realistic in the sense that we understand which biological process is mechanistically responsible for the regulation of the population size. A good procedure for developing such models is to determine beforehand which process, i.e., birth or death, has the strongest density dependence. The next step is to sketch a natural functional relationship between the biological process and the population density.

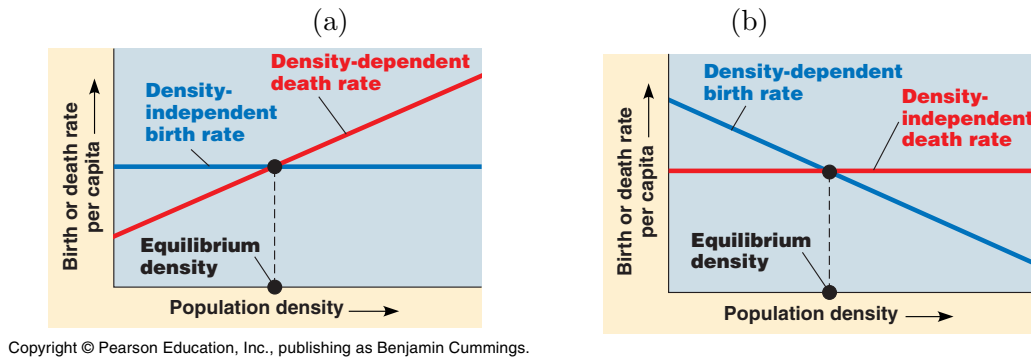


Figure 2.1: Graphs of the *per capita* birth and death rates. Equilibrium points correspond to the intersection points where the birth rate equals the death rate. From: Campbell and Reece (2008).

2.1 Density dependent death

If the death rate increases with the population size one could, for example, propose a simple linear increase of the *per capita* death rate with the population size (see Fig. 2.1a). This linear increase need not be realistic, but would certainly be a natural first extension of Eq. (1.9). Since we already have a normal death rate d in Eq. (1.9), a simple mathematical function for the graph in Fig. 2.1a is $f(N) = d + cN$, where d is the normal death rate that is approached when the population size is small, and where c is the slope with which the death rate increases with N . To incorporate the death rate of Fig. 2.1a into our model one can multiply the death rate parameter d in the $dN/dt = (b - d)N$ of Eq. (1.9) with a non-dimensional function like $f(N) = (1 + N/k)$, where the dimension of the parameter k is biomass, or individuals, and its exact interpretation is that the death rate has doubled when $N = k$. Because $f(N) = 1$ when $N \rightarrow 0$ the minimum *per capita* death rate (or maximum generation time) remains exactly the same. The full model becomes

$$\frac{dN}{dt} = [b - d(1 + N/k)]N. \quad (2.1)$$

At low population sizes the expected life span of the individuals remains $1/d$ time units, and they always have a birth rate b per time unit. Since the R_0 is a maximum fitness, it is computed for an individual under optimal conditions, which here means $N \rightarrow 0$. The fitness of individuals obeying Eq. (2.1) therefore equals $R_0 = b/d$.

To search for steady states of Eq. (2.1) one sets $dN/dt = 0$, cancels the trivial $N = 0$ solution, and solves from the remainder

$$b - d = dN/k \quad \text{that} \quad \bar{N} = k \frac{b - d}{d} = k(R_0 - 1) \quad (2.2)$$

is the non-trivial steady state population size. In ecology such a steady state is called the “carrying capacity”. A simple linear density dependent death rate is therefore sufficient to deliver a carrying capacity. Here, the carrying capacity depends strongly on the fitness of the population, i.e., doubling $(R_0 - 1)$ doubles the steady state population size.

To test whether these steady states are stable one could study the solution of Eq. (2.1) to see what happens when $t \rightarrow \infty$. Although this solution is known (see below), we prefer to introduce a graphical method for determining the stability of a steady state. Fig. 2.1a sketches the *per capita* birth and death rates as a function of the population size in one graph. When these lines intersect the birth and death rates are equal and the population is at steady state. To check the

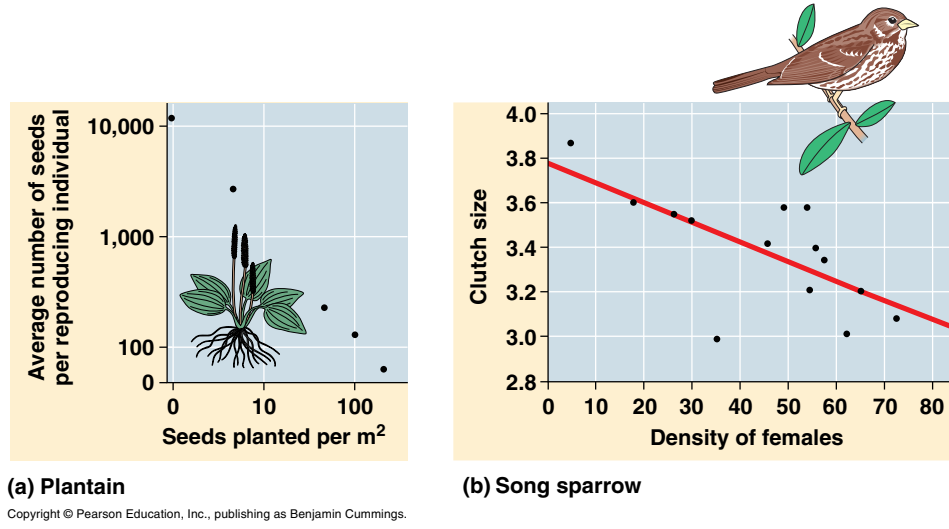


Figure 2.2: Panels (a) and (b) show for a plant species and a bird species that the *per capita* reproduction rate depends on the population size. From: Campbell and Reece (2002).

stability of the non-trivial steady state, one can study what happens when the population size is somewhat increased. Increasing N from the equilibrium density \bar{N} makes $dN/dt < 0$ because the death rate exceeds the birth rate. This forces the population back to its steady state value. Similarly, decreasing N makes $dN/dt > 0$ which pushes the population back to the steady state. We conclude that the non-trivial steady state is stable. The instability of the trivial steady state $N = 0$ can also be checked from Fig. 2.1a: increasing N from $\bar{N} = 0$ makes $dN/dt > 0$ whenever $b > d$, i.e., whenever the fitness $R_0 > 1$.

2.2 Density dependent birth

Alternatively, one may argue that the *per capita* birth rate b should decrease with the population size. Experimental evidence supporting a decreasing birth rate in two natural populations is shown in Fig. 2.2. The simplest functional relationship between the *per capita* birth rate and the population size is again a linear one (see Fig. 2.1b), and a simple mathematical description is $f(N) = b - cN$, where b is the birth rate at low population densities. Since we already have a maximum birth rate in the $dN/dt = (b - d)N$ of Eq. (1.9), we multiply the birth rate parameter, b , by the linear non-dimensional function, $f(N) = (1 - N/k)$, such that the model becomes

$$\frac{dN}{dt} = [b(1 - N/k) - d]N. \quad (2.3)$$

The dimension of the parameter k is again biomass, or individuals, and its exact interpretation now is that the birth rate becomes zero when $N = k$. The advantage of using this non-dimensional function, $f(N) \leq 1$, that approaches one when $N \rightarrow 0$, is that the interpretation of the maximum birth rate remains the same. At low population sizes the fitness of individuals obeying Eq. (2.3) therefore remains $R_0 = b/d$, which is natural because at a sufficiently low population size there should be no difference between the two models. The steady states now are $N = 0$ and solving

$$b - d = b \frac{N}{k} \quad \text{yields} \quad \bar{N} = k(1 - d/b) = k(1 - 1/R_0). \quad (2.4)$$

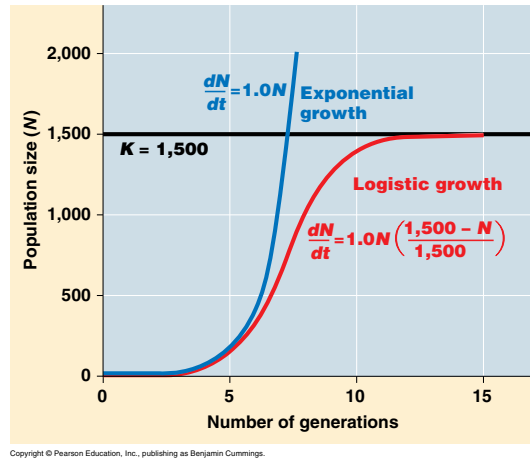


Figure 2.3: Logistic growth. From: Campbell and Reece (2008).

A simple linear density dependent birth term therefore also allows for a carrying capacity. When $R_0 \gg 1$, this carrying capacity approaches the value of k , and becomes fairly independent of the fitness. By the same procedure as illustrated above one can test graphically from Fig. 2.1b that the carrying capacity is stable, and that $N = 0$ is unstable.

2.3 Logistic growth

Since the model with density dependent death and the one with density dependent birth are both of the form $dN/dt = \alpha N - \beta N^2$, one can rewrite both models into the classical “logistic equation”:

$$\frac{dN}{dt} = rN(1 - N/K), \quad \text{with solution} \quad N(t) = \frac{KN(0)}{N(0) + e^{-rt}(K - N(0))}, \quad (2.5)$$

with a natural rate of increase of $r = b - d$, and where K is the carrying capacity of the population. One can easily see that all three are of the same form because they all have a positive linear and a quadratic negative term. The behavior of the three models is therefore the same: starting from a small initial population the growth is first exponential, and later approaches zero when the population size approaches the carrying capacity (see Fig. 2.3). Starting from a large initial population, i.e., from $N(0) > K$, the population size will decline until the carrying capacity is approached. Because Eq. (2.5) has no explicit death rate, the R_0 is not defined.

2.4 Stability and return time

The steady state $N = 0$ in Fig. 2.1 is not stable because small perturbations increasing N makes $dN/dt > 0$, which further increases N . The non-trivial steady states in Fig. 2.1 are stable because increasing N makes $dN/dt < 0$. It appears that steady states are stable when $\partial_N[dN/dt] < 0$, and unstable when this slope is positive (see Fig. 2.4). Note that ∂_N means the derivative with respect to N , i.e., $\partial_x x^2 = 2x$ and $\partial_t N = dN/dt$ (which is also written as N').

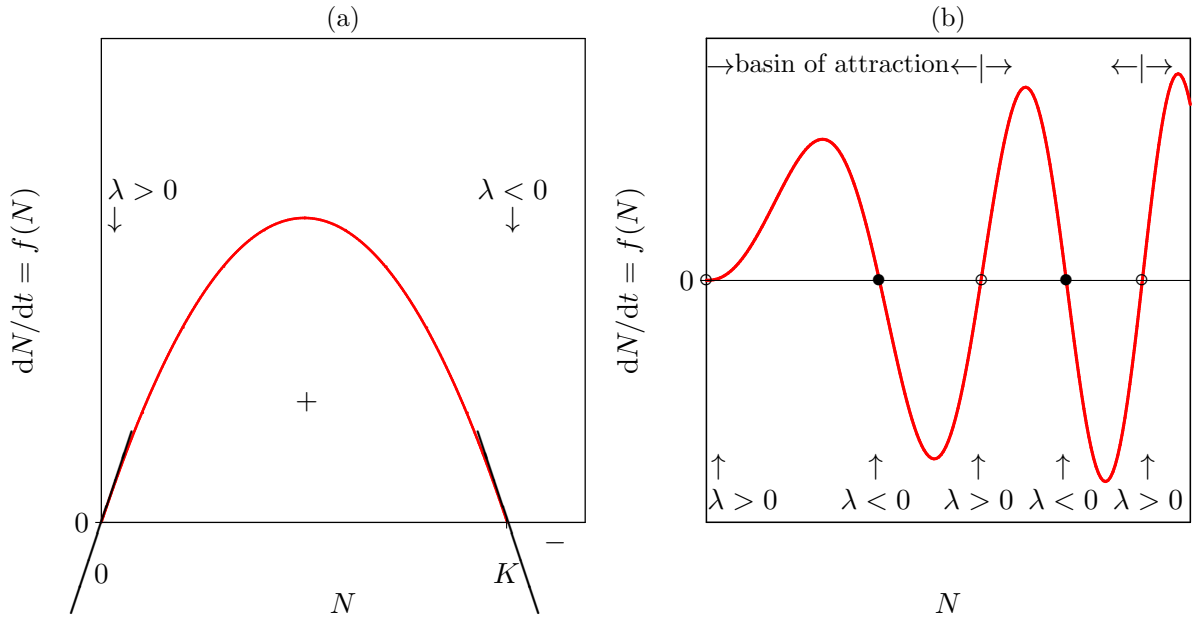


Figure 2.4: The stability of a steady state is determined by the local derivative (slope) of the growth function at the steady state. Panel (a) depicts the logistic growth function $f(N) = rN(1 - N/K)$ and Panel (b) depicts an arbitrary growth function.

Mathematically one can linearize any function $f(x)$ at any value of x by its local derivative:

$$f(x + h) \simeq f(x) + f'h, \quad (2.6)$$

where h is a small step, and $f' = \partial_x f(x)$ the derivative of $f(x)$ with respect to x (see Fig. ?? in the Appendix). To apply this to our stability analysis one rewrites $f(N)$ into $f(\bar{N} + h)$ where \bar{N} is the steady state population size and h is a small disturbance. Following Eq. (2.6) one rewrites $dN/dt = f(N)$ into

$$\frac{d\bar{N} + h}{dt} = f(\bar{N} + h) \simeq f(\bar{N}) + f'h = 0 + \lambda h, \quad (2.7)$$

where $\lambda = f'h$ is the derivative of $f(N)$ with respect to N . Because $d(\bar{N} + h)/dt = dh/dt$ we obtain

$$\frac{dh}{dt} = \lambda h \quad \text{with solution} \quad h(t) = h(0)e^{\lambda t}, \quad (2.8)$$

for the behavior of the disturbance around the steady state. Thus, whenever the local tangent λ at the equilibrium point is positive, small disturbances grow; whenever $\lambda < 0$ they decline, and the equilibrium point is stable. For an arbitrary growth function this dependence on the slope λ is illustrated in Fig. 2.4b. This figure shows that the unstable steady states, here saddle points, separate the basins of attraction of the stable steady states.

For example, for the logistic equation, $f(N) = rN(1 - N/K)$, one obtains $\lambda = r - 2rN/K$. At the carrying capacity of the logistic equation, i.e., at $N = K$, the local tangent is $\lambda = -r$, and at $N = 0$ we obtain $\lambda = r$ (see Fig. 2.4a), arguing that $N = K$ is a stable steady state, and $N = 0$ is an unstable steady state. The stability of a steady state can be expressed as a ‘Return time’

$$T_R = -\frac{1}{\lambda}, \quad (2.9)$$

i.e., the more negative λ the faster perturbations die out. For example, consider the return time of the logistic growth equation around its carrying capacity. Above we derived that at

$\bar{N} = K$ the tangent $\lambda = -r$. This means that $T_R = 1/r$, i.e., the larger r the shorter the return time. Populations that grow fast are therefore more resistant to perturbations. The paradigm of r -selected and K -selected species in ecology is built upon this theory. Finally, note that the dimensions are correct: because r is a rate with dimension “time⁻¹”, T_R indeed has the dimension “time”.

2.5 Summary

A stable non-trivial population size is called a carrying capacity. Replicating populations will only have a carrying capacity when the *per capita* birth and/or death rate depend on the population density. For non-replicating populations this is not the case because they approach a stable steady state without any population regulation (i.e., without density dependence [or homeostasis]). A steady state is stable if the local derivative of the growth function is negative. The steeper this derivative, the shorter the return time.

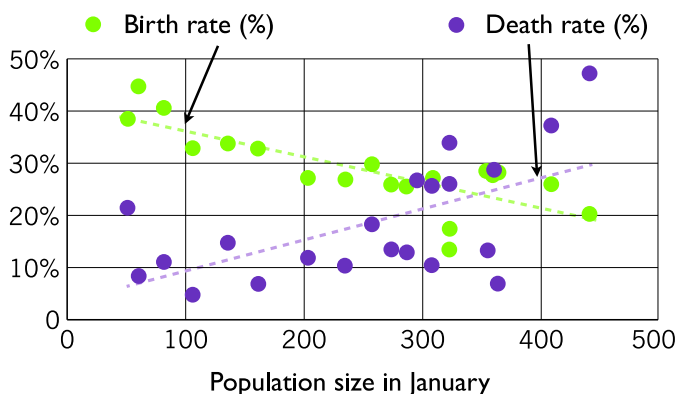
2.6 Exercises

Question 2.0. Read the chapter

- Give an intuitive definition of the R_0 concept.
- What is the difference between an R_0 and the natural rate of increase? Estimate the R_0 and the rate of growth of the human population.
- What is a density dependent death rate? Is the death rate in $dx/dt = f(x) - dx$ density dependent?
- What is a carrying capacity? What is a *per capita* growth rate?
- Define the concept ‘return time’. Can a steady state be unstable?

Question 2.1. Heck cattle

Heck cattle have been introduced to the ‘Oostvaardersplassen’ in the Netherlands as a semi-natural population of grazers. They prevent the outgrowth of trees and shrubs in this open wet landscape harboring many different bird species. The population was started with a small group of animals in 1983, and after approximately 20 years the density approached a carrying capacity of 300–400 cattle. People have measured birth and death rates over the years (see the Figure taken from an article in NRC Handelsblad on 11 December 2010):



Figures taken from NRC Handelsblad 11 Dec 2010 (left) and Wikipedia (right).

Because so many animals are dying from starvation every year, there have been vigorous debates in the public arguing that these animals are suffering too much. One solution would be to shoot animals to lower the population size, and hence the death by competition for resources. Please read the NRC article.

- a. How would you estimate the carrying capacity from the Figure, and what would it be?
- b. Since the birth and death rates obey the simple linear functions we defined in this chapter, the data in the Figure can be defined as

$$\beta(N) = b(1 - N/k_1) \quad \text{and} \quad \delta(N) = d(1 + N/k_2) ,$$

for the birth and death rate, respectively. From the Figure we can see that the maximum birth rate is approximately 0.4 per year, and is half maximal at $N = 400$, and that the minimum death rate is 0.03 per year, and is 11-fold larger, i.e., 0.33 when $N = 500$. Use this information to determine b , d , k_1 and k_2 .

- c. Incorporate these functions into a mathematical model, and compute the carrying capacity from your model.
- d. What fraction (or percentage) of the animals is dying every year when the population is at carrying capacity? How many dead animals is that?
- e. What is the R_0 of this population? Would you call this a logistic growth model?
- f. To reduce the number of animals dying from starvation it has been proposed to shoot a fixed number of animals per year. Calling the number of animals shot per year, s , the new model would become

$$\frac{dN}{dt} = [\beta(N) - \delta(N)]N - s .$$

Unfortunately, equilibria are no longer given by $N = 0$ and $\beta(N) - \delta(N) = 0$ and we have to find equilibria from solving the following quadratic equation

$$\bar{N}_{\pm} = \frac{(b-d)k_1k_2 \pm \sqrt{k_1k_2[(b-d)^2k_1k_2 - 4(dk_1 + bk_2)s]}}{2(dk_1 + bk_2)} \simeq 168 \pm 2.27\sqrt{5476 - 176s}$$

which has two positive solutions for $0 < s \leq 31$ animals per year. To get a better intuition about what these two equilibria represent note that equation $dN/dt = [\beta(N) - \sigma(N)]N$ can be rewritten as a standard logistic growth model and hence its graph corresponds to the parabola drawn in Fig. 2.4a. This parabola intersects the x axis at $N = 0$ and $\beta(N) - \delta(N) = 0$ equilibria. By introducing the term $-s$ this parabola is shifted downward, causing the $N = 0$ equilibrium to shift leftwards towards higher N values and the $\beta(N) - \delta(N) = 0$ to shift rightwards towards lower N values. From where the parabola lies above and below the x axis it follows that the lower equilibrium (the \bar{N}_- solution) is unstable and the higher equilibrium (the \bar{N}_+ solution) is stable:

s	\bar{N}_-	\bar{N}_+	$d(1 + \bar{N}_+/k_2)\bar{N}_+$	$s + d(1 + \bar{N}_+/k_2)\bar{N}_+$
0	0	336	78	78
10	30	307	66	76
20	68	269	51	71
30	136	200	30	60
31	158	178	24	55

Would you be in favor of this solution, and how many animals would you propose to shoot per year?

- g. Why is there no solution for $s > 31$ animals per year?
- h. What happens if the population is started with less than \bar{N}_- animals?
- i. Simulate this model at the GRIND computer practical to see if the population growth resembles the data.

Question 2.2. Density dependent growth

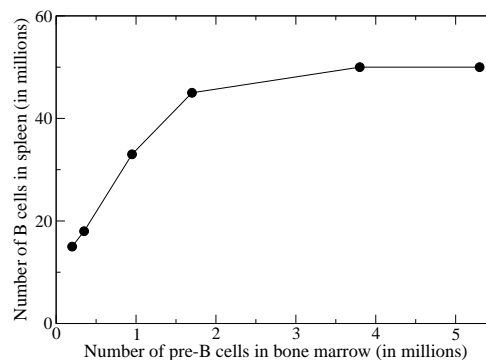
A density dependent birth rate need not decline linearly with the population density. Consider a population with a density dependent growth term:

$$\frac{dN}{dt} = (bf(N) - d)N \quad \text{with} \quad f(N) = \frac{1}{1 + N/h}.$$

- Sketch how the *per capita* birth rate depends on the population density N .
- Sketch how the birth rate of the total population depends on the population density N .
- Compute the steady states of the population.
- What is the R_0 and express the steady state in terms of the R_0 ?
- Is $f(N)$ a Hill function (see Chapter ??)?

Question 2.3. Freitas

Agnes et al. (1997) at the Pasteur Institute manipulated the number of cells in the bone marrow (pre-B cells) producing naive B cells (e.g., in the spleen), and found the following:



The simplest model for the naive B cell population is $dB/dt = m - dB$ where m is the bone marrow production, and $1/d$ is the average life span of naive B cells. The rate of naive B cell production is proportional to the number of pre-B cells, i.e., $m = \alpha P$, where P is the number of pre-B cells. Note that in the graph the horizontal axis corresponds to m and that the vertical axis depicts \bar{B} .

- Is this simple model compatible with the data shown?
- If not, how would you extend the model?
- Do the data require homeostasis, i.e., density dependent regulation?
- Is $dB/dt = m - dB$ accounting for homeostasis?

Question 2.4. Stem cells

Stem cells are maintained by continuous division. A fraction of the daughter cells differentiates and obtains other phenotypes. A convenient model for stem cell growth is the logistic equation $dS/dt = rS(1 - S/k)$.

- Expand the model with differentiation of stem cells
- Write a simple model for the differentiated cells
- Compute the steady state population sizes of this model.

Question 2.5. Density dependent death

Consider a replicating population where most of the death is due to competition with other

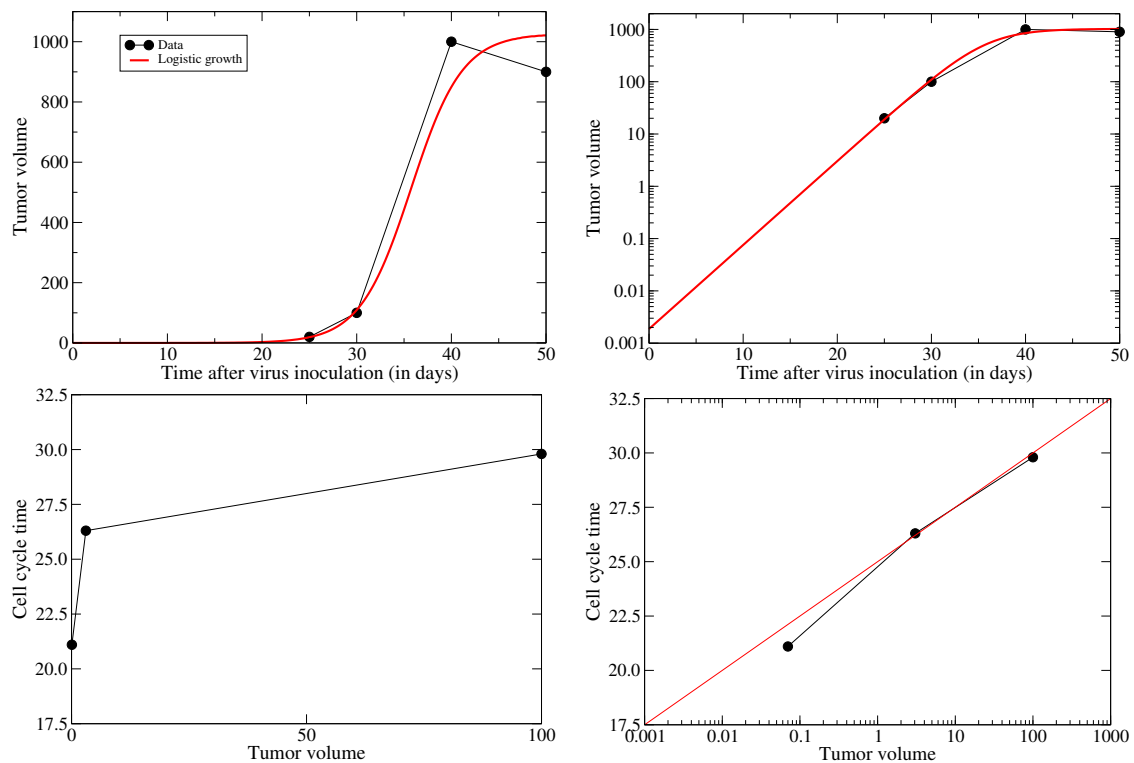


Figure 2.5: The growth of a sarcoma as measured by Zobl et al. (1975). The symbols denote the data and the lines our best description of this data by fitting a mathematical model.

individuals, i.e., let $f(N) = cN$ in a model where $dN/dt = (b - f(N))N$.

- Sketch the *per capita* death rate as a function of N .
- Sketch the *per capita* net growth rate as a function of N .
- Compute the steady states.
- Why is the R_0 not defined?
- What is the return time in the non-trivial steady state?

Question 2.6. Logistic growth of a tumor

Zobl et al. (1975) have studied the growth functions of tumors by inducing novel sarcomas in the kidneys of rats using Polyoma virus. These tumors initially grow exponentially and then approach a steady state volume. This growth function can reasonably be described with a logistic growth function, $dN/dt = rN(1 - N/K)$, where r defines the maximum growth rate, and K is the “carrying capacity”. To visualize that the initial growth rate is truly exponential we plot their data both on a logarithmic and a linear scale in Fig. 2.5. In this figure the symbols denote the data with the volume in mm^3 , and the heavy line is the best fit of the classical logistic equation to the data (with $r = 0.37$ per day, $K = 1027 \text{ mm}^3$, and $N(0) = 1.87 \times 10^{-3} \text{ mm}^3$). The Mathematica code to fit the logistic growth function to this data is available on the website as the file `tumor.nb`.

In the paper Zobl et al. (1975) also measure the cell cycle times of the tumor cells. They find that the cell cycle time, T , is approximately 21h at day 10, 26h at day 20, and 30h at day 30. Reading the size of the tumor from the fitted curve at these time points we find that $T \simeq 21\text{h}$ when $N \simeq 0.07$, $T \simeq 26\text{h}$ when $N \simeq 3$, and $T \simeq 30\text{h}$ when $N \simeq 100$. Plotting T as a function of $\log_{10} N$ reveals that the division time increases approximately linearly with the log tumor size, i.e., the diagonal line in Panel (d) obeys $T = 25 + 2.5 \log_{10}[N]$.

- a. Can you give a biological explanation for the carrying capacity observed at a tumor size of $K = 1027 \text{ mm}^3$?
- b. Note that we have fitted 4 data points with a function requiring at least 3 parameters (r , K , and $N(0)$). One could also try to make the model more realistic and distinguish between cell division and cell death by writing $dN/dt = bN(1 - N/k) - dN$. What is now the biological interpretation of k ? Do you think one can estimate the values of all parameters of the more realistic model with the same data?
- c. What would be your best estimate for the cell cycle time in a tumor of 10^{-3} mm^3 ? What do you expect for the cell cycle time at day 50?
- d. Write a simple equation for how the cell division rate depends on the tumor volume (the division rate $B(N)$ is the inverse of the cell cycle time $T(N)$).
- e. Write a model implementing this division rate and compute the new steady state.
- f. Estimate the death rate realizing that we should obtain the same steady state with the new model. Using this new death rate compute the net replication rate of the tumor and compare this to the net replication rate described by r in the logistic model that we started out with. What could be causing the difference?
- g. Why are we now able to estimate the death rate, whereas in b we argued that we could not determine the birth and death rates but only the net replication rate?

Question 2.7. Negative birth (Extra exercise for cool students)

The *per capita* birth rate function $f(N) = b(1 - N/k)$ of Eq. (2.3) is not completely correct because the birth rate becomes negative when $N > k$. This can be repaired by writing $f(N) = \max[0, b(1 - N/k)]$ which equals zero when $b(1 - N/k) \leq 0$ because the $\max[]$ function returns the maximum of its arguments. Will this change the steady states analyzed in this Chapter?

Chapter 3

Lotka Volterra model

In the next two chapters we will develop a number of classical ecological models. The famous Lotka-Volterra model that we will analyze here was developed around 1925 by Vito Volterra and Alfred Lotka, and in 1934 Gause formulated the competitive exclusion principle (see Chapter 5). Theoretical models are common in ecology, and a number of ecological concepts, like “niche” and the relationship between “stability and complexity” originate from theoretical work (May, 1974). We will start with the Lotka-Volterra model that was originally developed for modeling host-parasite and predator-prey interactions, and has since been used in many situations where some expanding population is controlled by another population (e.g., growing tumors or infections controlled by immune responses).

Suppose one has measurements for the interaction between a certain prey species and a certain predator, e.g., mice and owls. These measurements are summarized in Fig. 3.1, and suggest that the mice have a linear density dependent birth rate (a) and a density independent death rate (b). This can be modeled with Eq. (2.3). Panel (c) suggests that the rate at which owls catch mice is proportional to the mouse density, i.e., if the mouse population size were to double, the owls would consume twice as many mice. For this linear density dependence and linear predation term one obtains the prey equation of the famous Lotka-Volterra predator-prey model:

$$\frac{dR}{dt} = [bf(R) - d]R - aNR \quad \text{where} \quad f(R) = 1 - R/k, \quad (3.1)$$

with maximum birth rate b , death rate d , and a predation term aNR . In the previous chapters we have seen that $R_0 = b/d$ for this prey population. We have also seen that the steady state of a prey population in the absence of predators is

$$\bar{R} = k(1 - d/b) = k(1 - 1/R_0) = K, \quad (3.2)$$

where K defines the “carrying capacity” (see Chapter 2). Theoretical ecologists typically do not split birth from death in the Lotka-Volterra model. Rather, the prey equation is written with a logistic growth $dR/dt = rR(1 - R/K)$, where r is a net rate of increase (cf. Eq. (2.5)), and which immediately has the steady state $\bar{R} = K$ (see Fig. 2.3), but here we prefer to have explicit birth and death rates (and hence have an R_0).

The owl “measurements” in Fig. 3.1 suggest the *per capita* birth rate of the owls is proportional to the number of mice eaten per owl, i.e., to aR . Since the owl death rate is density independent, one would write

$$\frac{dN}{dt} = [caR - \delta]N, \quad (3.3)$$

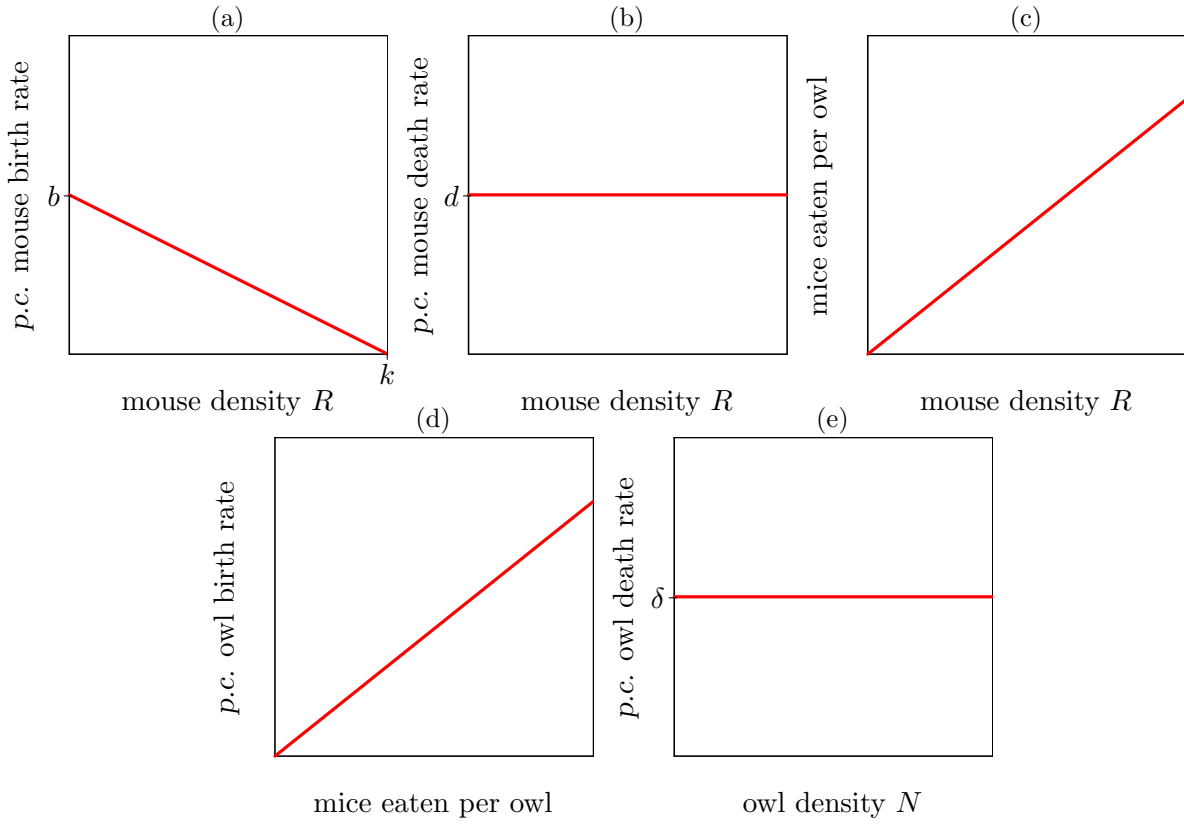


Figure 3.1: Population dynamical characteristics of a mouse and owl population. The *p.c.* in the figure means *per capita*.

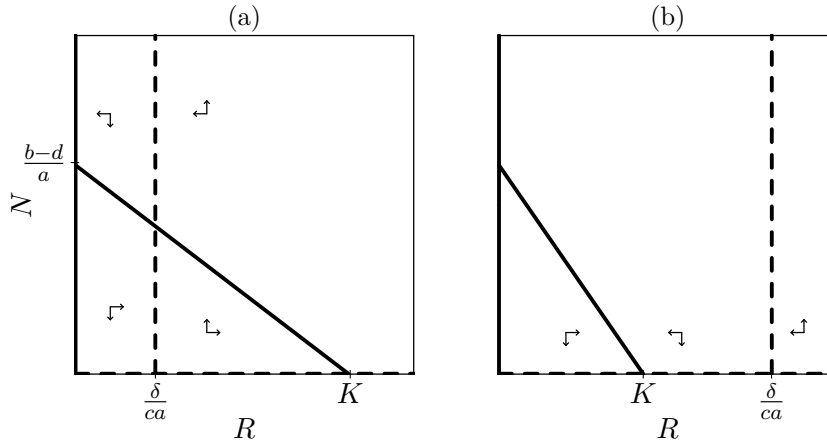


Figure 3.2: The Lotka-Volterra model. The heavy lines are the nullclines of the prey; the dashed lines those of the predator.

where $1/\delta$ is the expected life-span of the predators. The parameter c converts “eaten prey biomass” into “predators born”. Because the predator birth rate, caR , depends on the availability of prey, one typically takes the maximum prey density, $R = K$, to compute the R_0 of the predator (see below).

To compute the steady states of the full Lotka-Volterra model, one substitutes $f(R)$ in Eq. (3.1),

and sets $dR/dt = dN/dt = 0$. Setting $dR/dt = 0$ yields

$$\bar{R} = 0 \quad \text{and} \quad \bar{N} = \frac{1}{a} [b(1 - R/k) - d] , \quad (3.4)$$

and setting $dN/dt = 0$ gives

$$\bar{N} = 0 \quad \text{and} \quad \bar{R} = \frac{\delta}{ca} . \quad (3.5)$$

The model has three steady states. Since both species are replicating populations $(\bar{R}, \bar{N}) = (0, 0)$ is a (trivial) steady state. The second steady state was already obtained in Eq. (3.2) for a prey population without predators, i.e., $(\bar{R}, \bar{N}) = (K, 0)$, where K is the “carrying capacity” of the prey population. The third steady state is called non-trivial because both populations are present. By Eq. (3.5)b we know that $\bar{R} = \delta/(ca)$, which when substituted into Eq. (3.4)b yields

$$\bar{N} = \frac{1}{a} \left[b \left(1 - \frac{\delta}{cak} \right) - d \right] . \quad (3.6)$$

We proceed by sketching the phase space with nullclines of the model. The predator, $dN/dt = 0$, nullcline is given by Eq. (3.5), which in Fig. 3.2 corresponds to the horizontal axis and a vertical line at $R = \delta/(ca)$. The $dR/dt = 0$ nullcline is given by Eq. (3.4) and corresponds to the vertical axis in Fig. 3.2, and the diagonal line intersecting the vertical axis at $N = (b - d)/a$ and intersecting the horizontal axis at $R = K = k(1 - 1/R_0)$. The phase space has two qualitatively different possibilities: when $\delta/(ca) < K$, the non-trivial steady state exists, which means that predator and prey can coexist. If $\delta/(ca) > K$ the maximum prey density K is insufficient for predator growth (Fig. 3.2b). Under such circumstances the carrying capacity of the prey is the one and only attractor of the system.

The vector field shows that the steady state $(0, 0)$ is unstable. The $(K, 0)$ steady state is unstable in Fig. 3.2a, and is stable in Fig. 3.2b. Now let us study the stability of the non-trivial steady state in Fig. 3.2a. The vectorfield indicates a rotating type of dynamics, however such dynamics may arise from either a stable or unstable spiral, a center point, and a subset of stable and unstable nodes. Therefore we have to look in more detail at the vectorfield and determine the local feedback of the prey and predators on themselves. For the prey, starting from the equilibrium we add a few prey (we move a bit to the right on the phase plane) and examine what the local vectorfield tells us about the dynamics of the prey (we consider the horizontal part of the vectorfield at that location). We see that upon adding a few prey the number of prey tend to decrease. Thus a destabilisation of the number of prey from the number in the equilibrium will become restored. Similarly, for the predators, starting from the equilibrium point we add a few predators (we move a bit upward on the phase plane). Next we examine the local dynamics of the prey (vertical part of the local vectorfield). We see that we are exactly at the nullcline and that hence the vertical part of the vectorfield is zero. Thus, while an increase in predators does not become restored, it also does not get exaggerated through a further increase in predator numbers. Together this information suggests that the nontrivial equilibrium point is stable.

Finally, we use the R_0 of the predator to simplify the expression for the non-trivial steady state. This will tell us something about the effect the predator has on the prey density. Having $\bar{R} = K$ as the maximum prey density, the maximum predator birth rate is caK . With an expected life span of $1/\delta$ one can define the R_0 of the predator as $R_0 = \frac{caK}{\delta}$. This allows us to rewrite the equilibrium prey density defined in Eq. (3.5) as $\bar{R} = K/R_0$. Interestingly, this tells us that the depletion of the prey population is proportional to the fitness of the predator. Thus, a predator that realizes a reproduction of ten offspring per generation at a maximum prey availability $R = K$, is expected to reduce its prey population by a factor ten.

3.1 Summary

Sketching the nullclines and the vector field help one to find the different steady states of a model, and to determine their type and stability. Simple models can deliver surprising results. For instance, in the Lotka Volterra model the population density of the prey is completely determined by predator parameters, and is independent of the prey's birth and death rates, and the carrying capacity. The mathematical reason for this is that the predator cancels from the predator's ODE, such that we have to solve the prey density from the predator's equation.

3.2 Exercises

Question 3.0. Read the chapter

- What is a phase space? What is a nullcline? What is a vector field? What is a trajectory?
- How do you recognize the steady states from a phase plane with nullclines? Why is that the case?
- How many steady states are there in the Lotka Volterra model?
- Write them all in terms of the parameters, and give each of them a simple biological interpretation.
- Which of them are non-trivial? Which of them are stable?
- What is the expected population size of a prey population with carrying capacity K , and which is controlled by a predator with a fitness R_0 ?

Question 3.1. Algae and zooplankton

In fresh water lakes green algae are eaten by several zooplankton species. Let us model this with the simple Lotka-Volterra model

$$\frac{dA}{dt} = rA(1 - A/K) - bAZ \quad \text{and} \quad \frac{dZ}{dt} = cbAZ - dZ ,$$

where we have collapsed the birth and death processes of the algae into a net growth term known as logistic growth.

- Sketch the nullclines and determine the stability of all the steady states for the case with a non-trivial steady state.
- Consider a lake with algae and zooplankton coexisting at steady state. Eutrophication of the lake with nitrogen and phosphate increases the availability of food for the algae. In this model this means that the carrying capacity parameter K increases by eutrophication. Sketch in the same phase space the nullclines of a lake with and without eutrophication.
- Which of the two populations increases most by the eutrophication?

Question 3.2. Seals

Assume that seals in the Waddenzee have a density dependent birth rate and a density independent death. Healthy seals S live on average $1/d$ days, and can become infected with a virus carried by infected seals I . Infected seals die after a short period averaging about $1/\delta$ days. We write the following model:

$$\frac{dS}{dt} = bS(1 - S/k) - dS - \beta SI \quad \text{and} \quad \frac{dI}{dt} = \beta SI - \delta I \quad \text{where} \quad \delta \gg d .$$

- What are the steady states of the seal population in the absence of the infection?

- b. What is the R_0 of the seals? What is the R_0 of the infection?
- c. Express the steady state from **a.** in terms of the R_0 of the seals.
- d. Suppose that pollution with chemicals (like PCBs) halves the birth rate of the seals. What is the steady state of the seal population under polluted circumstances?
- e. How many healthy seals S do you expect in a population chronically infected with this deadly virus?
- f. How is this healthy seal population size in the infected steady state changing by water pollution with chemicals?
- g. Sketch the nullclines of the model and determine the stability of all the steady states.
- h. Sketch the nullclines of the model in the presence and the absence of PCBs in one picture (for the case where the virus is present).

Question 3.3. Solving the steady state

Find the non-trivial steady state value of the population B in the following food chain assuming that all species are present:

$$\frac{dA}{dt} = rA(1 - A/K) - cAB, \quad \frac{dB}{dt} = cAB - dB - eBC, \quad \frac{dC}{dt} = eBC - fC.$$

Question 3.4. Density dependent birth

In the Lotka-Volterra model (i.e., Eqs. 3.1 & 3.3) we assumed a linear decrease in the prey birth rate with the prey density, i.e., $f(R) = 1 - R/k$. Now consider the curved function $f(R) = 1/(1 + R/k)$ introduced in Question 2.2. Make sure you know how to sketch this function.

- a. Sketch the nullclines for the case with a non-trivial steady state (compute the intersects with the axis and asymptotes of the new nullcline).
- b. Write an expression for the new carrying capacity K of the prey.
- c. What is the R_0 of the predator?
- d. Note the similarity in the expressions for the non-trivial steady state of the prey, \bar{R} , and the R_0 of the predator. Can you simplify the expression for \bar{R} using the R_0 of the predator?
- e. Determine the stability of the steady states.
- f. Do you find this model very different from the Lotka-Volterra model?

Question 3.5. Malaria

Consider an infection of red blood cells that are produced at a fixed rate by the bone marrow.

$$\frac{dB}{dt} = \sigma - dB - aBI \quad \text{and} \quad \frac{dI}{dt} = aBI - \delta I$$

where B are uninfected red blood cells and I are infected cells.

- a. Sketch the nullclines for the case where the infection can maintain itself (do compute the asymptotes).
- b. Write an expression for the “carrying capacity” K of the red blood cells.
- c. What is the steady state \bar{B} during a chronic infection?
- d. Express this steady state \bar{B} in terms of the carrying capacity K and the R_0 of the infection.
- e. Determine the stability of the steady states.
- f. What are the major differences between this model and the Lotka-Volterra model?

Question 3.6. Growth of insects

Consider an insect population consisting of larvae L and adults A :

$$\frac{dL}{dt} = aA - dL(1 + eL) - cL \quad \text{and} \quad \frac{dA}{dt} = cL - \delta A .$$

- a. Interpret all terms of the model.
- b. Sketch the nullclines and the vector field (see Section ??).
- c. Determine the stability of the steady state(s).

Chapter 4

The predator functional response

In the previous chapter we derived the Lotka-Volterra model for a predator-prey interaction. That model assumed that the number of prey caught per predator is proportional to the prey density. Because at high prey densities the predator will become satiated, and/or needs time to handle the prey it has caught, this assumption may sometimes be unrealistic. When these effects happen at prey densities below the carrying capacity (i.e. prey densities that may actually occur in the system), we need saturation functions to improve the predation term. Let us define the concept of a “functional response”, which describes the expected number of prey eaten per predator as a function of the prey density. The Lotka-Volterra model has a linear functional response (see Fig. 4.1a).

We rewrite the Lotka-Volterra model with a function $f(R)$ to incorporate the functional response:

$$\frac{dR}{dt} = rR(1 - R/K) - Nf(R) \quad \text{and} \quad \frac{dN}{dt} = cNf(R) - dN, \quad (4.1)$$

where $f(R)$ is the amount of prey biomass eaten by one predator per unit of time. For simplicity we have collapsed the prey birth and death processes into a net growth term (i.e., into logistic growth). The parameter c is again a conversion factor. The three Holling (1959) functional

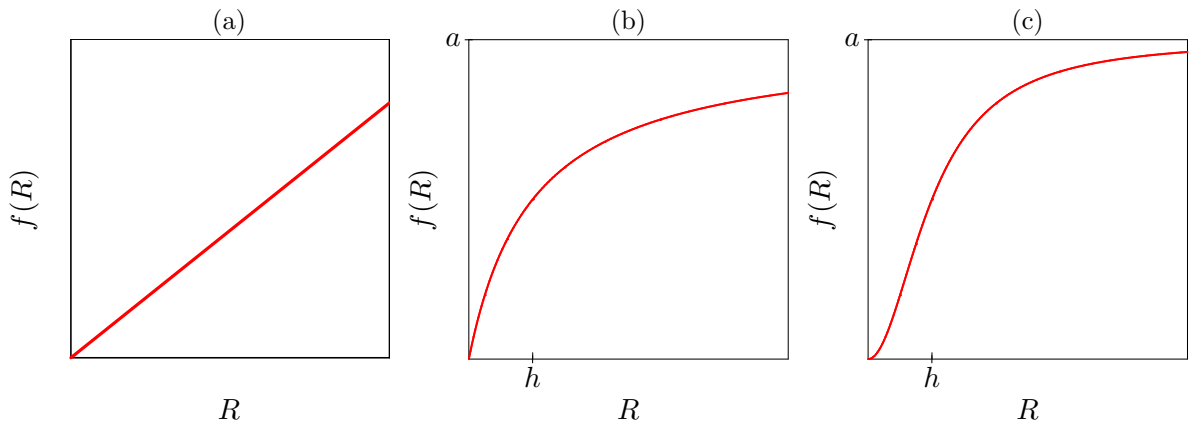


Figure 4.1: Plotting the number of prey eaten per predator as a function of the prey density R . A linear (a), a Monod saturated (b), and a sigmoid (c) functional response.

responses are depicted in Fig. 4.1, and can be defined by the following three equations:

$$f(R) = aR, \quad f(R) = \frac{aR}{h+R} \quad \text{and} \quad f(R) = \frac{aR^2}{h^2+R^2}, \quad (4.2)$$

which define the linear response of the Lotka-Volterra model, the “Monod saturation”, and a sigmoid functional response, respectively. Ecologists also call the latter two the Holling type II and type III functional responses (Holling, 1959). More generally speaking, the latter two functions are “Hill functions” as explained in the Appendix (Chapter ??). The Hill-functions in Eq. (4.2) have the pleasant property that $f(R) \rightarrow a$ when $R \rightarrow \infty$, and that $f(R) = \frac{1}{2}a$ when $R = h$. The parameter a in the two functions is therefore the maximum prey biomass that a predator can consume per unit of time. The saturation constant h is the prey density at which predator consumption is half of this maximum. The value of h is partly determined by the “handling time” (see our Theoretical Ecology course (De Boer, 2004)).

We will here study the model with a Monod functional response

$$\frac{dR}{dt} = rR(1 - R/K) - \frac{aNR}{h+R} \quad \text{and} \quad \frac{dN}{dt} = \frac{caNR}{h+R} - dN. \quad (4.3)$$

To sketch the nullclines we write $dR/dt = 0$ to find

$$R = 0 \quad \text{and} \quad N = (r/a)(h+R)(1 - R/K), \quad (4.4)$$

where the latter describes a parabola that equals zero when $R = -h$ and $R = K$ (i.e., the latter is of the form $y = \alpha(h+x)(1-x/K)$). For the predator nullcline we write $dN/dt = 0$ to find

$$N = 0 \quad \text{or} \quad R = \frac{h}{ac/d - 1}, \quad (4.5)$$

which are horizontal and vertical lines in the phase space.

To simplify we again define an R_0 . Because we have collapsed birth and death into one logistic equation, the R_0 of the prey is not defined. To define an R_0 of the predator we can now employ the fact that predator consumption is saturated. Indeed for an infinite prey population the *per capita* predator birth rate approaches ac , and over an expected life span of $1/d$ time units, we obtain a maximum fitness of $R_0 = ac/d$. From Eq. (4.3)b one can easily check that $R_0 > 1$ is a minimum requirement for predator survival. The location of the predator nullcline in Eq. (4.5) can now be written as $R = h/(R_0 - 1)$.

The prey nullcline is the parabola depicted in Fig. 4.2. The point where the parabola intersects the horizontal axis is the carrying capacity of the prey ($R = K$). The prey population increases below the parabola (e.g., below its carrying capacity when $N = 0$). The predator nullcline is a vertical line at $\bar{R} = h/(R_0 - 1)$, see Fig. 4.2. If $\bar{R} > K$ the maximum prey density, $R = K$, is insufficient for predator growth, and a prey population at carrying capacity is the only attractor of the system. If $h/(R_0 - 1) < K$ the two nullclines intersect in a non-trivial steady state. However, there are two qualitatively different possibilities. The situation where the predator nullcline intersects at the right side of the top of the parabola (i.e., if $\bar{R} > (K - h)/2$) differs from that where it intersects at the left side of the top. In Fig. 4.2a, where $\bar{R} > (K - h)/2$, there is a negative feedback of the prey on itself, and a zero feedback of the predators on itself, similar to the situation in the Lotka-Volterra model, and hence we expect a stable equilibrium. The heavy line in Fig. 4.2a is a trajectory, representing the invasion of a few predators in a prey population at carrying capacity, which ultimately approaches the steady state (see Fig. 4.2d for a time plot).

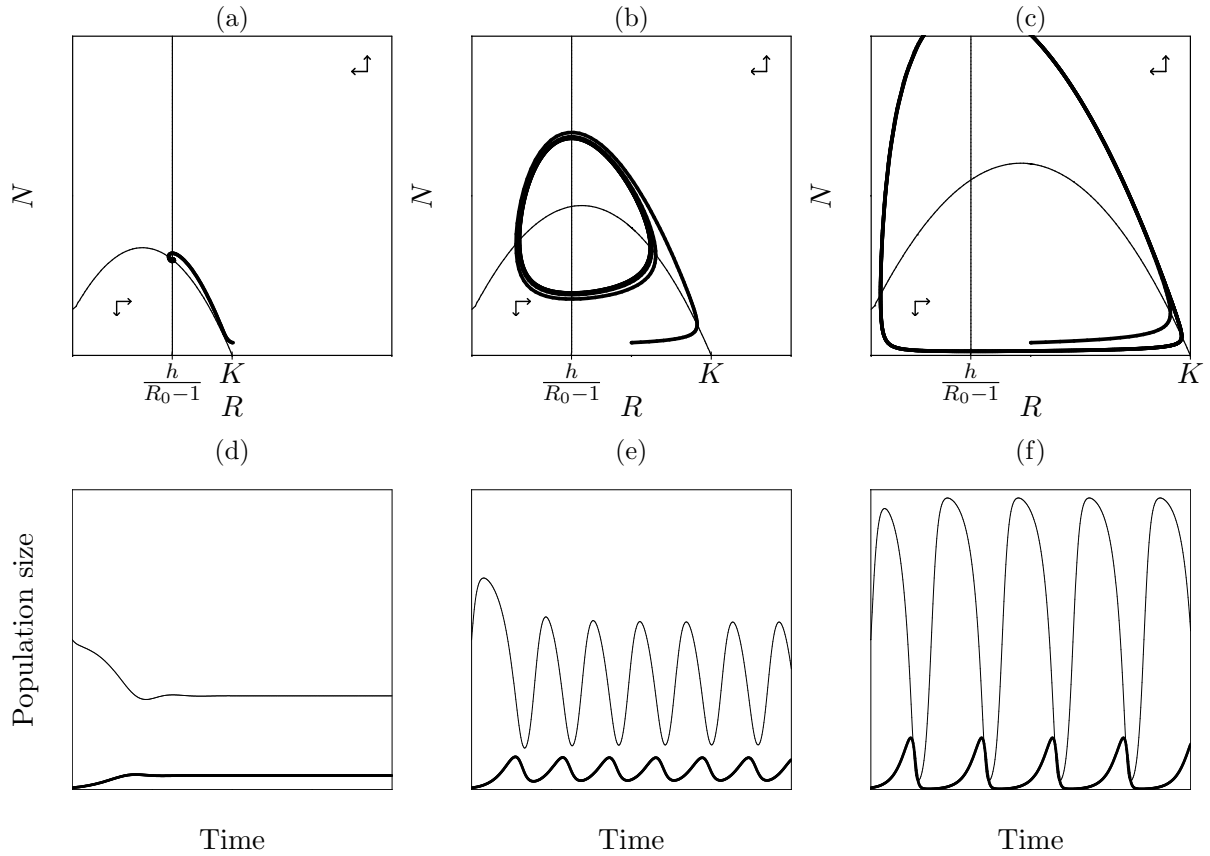


Figure 4.2: The nullclines and trajectories of a predator prey model with a Monod functional response, see Eq. (4.3). The carrying capacity K is indicated. The predator nullcline is the vertical line located at $R = h/(R_0 - 1)$. From left to right the carrying capacity increases. In the two panels on the right the model behavior approaches a stable limit cycle. The heavy line in the time plots is the predator.

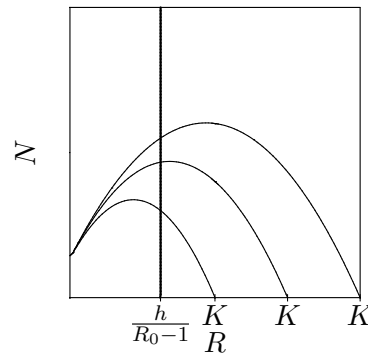


Figure 4.3: The nullclines of a predator prey model with a Monod functional response Eq. (4.3) for three values of the carrying capacity. The picture shows that the steady state remains located at a prey density of $R = h/(R_0 - 1)$, and switches from stable to unstable when the carrying capacity is increased.

In Fig. 4.2b & c, where we have increased the carrying capacity such that $h/(R_0 - 1) < (K - h)/2$, the predator isocline intersects the parabola at the left side of the top. In this situation the prey have a positive feedback on themselves, while the predators still have zero feedback on themselves. Thus the equilibrium is now unstable. The trajectory starting at the same point in phase space as in Fig. 4.2a now approaches a stable limit cycle (see Fig. 4.2e & f for time dynamics). Note that as the intersection point shifts more and more to the left of the equilibrium

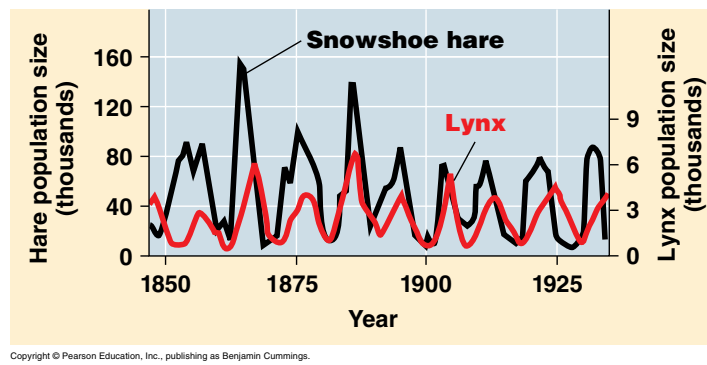


Figure 4.4: Population cycles in the snowshoe hare and lynx. From: Campbell and Reece (2008).

the size of the limitcycle and hence the amplitude of the oscillations increases.

For the parameter condition $h/(R_0 - 1) = (K - h)/2$ the predator isocline intersects the prey parabola exactly at its maximum. At this parameter conditions a so-called Hopf bifurcation occurs. Close to this bifurcation point we know that at one side the steady state is a stable spiral, and at the other side it is an unstable spiral, surrounded by a stable limit cycle (see Fig. 4.2). If one were to increase the parameter K gradually starting from a situation with a stable non-trivial equilibrium one would at some point run into a K value at which the steady state becomes unstable, and the model behavior becomes oscillatory. Because at the bifurcation point one goes from a stable spiral to a small stable limit cycle surrounding the same steady state, this Hopf bifurcation is not a catastrophic bifurcation (see Chapter 7). Instead, the amplitude of the limit cycle gradually increases when one moves away from the Hopf bifurcation. The most famous example of predator-prey oscillations is that of snowshoe hares and lynxes (see Fig. 4.4).

A non-intuitive property of the predator prey models described thus far is that the prey population fails to increase when its food availability is increased. This interesting phenomenon is known as the “Paradox of Enrichment” (Rosenzweig, 1971), and has been studied intensively. Fig. 4.5 shows an example of a bacterial food chain providing strong support for the existence of this paradox in real life (Kaunzinger and Morin, 1998). If the prey *Serratia marcescens* grows on its own, the steady state density increases with nutrient availability. (Fig. 4.5b). However, if the prey *Serratia* grows together with the bacterivorous ciliate *Colpidium striatum*, it is largely the predator density that increases with nutrient availability (Fig. 4.5a).

4.1 Summary

Simple saturation effects complicate the Lotka-Volterra model into a system where the non-trivial steady state need not be stable. Oscillatory behavior therefore seems a very natural behavior of a biological system, and is here brought about by a local positive feedback of the prey onto itself. One can now compute an R_0 of the predator for an infinite prey density. Like in the Lotka Volterra model, feeding the prey is not always increasing the prey density.

There are many textbooks on Theoretical Ecology. The books of Yodzis (1989), Case (2000), and Hastings (1997) give a good background to the material covered here.

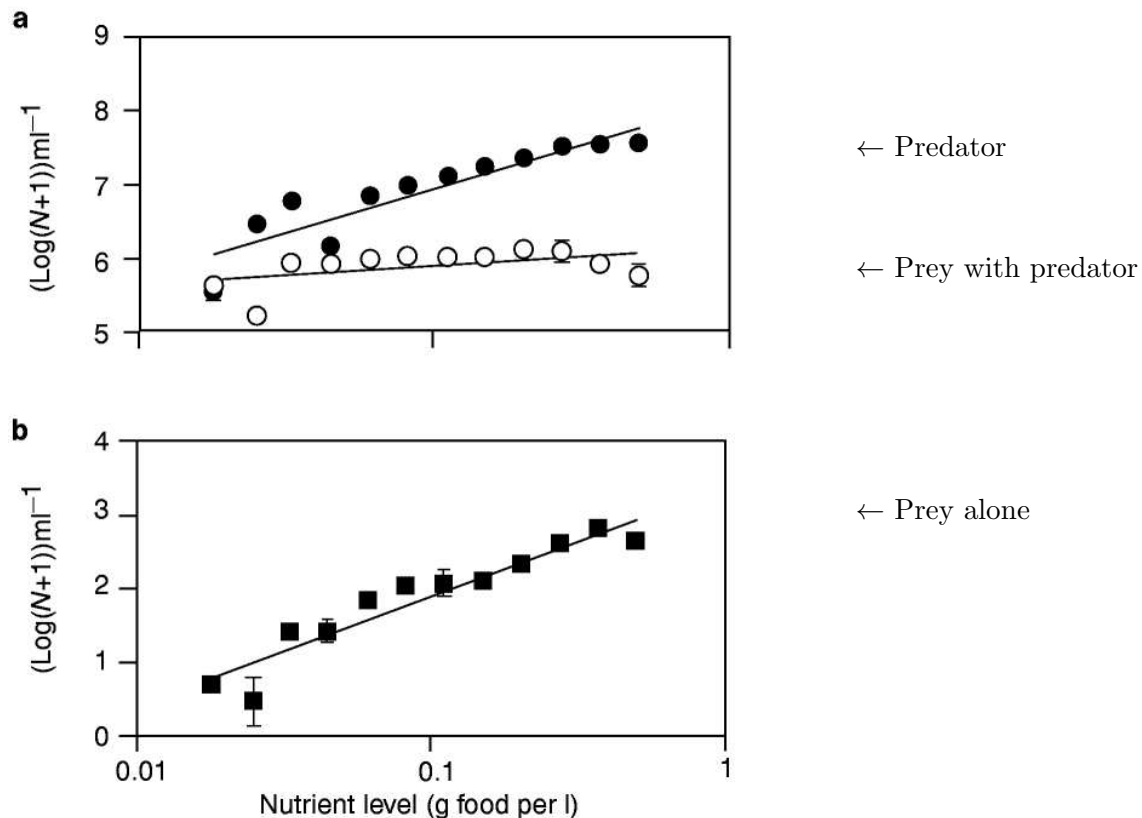


Figure 4.5: The effect of nutrients on the density of the prey *Serratia marcescens* growing on its own (b: filled squares); and on that of the prey *Serratia* (a: open circles) growing with a predator *Colpidium striatum* (a: closed circles). From: Kaunzinger and Morin (1998).

4.2 Exercises

Question 4.0. Read the chapter

- What is a saturation function? Why do we use them for predators?
- What is the meaning of the parameters a and h in $y = ax/(h + x)$?
- What is an oscillation and what causes a system to oscillate?
- What is a Hopf bifurcation?
- Which population increases most in a predator prey model when one feeds the prey?

Question 4.1. Paradox of enrichment

Rosenzweig (1971) analyzed eutrophication of lakes with algae and zooplankton. Water pollution was at that time an even larger problem than it is now. For instance, the large lakes like lake Erie were nearly dead. It was well known at that time that the pollution was largely due to the nutrients (nitrogen and phosphate), but it was unclear how such an enrichment of a lake would drive ecosystems to extinction. As always in biology, one can argue for several factors contributing to the negative effects of pollution:

- eutrophication leads to growth of the algae which leads to high concentrations of oxygen during the day, but to low concentrations at night due to oxygen consumption;
- in addition to the eutrophication, water pollution involves toxic waste that kills fish, zooplankton and/or algae;

- eutrophication leads to a shift from edible green algae to toxic blue algae; etcetera.
- Summarizing, water pollution is a complex mixture of factors that are difficult to disentangle. The contribution of Rosenzweig was to develop a solid expectation for the effects of eutrophication by a modeling study. Mathematical models were used to “think clearly” (May, 2004). Rosenzweig argued that due to saturation effects the algae nullcline should typically have a maximum, and that the zooplankton nullcline should typically be vertical (like the ones in Fig. 4.2). He showed that the stability of the system depends on the location of the zooplankton nullcline, and argued that increasing the carrying capacity of the algae by eutrophication was **expected** to destabilize the system (Rosenzweig, 1971).
- a. Rosenzweig was criticized by McAllister et al. (1972) who was growing salmon in ponds. To increase the salmon production he added nutrients to the ponds to feed the algae. His criticism was that the system remained healthy. The water remained clear, i.e., the density of algae, was not increasing, and the zooplankton density increased markedly (8-fold). Does this criticism invalidate Rosenzweig’s analysis?

Extra questions for interested students:

- b. Large studies comparing various lakes show that the density of the algae is increasing with eutrophication. This increase is much larger however when there are no zooplankton (Persson et al., 2001). Extend Eq. (4.3) with a small density dependent death for the zooplankton, and sketch the nullclines.
- c. What do you now expect for the algal density after eutrophication in the presence and in the absence of zooplankton?

Question 4.2. Enriching oligotrophic lakes

Consider a oligotrophic lake (i.e., a lake with very low concentrations of nutrients). The lake has a low stable density of algae. Invasion of zooplankton is never successful because an algal population at carrying capacity is insufficient for the survival of the zooplankton.

- a. Model this lake with Eq. (4.3) and sketch the nullclines for this situation.
- b. What is the parameter condition for this situation?
- c. What happens if one adds nutrients to such a lake?
- d. Does eutrophication of lakes always lead to a decrease of ecosystem diversity?

Question 4.3. Ditch

A local ditch is polluted with chemicals that are toxic for zooplankton, but have little effect on the algae.

- a. What parameter(s) of Eq. (4.3) change due to this form of water pollution?
- b. Sketch the nullclines with and without pollution in one diagram and predict the effect of pollution on the algae and the zooplankton.

Question 4.4. Bacterial oscillations

The bacterium *Streptococcus pneumonia* can be grown in a chemostat with a constant supply of resources and a constant environment. The bacteria replicate very fast, and –despite the constant environment– their densities oscillate over several orders of magnitude (Cornejo et al., 2009). It can be shown that the bacteria produce a toxin, and that the toxin concentration also oscillates with the same period. Peaks in the toxin concentration more-or-less coincide with peaks in the bacterial population size. It has been established decades ago by Monod that the replication rate of bacteria follows a simple saturation function of the resource densities. A natural model would therefore be

$$\frac{dR}{dt} = s - wR - \frac{aNR}{h + R}, \quad \frac{dN}{dt} = \frac{bNR}{h + R} - wN - xNT \quad \text{and} \quad \frac{dT}{dt} = pN - wT,$$

where w is the “wash out” rate of the chemostat, R is the resource concentration, N is the bacterial density, and T is the concentration of the toxin. Toxin is produced at a rate p per bacterium per hour.

- Why do all populations have the same “death rate” w ?
- What is the interpretation of the xNT term?
- Simplify the model by applying a quasi steady state assumption for the toxin (explained in more detail in the next chapter). For this we set $dT/dt = pN - wT = 0$ which gives us the equation for T $T = (p/w)N$. Next, we substitute this equation for T into the equations dR/dt and dN/dt and obtain a simplified 2-dimensional model. (Note that since we now have an equation for T we no longer use dT/dt).
- Sketch the nullclines of the simplified model (assuming that bacteria survive).
- Do you indeed expect oscillations?
- Consider the model in the absence of the toxin, i.e., set $p = x = 0$, and compare it to the predator-prey model of Eq. (4.3) on Page 26. Do you expect oscillations in predator-prey systems if the resource is maintained by a constant source rather than by logistic growth?
- Computer exercise that you can do after completing Chapter 12. Cornejo et al. (2009) actually used a model with an autocatalytic production of the toxin, and made the production of the toxin proportional to the toxin concentration, i.e., $dT/dt = pNT - wT$. This model does not allow for a quasi steady state assumption for the toxin, and needs to be studied numerically in its full 3-dimensional form. Use GRIND to test whether the bacteria in their model are expected to oscillate. On the website we provide their model and parameters in the files `toxin.grd` and `toxin.txt`. The authors are concerned that the high densities reached by the bacteria in the chemostat are much higher than those in their natural habitat, the human nasopharynx. If you were to do the chemostat experiment, which parameter would you change to have lower bacterial densities? What happens when you change that parameter? What kind of bifurcation is that?

Question 4.5. Pump

A small lake with algae and zooplankton is dirty and green of the high algal densities. Biologists attempt to clean up the water by putting in a water pump that selectively filters the algae out of the water, and leaves the zooplankton in. The pump has been in place for months and the lake has approached a new steady state.

- Extend Eq. (4.3) with this device.
- Sketch the nullclines before and after the installation of the pump in one diagram, and predict the effect of the pump on the algae and the zooplankton.

Question 4.6. Sigmoid functional response

In Fig. 2.1 we plotted growth and death functions to find the steady states by means of a graphical analysis. This technique has also been used to sketch nullclines of predator prey models with a sigmoid functional response (Noy-Meir, 1975). Thus consider Eq. (4.1) and substitute Eq. (4.2)c.

- Write the full model.
- Compute the predator nullcline, and express it in terms of the R_0 of the predator. Is this nullcline very different from that of Eq. (4.3)?
- Now turn to the prey nullcline. One can cancel the $R = 0$ solution from the equation, but it remains complicated to find a simple algebraic solution. The nullcline is therefore constructed graphically. First split dR/dt into its positive and negative terms (for $0 \leq R \leq K$):

$$f(R) = rR(1 - R/K) \quad \text{and} \quad f(R, N) = \frac{aNR^2}{h^2 + R^2}.$$

Now sketch the logistic term as a function of R . In the same graph sketch $\frac{aNR^2}{h^2+R^2}$ for several values of N .

d. Whenever the graphs in your picture intersect, the positive and negative terms in dR/dt are equal such that $dR/dt = 0$. Thus, for the various values of N you can read from the previous picture at what values of R you find the $dR/dt = 0$ nullcline. Sketch the prey nullcline.

e. Sketch the nullclines of this predator prey model with a sigmoid functional response for all qualitatively different situations. Determine the stability of the steady states, and discuss the behavior of the model.

Chapter 5

Competitive exclusion

Competitive exclusion is a very general outcome of mathematical models. It occurs when two species compete for the same resource, e.g., when two viruses compete for the same target cells, or when two ecological species compete for the same niche. In Exercise 8.5 you showed that there can be no two immune response controlling one virus in steady state.

To illustrate the concept in its most general form consider some “resource” R that is used by two populations N_1 and N_2 . For simplicity we scale the maximum resource density to one. An example would be the total amount of nitrogen in a lake, which is either available for algae to grow on, or is unavailable being part of the algal biomass. A simple Lotka-Volterra competition model is:

$$R = 1 - N_1 - N_2, \quad \frac{dN_1}{dt} = N_1(b_1R - d_1), \quad \frac{dN_2}{dt} = N_2(b_2R - d_2), \quad (5.1)$$

where R is the amount of nitrogen available for growth of the algae. The two populations have an R_0 of b_1/d_1 and b_2/d_2 , respectively. Substitution of $R = 1 - N_1 - N_2$ into dN_1/dt yields

$$\frac{dN_1}{dt} = N_1(b_1(1 - N_1 - N_2) - d_1), \quad (5.2)$$

which has nullclines $N_1 = 0$ and

$$N_2 = 1 - \frac{1}{R_{0_1}} - N_1. \quad (5.3)$$

Similarly the $dN_2/dt = 0$ nullcline is found by substituting the amount of resource, R , into $dN_2/dt = 0$ and has nullclines $N_2 = 0$ and

$$N_2 = 1 - \frac{1}{R_{0_2}} - N_1. \quad (5.4)$$

Thus, plotting N_2 as a function of N_1 the two nullclines run parallel to each other with slope -1 . The fact that they are parallel means that there is no steady state in which the two populations coexist. The intersects with the vertical N_2 axis are located at $N_2 = 1 - 1/R_0$. Thus the species with the largest fitness, R_0 , has the “highest” nullcline, and wins the competition (Fig. 5.1).

Competitive exclusion is a paradoxical result because many biological systems are characterized by the co-existence of many different species that seem to survive on very few resources. Examples are the incredible number of different bacterial species living in the gut, the number of algae species living in fresh or salt water, and the millions of lymphocyte clones comprising the adaptive immune system. A lot of research effort is devoted to explaining how spatial heterogeneity, tradeoffs and division of labor may help explain this observed diversity.

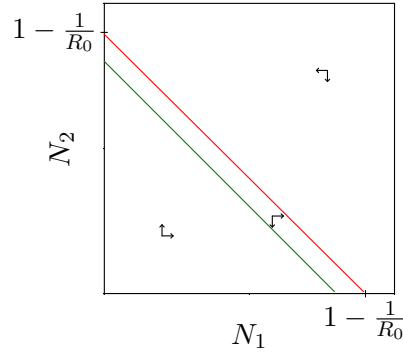


Figure 5.1: The parallel nullclines of Eq. (5.1).

5.1 Exercises

Question 5.0. Read the chapter

- Give an intuitive definition of competitive exclusion.

Question 5.1. Saturated proliferation

Consider two immune responses to the same pathogen, and assume that the immune responses reduce the pathogen concentration to

$$A = 1 - kE_1 - kE_2 ,$$

where A reflects the amount of antigen present. The maximum proliferation rate is a saturation function (i.e., a Hill function) of the pathogen concentration. Thus, let the immune responses be described by

$$\frac{dE_1}{dt} = \frac{pE_1 A}{h_1 + A} - dE_1 \quad \text{and} \quad \frac{dE_2}{dt} = \frac{pE_2 A}{h_2 + A} - dE_2 ,$$

where $h_2 > h_1$ means that the second response requires a higher pathogen concentration for obtaining the same proliferation rate. Because the proliferation is saturated it seems that exclusion would be less likely.

- Sketch for a fixed antigen concentration the *per capita* proliferation rates as a function of the concentration of antigen.
- Draw the nullclines in a phase space of E_1 and E_2 .
- Can the two responses coexist?
- What is the difference with Fig. 5.1?

Question 5.2. Competitive proliferation

Consider two immune responses to the same pathogen, and assume that the immune responses reduce the pathogen concentration to

$$A = 1 - kE_1 - kE_2$$

and let the immune responses be described by

$$\frac{dE_1}{dt} = \frac{pE_1 A}{1 + c_1 E_1} - dE_1 \quad \text{and} \quad \frac{dE_2}{dt} = \frac{pE_2 A}{1 + c_2 E_2} - dE_2 ,$$

where $c_2 > c_1$ means that the second response has a stronger intra-specific competition.

- Sketch for a fixed antigen concentration the *per capita* proliferation rates as a function of

the clone size.

- b. Draw the nullclines in a phase space of E_1 and E_2 .
- c. Can the two responses coexist?
- d. What is the difference with Fig. 5.1?

Question 5.3. Virus competition experiments (Extra exercise for cool students)

To determine the relative fitness of two variants of a virus one typically grows them together in conditions under which they grow exponentially. Thus, consider two variants of a virus that grow exponentially according to

$$\frac{dV_1}{dt} = rV_1 \quad \text{and} \quad \frac{dV_2}{dt} = r(1+s)V_2 ,$$

where s is the conventional selection coefficient. One way to represent the data is to plot how the fraction $f \equiv V_2/(V_1+V_2)$ evolves in time. To compute how the fraction $f(t)$ changes one needs to employ the quotient rule of differentiation: $[f(x)/g(x)]' = (f(x)'g(x) - f(x)g(x)')/g(x)^2$. Thus, using $'$ to denote the time derivative, one obtains for df/dt :

$$\begin{aligned} \frac{df}{dt} &= \frac{V_2'(V_1+V_2) - (V_1'+V_2')V_2}{(V_1+V_2)^2} , \\ &= \frac{V_2'V_1 - V_1'V_2}{(V_1+V_2)^2} , \\ &= \frac{r(1+s)V_2V_1 - rV_1V_2}{(V_1+V_2)^2} , \\ &= r(1+s)(1-f)f - rf(1-f) , \\ &= rsf(1-f) , \end{aligned}$$

which is the logistic equation with growth rate rs and steady states $f = 0$ and $f = 1$. Thus one expects a sigmoidal replacement curve of the two variants.

- a. Now write a differential equation of the ratio $\rho = V_2/V_1$ of the two populations.
- b. Virologists plot the logarithm of the ratio in time to determine the relative fitness (Holland et al., 1991). What is the slope of $\ln[\rho]$ plotted in time?

Chapter 6

Alternative Model Formalisms

In the previous chapters we discussed the use of ordinary differential equations (ODEs) to model biological processes. Inherent to ODE models is that the variables take on continuous values, that is they can not only take on integer values 0, 1, 2, 3 . . . 1000, .., n but also 0.1, 1.3, 2.74, 3000.2 etc. Such continuous values are not problematic if they describe molecules, cells or individuals present at high numbers since for example 1000.3 is a reasonably good approximation for 1000 individuals. However, if entities are present at low numbers continuous values become problematic since 0.03 molecules or 0.2 rabbits are biologically non-sensical and in effect imply that the chemical substance is absent or the rabbit population is extinct. In these types of situations different model formalisms in which individual entities are represented by discrete values are more appropriate.

In this chapter we will discuss two types of such alternative model formalisms namely Cellular Automata (CAs) and Individual Based Models (IBMs), focusing on their use for modeling entities in a discrete rather than continuous manner. In the chapter on spatial patterning, we will come back to these alternative model formalisms, shifting focus now to their application for the study of pattern forming processes.

6.1 Cellular Automata

In this section we give a simplified introduction to Cellular Automata (CAs). CAs are a modeling formalism that allows one to study processes with discrete entities (molecules, organisms) within a spatial setting. Both time and space are discrete in this model formalism. With regard to space, a CA consists of a regular grid of points. Each grid point has a **state**, and a local **neighborhood** of nearby grid points. The future state of a point depends on its own state and the states of neighbouring points (see Fig. 6.3). The simplest CA has only two possible states for each grid point, 0 (white) and 1 (black). This can mean that it's dead or alive, or empty versus occupied by an organism or molecule, respectively. In more complex CAs, a larger number of states is used.

Time in a CA model consists of discrete steps. Each time step, a new state is determined for each grid point, based on its own previous state and on the state of neighboring gridpoints. The update rules determining the next state of a grid point are often given as a table (see Fig. 6.3).

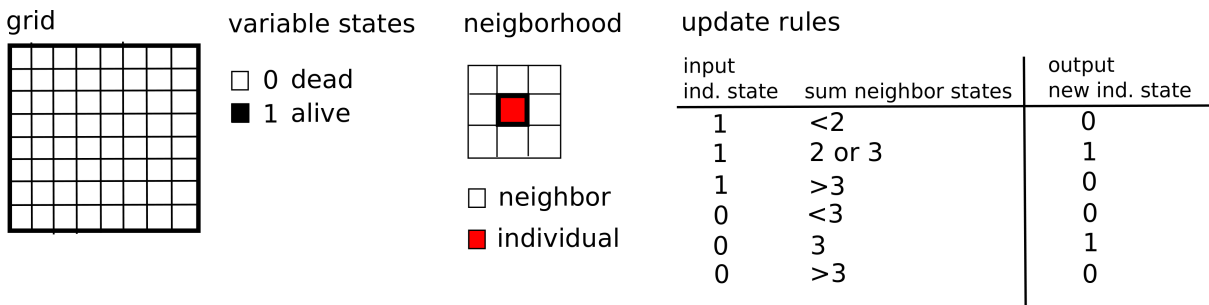


Figure 6.1: Overview of the ingredients of a CA model. The model contains a grid of discrete points that can be in different states (left). Each point has a local neighborhood consisting of itself and neighboring points, that will determine the state of the point at the next time step (middle). A set of update rules takes the state of the point itself and that of its neighbours, and gives the state of the point at the next time step (right).

As an example let us consider modeling a predator prey system in a CA. Each CA lattice point can have one of three states 0: empty, 1: prey, 2: predator. Updating occurs according to the following rules:

1. if the state is 0 (empty)
 - a. if there are one or more prey in neighboring points and $p < \alpha$: next state is 1 (reproduction prey)
 - b. else next state is 0 (nothing happens)
2. if the state is 1 (prey)
 - a. if one or more neighboring states are 2 and $p < \gamma$: next state is 2 (prey is eaten and hence disappears, and the predator reproduces)
 - b. else if $p < \beta$: next state is 0 (standard death of the prey)
 - c. else next state is 1 (nothing happens)
3. if the state is 2 (predator)
 - a. if $p < \delta$: next state is 0 (standard death of the predator)
 - b. else next state is 2 (nothing happens)

where p denotes the chance for a certain event to happen, and α , β , γ and δ are the probabilities for the different events. In the exercises we will study the behavior generated by this type of model and to what extent it is similar to or differs from the Lotka-Volterra differential equations model we studied earlier.

In the first example CA shown in Fig. 6.3 the rules are **deterministic**, that is if the state of the grid point and its neighbors are X then the next state is always Y . In the second example CA, the rules are **probabilistic**, that is if the state of the grid point and its neighbors are X then there is a chance p that Y occurs, and else Z occurs.

6.2 Individual Based Models

In this section we give a simplified introduction to Individual Based Models. An alternative term for Individual Based Models is Agent Based Models. IBMs share certain characteristics with CA models. Like CAs, IBMs describe variables in a discrete manner. In addition, again similar to CAs, IBMs explicitly model a one, two or three dimensional spatial setting inhabited by the variables. Finally, once more similar to CAs, IBMs are governed by a set of rules that

determine the dynamics of populations of entities.

However, there are also some differences between IBMs and CAs. An important difference concerns how space is incorporated in these different models. As we saw earlier, in CAs space is modeled as a lattice consisting of discrete sites that can be either empty or contain one or a few entities. In contrast, in IBMs space can be continuous and there is often no maximum number of entities per surface unit imposed.

Furthermore, in CAs the rules are applied on a per lattice site basis, while in IBMs the rules are applied on a per individual basis. Let us explain this in more detail for an example case: determining whether reproduction will take place. In the case of a CA, we start out by determining for each lattice site whether it is empty, as it is only in empty sites that newborn individuals can be placed. Next, we count the number of non-empty neighboring lattice sites, thus assuming that the number of individuals next to the empty lattice site influences the chances that a local reproduction event will occur. The discrete lattice space and the need for empty space to create new entities necessarily leads to an implicit competition for space between entities in CA models. As opposed to this, in an IBM we start out by determining for each individual its current chances of reproduction. If reproduction occurs we next determine where this newborn individual will be placed. In the presence of a continuous space, and in the absence of maximum densities, no implicit competition for space will occur.

Like CAs Individual Based Models can be used to test the effect of discrete population numbers on population dynamics, and it is for this purpose that we discuss them here as you will see in the exercises at the end of this chapter. However, IBMs are useful for the study of many more phenomena in biology. For fun, for illustration purposes, and to give an explicit example of the building blocks and workings of an IBM model we here consider a model for bird flock dynamics modeled by (Hemelrijk and Hildenbrandt, 2011).

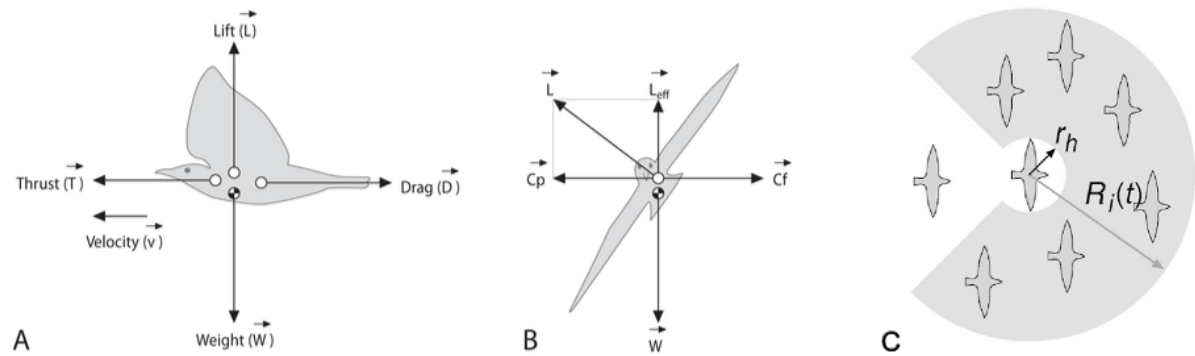


Figure 6.2: Building blocks of the sterling flocking model. **A** Forces involved in simulating aerodynamically realistic flight. **B** As the bird reorients, for example during banking (see text) the forces are also reoriented. **C** Birds perceive the neighbors in front and to their sides but not behind them. Based on the perceived neighbors direction and speed of movement and orientation are adjusted. Figure adjusted from (Hemelrijk and Hildenbrandt, 2011)

The model of sterling flocking dynamics consists of a limited three dimensional space in which a number of *in silico* sterlings are flying around. Each individual bird has the following properties:

1. current location
2. speed and direction of movement
3. set of visible neighbours

In addition, realistic aerodynamic properties of bird flight such as lift, drag and banking are

included in the model. For each individual simulated sterling the following rules are applied:

1. if neighbors are too close, move further away (repulsion)
2. if neighbors are too far, move closer (attraction)
3. align your direction towards direction of neighbors (alignment)

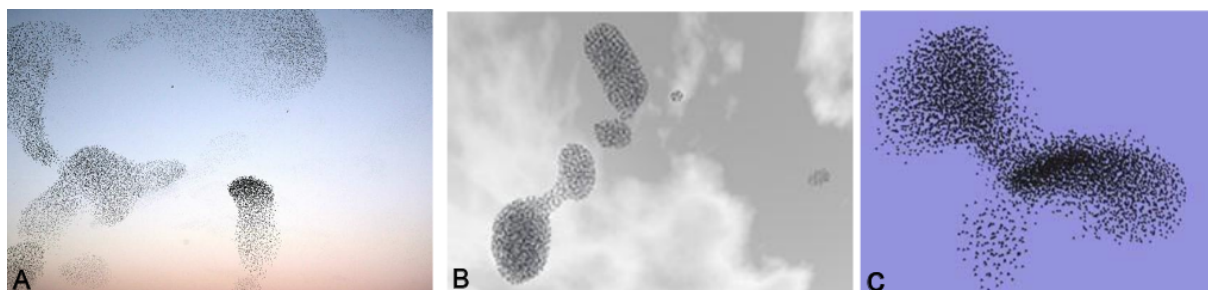


Figure 6.3: Comparison of actual (**A**) and simulated (**B,C**) sterling flocking dynamics. Figure **A** was taken from Ballerini et al, PNAS, 2008. Figures **B**, **C** were taken from the website of Prof. Hemelrijk and Dr. Hemelbrandt, respectively

Moving further further away or closer by can be achieved by adjusting speed, and direction of movement. As one might expect, these rules cause the *in silico* birds to maintain an approximately constant distance, resulting in an alignment of their flight direction. However, these rules also cause the abrupt turnings of the entire flock that give rise to the spectacular shapes and moves typical of sterling flocks, something that can not easily be deduced from the rules. Indeed, it turns out that this dynamical behavior is the result of the movement rules combined with the incorporation of realistic aerodynamic flight behaviour, so-called banking: when birds make a turn to the left or right they also rotate in the third dimension, positioning their inside wing lower than the outside wing (Hemelrijk and Hildenbrandt, 2011). For movies of the simulated flock dynamics go here: <http://beheco.oxfordjournals.org/content/suppl/2010/08/19/arq149.DC2>

This model is an illustration of how simple rules applied to simple and identical individuals can give rise to complex dynamics and emergent patterns. Indeed, CAs and IBMs play an important role in understanding complex processes with emergent properties, not only in biology but also in fields such as economy and social sciences.

6.3 Summary

Cellular Automata and Individual Based Models are alternative model formalisms. While models based on ordinary differential equations describe variables as having continuous values, CAs and IBMs allow us to describe entities such as molecules, cells or individuals using discrete values. In situations in which entities are present at low numbers models allowing for discrete values are more appropriate. Apart from their usefulness for investigating the effect of discrete valued variables, CAs and IBMs are used for a great many more purposes. We will come back to these modeling formalisms when discussing spatial pattern formation.

6.4 Exercises

Question 6.0. Exponential Population Growth

Assume we wish to model exponential growth (i.e. absence of density dependence). Of the two model formalisms discussed in this chapter, Cellular Automata and Individual Based Models, which do you think is more suited for modeling exponential growth and why? Which of the two models have an inherent carrying capacity and what determines this carrying capacity?

Question 6.1. Two populations

Assume there are two populations, living, reproducing and dying in the same environment. They do not eat the same food, they do not eat or kill each other. We model these populations in a CA model.

- Are these two populations truly independent?
- What do you expect if at the start of the simulation one population is 10 times bigger than the other population? (Assume the individuals of the two populations are randomly distributed over the simulation grid)

Question 6.2. Rabbits and Grass

Study an IBM type model containing grass and rabbits written in NetLogo. For this model we can use the NetLogo program as installed here on the local computers. To use NetLogo go to: **All Programs** → **Standard Applications** → **Computing Sciences** → **NetLogo4.0.4**

Then, to select the right model in NetLogo go to: **File** → **Models Library** → **Biology** → **Rabbits Grass Weeds**

We will run the model without Weeds.

Grass grows at random locations at a constant rate. (Note that this implies that grass seeds spread by the wind and hence new grass not necessarily grows next to older grass. In addition it also implies that an excess of seeds are produced such that the amount of present grass is not determining the amount of new grass that can grow). However grass can only grow at empty spots. Note how this assumption is a bit more CA like: available space is a limiting factor for grass growth. Rabbits move around randomly, reproduce and when encountering grass eat it. Grass dies due to being eaten by rabbits. To reproduce rabbits need to have eaten enough grass, if in contrast they have not eaten sufficient grass they will die (rabbits have an internal state counting the amount of grass they have eaten). Run the model and play around with the parameters

- Is it easy to obtain stable coexistence between rabbits and grass?
- Which ODE equations would be a good description of this computer model? Analyse the behavior of this system of equations.
- Which long term behaviour do you expect for the ODE model? And for the IBM computer model?
- Which of the two do you consider to be more realistic?

Question 6.3. Wolves, Sheep and Grass

Let us study another IBM type model written in NetLogo containing wolves, sheep and grass. This model can be found in NetLogo under:

File → **Models Library** → **Biology** → **WolfSheepPredation**.

The model can be run with and without grass. We start studying the model without grass. Wolves and sheep move around randomly. Sheep get born at a constant rate, and die by getting eaten by wolves. Wolves eat sheep when encountering them, thus adding to their internal energy level. If their energy level is sufficiently high they can reproduce, if is too low they die.

- a. Run the model without grass. Is it possible to get coexistence between wolves and sheep?
- b. Write ODE equations that would give a good description of this computer model. Analyse the behavior of this system of equations.
- c. What is the difference between ODE and computer model? Can you now explain the behavior of the computer model?
- d. Now we study the model with grass. In this case, the sheep eat grass when encountering it, increasing their internal energy level. As for the wolves, sheep need a certain level of energy to reproduce, and die below a certain energy threshold or due to predation. Grass dies due to predation by sheep and can only regrow after a certain amount of time. Regrowth is limited to empty spots. Thus, with regards to grass the model is more CA like.

Run the model with grass. Is it possible to get coexistence between wolves and sheep?

- e. How would you write the ODE equation for grass (Hint: what does limited space in fact mean for the growth of grass)? How would you rewrite the ODE equation for the sheep?
- f. If not explicitly modeling grass, how would you write the ODE equation for sheep and how does this explain the altered model behavior?

Chapter 7

Gene regulation

A central dogma in biology is “DNA makes RNA and RNA makes protein”. Protein synthesis is a pathway depending on DNA transcription in the nucleus, producing mRNA molecules, and on translation of mRNA at ribosomes, producing proteins. Species like *Homo sapiens* have tens of thousands of genes that interact in complicated networks. Understanding the workings of gene regulation is fundamental for developmental biology because cells differentiate into various phenotypes by changing the expression of their genes (and not by changing genotype). Genes regulate each other by coding for transcription factors that can bind regions of the DNA (like operons) that regulate whole sets of other genes. Nowadays one can study the expression of all genes of specific tissues under particular circumstances by RNA-chips that allow one to measure all mRNA levels in a single experiment. Another exciting recent development is to experimentally record the expression of a single gene, and fit these data to mathematical models (Golding et al., 2005; Golding and Cox, 2006; Raj et al., 2006). This recent work has demonstrated that transcription occurs in stochastic bursts delivering one or a few mRNA molecules.

7.1 Models

One can write simple models for the intracellular concentration of the mRNA that is produced by transcribing DNA, and the corresponding protein concentration resulting from the translation of the mRNA:

$$\frac{dM}{dt} = c - dM \quad \text{and} \quad \frac{dP}{dt} = lM - \delta P, \quad (7.1)$$

where c is the transcription rate, in molecules per hour, and l is the translation rate (per hour). The d and δ parameters are the decay rates, or turnover rates, of mRNA and protein, respectively. The mRNA equation is an example of a non-replicating population that we have studied in earlier chapters, and has the stable steady state $\bar{M} = c/d$ molecules. Solving the $dP/dt = 0$ nullcline yields the straight line $M = (\delta/l)P$ (see Fig. 7.1a). The nullclines intersect in one unique steady state, which can be solved from $c/d = (\delta/l)P$, giving $(\bar{P}, \bar{M}) = (c/d\delta, c/d)$ molecules. The vector field around the steady state shows that the point is stable. The behavior of the model will always be an approach to this unique stable steady state.

Transcription factors can inhibit the transcription of their own mRNA. Let us model this by a

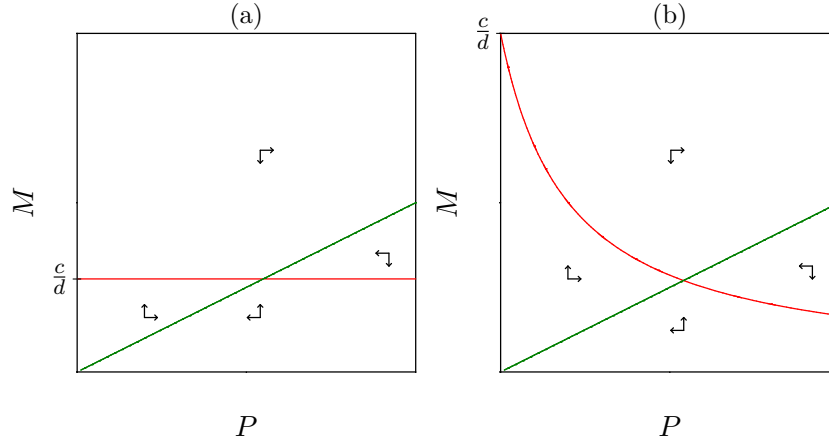


Figure 7.1: The nullclines of Eq. (7.1) in Panel (a) and Eq. (7.2) in Panel (b). In both cases there is only one possible phase space with one stable steady state.

declining Hill function $1/(1+x)$ (see Chapter ??):

$$\frac{dM}{dt} = \frac{c}{1+P/h} - dM \quad \text{and} \quad \frac{dP}{dt} = lM - \delta P, \quad (7.2)$$

where c now is the maximum transcription rate (molecules per hour), and l remains the translation rate. When $P = 0$ the gene is “on”, and the transcription rate is maximal (c). When $P \rightarrow \infty$ the gene is “off” and the transcription rate approaches zero. When $P = h$ molecules, the actual transcription rate is $c/2$ molecules per hour, which is half-maximal. To analyze this slightly more complicated model we again draw nullclines. Setting $dM/dt = 0$ the simplest function to obtain is $M = \frac{c/d}{1+P/h}$, which is an inverse Hill function with maximum c/d when $P = 0$ (see Fig. 7.1b). Solving $dP/dt = 0$ for M yields the same straight line $M = (\delta/l)P$ as above (see Fig. 7.1b). The nullclines again intersect in only one steady state. The vector field around the steady state shows that the point remains stable in the presence of this negative feedback on the transcription rate.

7.2 Separation of time scales

One often simplifies models by distinguishing slow and rapid time scales. This is a very important technique. For fast variables one can do a “quasi steady state” (QSS) approximation. This means that the QSS variable is in steady state with the rest of the system, i.e., with the slow part of the system. When the slow part changes the QSS variable walks along. By a QSS approximation one basically replaces a differential equation with an algebraic equation. A simple example of a QSS approximation would be the position of a fast fighter jet that is following a slow Boeing 747. If the pilot of the fighter jet has the order to tail the Boeing, one can describe the location of the fighter jet as a short distance behind the Boeing. Whenever the Boeing changes course, the rapid fighter jet will immediately follow. If the fighter jet were a slow plane, this would not be a valid assumption. This story was originally told by Lee Segel from Israel. He was the “father of the quasi steady state assumption” (Segel, 1988; Borghans et al., 1996), and a great story teller.

Conversely, variables that are much slower than the other variables of a model can be approximated by constants that do not change at all on the time scale of interest. One example will

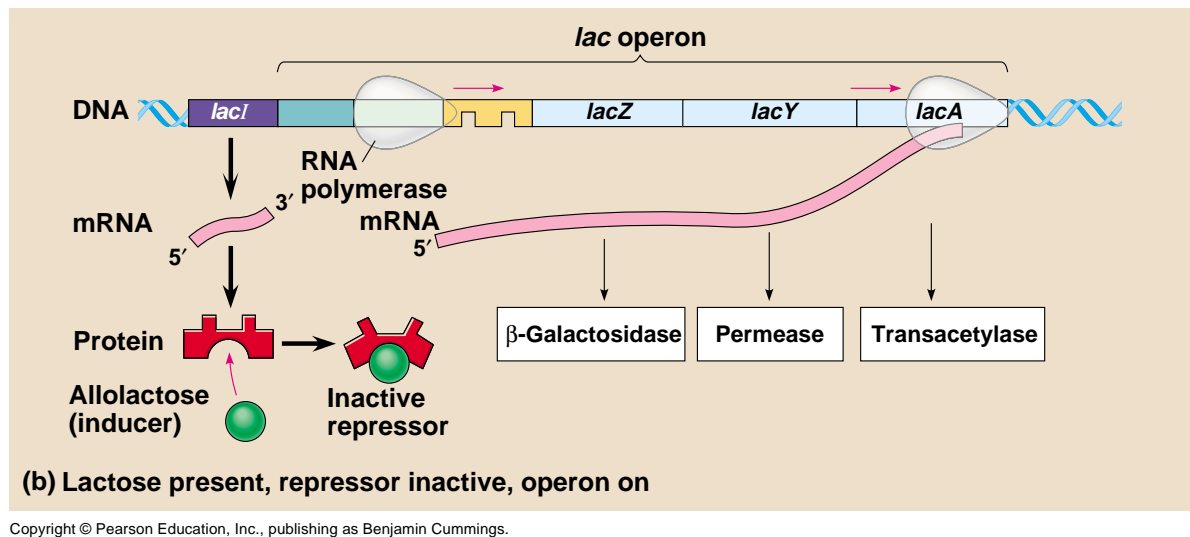


Figure 7.2: The *lac* operon: regulated synthesis of inducible enzymes. From: Campbell and Reece (2008).

be the assumption that the immune response is not changing during anti-retroviral therapy in Chapter 8. In this course we will use both techniques in order to obtain natural simplifications of our models.

For instance, assuming that proteins are degraded rapidly, i.e., assuming that the turnover of proteins is much faster than the turnover of mRNA molecules, the protein concentration will typically be close to its steady state value given the concentration of its mRNA. The quasi steady state of Eq. (7.2)b is obtained by solving P from $dP/dt = 0$, giving $P = (l/\delta)M$. In this simple case, the QSS assumption boils down to assuming that the protein concentration is proportional to the concentration of its mRNA (Golding et al., 2005). Substituting $P = (l/\delta)M$ into dM/dt yields the simplified quasi steady state model

$$\frac{dM}{dt} = \frac{c}{1 + (l/\delta)M/h} - dM = \frac{c}{1 + M/h'} - dM, \quad (7.3)$$

where $h' = h\delta/l$ is the new saturation constant. If this quasi steady state is a fair assumption, the behavior of the simplified model should be very similar to that of the full model.

7.3 Lac-operon

Bacteria can use several external substrates for cellular growth and switch the corresponding intracellular pathways on and off depending on the available resources. One of the possible substrates is the sugar lactose, and the regulation of the “Lac-operon” was one of the first circuits of gene regulation that was revealed (Jacob and Monod, 1961). Regulation of the Lac-operon involves a positive feedback because the sugar allolactose, A , activates gene expression by deactivating a repressive transcription factor, R . Allolactose is an isomer of lactose that is formed in small amounts from lactose. The intracellular lactose concentration is determined by an enzyme permease that is produced by this gene complex. The gene complex also codes for the enzyme β -galactosidase that hydrolyzes the disaccharide allolactose into glucose and galactose.

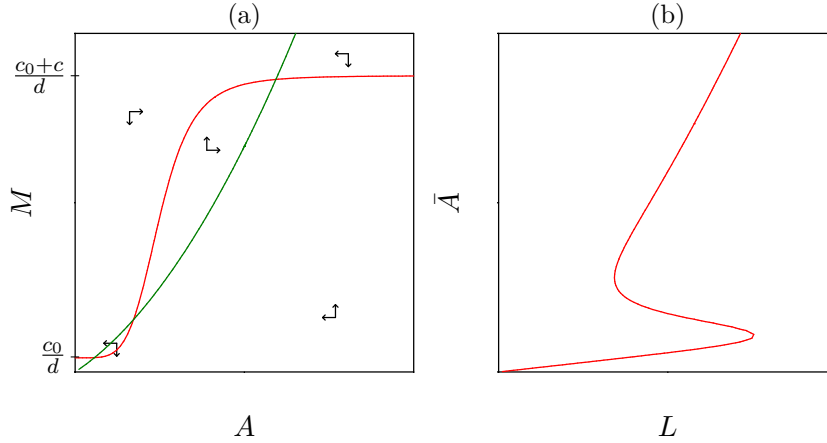


Figure 7.3: Nullclines of Eq. (7.4). Parameters: $L = c = d = 1$, $c_0 = 0.05$, $v = 0.25$, $n = 5$, and $\delta = 0.2$.

Making the same quasi steady state assumption as we did above in Eq. (7.3), i.e., assuming that these protein concentrations of permease and β -galactosidase remain proportional to the concentration of their mRNA, this can be summarized into the following model:

$$\begin{aligned}
 R &= \frac{1}{1 + A^n}, \\
 \frac{dM}{dt} &= c_0 + c(1 - R) - dM = c_0 + \frac{cA^n}{1 + A^n} - dM, \\
 \frac{dA}{dt} &= ML - \delta A - vMA,
 \end{aligned} \tag{7.4}$$

where $0 < R \leq 1$ is a sigmoid Hill function representing the “concentration” of active repressor. Setting $n = 5$ one obtains that the operon tends to switch between on and off. M is the mRNA concentration, L is a parameter representing the extracellular lactose concentration, and A is allolactose. The allolactose concentration increases when the gene complex is active, i.e., when permease is present, and extracellular lactose L is transported from the extracellular to the intracellular environment. This is formulated as a simple “mass action term” of the external lactose concentration, L , and the permease M . Allolactose is hydrolyzed according to another mass action term depending on the enzyme β -galactosidase (the concentration of which is again assumed to be proportional to the amount of mRNA M). Overall there is a positive feedback because increasing M increases A , which increases M (Griffith, 1968).

To analyze the model we draw nullclines. Setting $dM/dt = 0$ yields

$$M = \frac{c_0}{d} + \frac{(c/d)A^n}{1 + A^n}, \tag{7.5}$$

which is a sigmoid Hill function with an offset $M = c_0/d$ when $A = 0$ (see Fig. 7.3a). One obtains the vector field by noting that $dM/dt > 0$ when A is large and M is small. The $dA/dt = 0$ nullcline is solved from

$$M(L - vA) = \delta A \quad \text{or} \quad M = \frac{\delta A}{L - vA}, \tag{7.6}$$

which is of the form $y = ax/(1 - bx)$. The nullcline goes through the origin, and has a horizontal asymptote $M = -\delta/v$, and a vertical asymptote $A = L/v$. Around the origin $M \simeq (\delta/L)A$, which is a straight line with slope δ/L . Increasing the external lactose concentration, L , therefore shifts the vertical asymptote to the right and decreases the slope in the origin. Fig. 7.3a depicts the nullclines for the situation where the hyperbolic $dA/dt = 0$ nullclines intersects the sigmoid

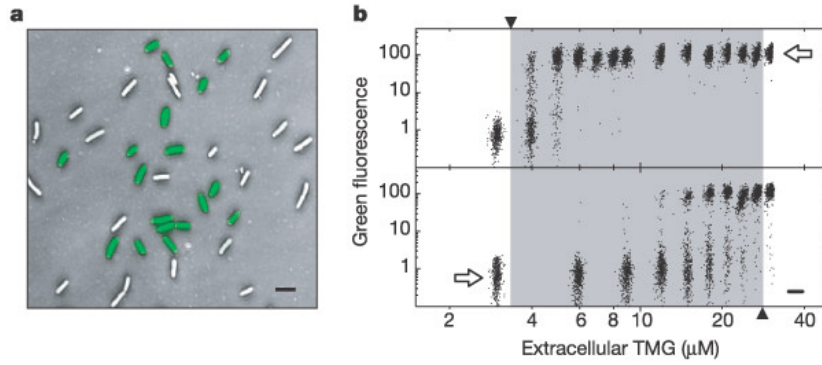


Figure 7.4: Figure 2 in Ozbudak et al. (2004): Hysteresis and bistability in single cells. **a**, Overlaid green fluorescence and inverted phase-contrast images of cells that are initially uninduced for lac expression, then grown for 20 h in $18\mu\text{M}$ TMG (which is an analogue of lactose). The cell population shows a bimodal distribution of lac expression levels, with induced cells having over one hundred times the green fluorescence of uninduced cells. Scale bar, $2\mu\text{m}$. **b**, Behavior of a series of cell populations, each initially uninduced (lower panel) or fully induced (upper panel) for lac expression, then grown in media containing various amounts of TMG. Scatter plots show $\log[\text{green fluorescence}]$ versus $\log[\text{red fluorescence}]$ for about 1,000 cells in each population. Each scatter plot is centered at a position that indicates the underlying TMG concentration. White arrows indicate the initial states of the cell populations in each panel. The TMG concentration must increase above $30\mu\text{M}$ to turn on initially uninduced cells (up arrow), whereas it must decrease below $3\mu\text{M}$ to turn off initially induced cells (down arrow). The gray region shows the range of TMG concentrations over which the system is hysteretic.

$dM/dt = 0$ nullcline three times. For the vector field one can see that when the concentration of mRNA is high, and that of allolactose A is low, the allolactose concentration increases ($dA/dt > 0$). The vector field shows that the steady state in the middle is a saddle point, and that the two at the boundaries are stable nodes.

For one specific concentration of lactose, L , the operon can therefore be “on” or “off”, i.e., in one of the two stable steady states. The effect of the lactose concentration can better be visualized by making a quasi steady state assumption for the mRNA equation, i.e., by assuming that the transportation and degradation of allolactose has a slow time scale. Substituting Eq. (7.5) into dA/dt in Eq. (7.4) yields the one-dimensional quasi steady model

$$\frac{dA}{dt} = -\delta A + (L - vA) \left(\frac{c_0}{d} + \frac{(c/d)A^n}{1 + A^n} \right). \quad (7.7)$$

Since the model has only one variable, the $dA/dt = 0$ nullcline gives the \bar{A} equilibrium, which can now be sketched as a function of one of the parameters, e.g., the external lactose concentration L . This can no longer be done by hand, but using the computer program GRIND (see Chapter 12) the \bar{A} equilibrium is depicted as a function of the lactose concentration in Fig. 7.3b. The curve in Fig. 7.3b is basically a bifurcation diagram: it depicts the steady state allolactose concentration, \bar{A} , as a function of a parameter, L , the extracellular lactose concentration. The upper and lower branches are stable and the branch in the middle is unstable. Bacteria growing in an environment that is extremely poor in lactose are in a state with low intracellular levels of allolactose, because the Lac-operon is off. Bacteria growing in an environment rich in lactose have an active Lac-operon and high intracellular allolactose concentrations. Bacteria growing in an environment with an intermediate lactose concentration can be in either of these two states however (Novick and Weiner, 1957; Ozbudak et al., 2004; Van Hoek and Hogeweg, 2006); see Fig. 7.4. At these concentrations the bacteria have “alternative stable states” (May, 1977; Scheffer et al., 2001; Ozbudak et al., 2004), and it depends on the history of the bacteria in which state

they will be. Indeed, the curve in Fig. 7.3b implies a form of “hysteresis”. If one decreases the extracellular lactose concentration from very high to very low, one follows the upper branch. At a critical lactose concentration, L_1 , the bacteria suddenly switch to the state with a closed operon. On the other hand, if one increases the lactose concentration from low to high, one switches from bacteria with a repressed operon to an expressed operon at lactose concentration L_2 . Fig. 7.3b shows that $L_2 > L_1$. Thus, the system has a form of memory, and tends to remain in the state where it was. This is called hysteresis.

The two transition points are catastrophic bifurcations. The system has a discontinuity and jumps to an alternative attractor. The bifurcations in Fig. 7.3b are called “saddle-node” bifurcations because a saddle point and a stable node merge and annihilate each other.

7.4 Gene networks

Models of gene regulation have recently attracted much more attention because one can nowadays read the mRNA expression of thousands of genes in a single RNA-chip experiment. To understand the properties of complicated networks of genes influencing each other, people are studying models composed of many equations, one for each of the genes in the network. To write a simple phenomenological (i.e., non-mechanistic) ODE for a gene producing protein “one”, P_1 , that is down-regulating its own transcription, but is up-regulated by another gene product, P_2 , one could write something like

$$\frac{dP_1}{dt} = c \frac{h_1}{h_1 + P_1} \frac{P_2}{h_2 + P_2} - dP_1, \quad (7.8)$$

where one uses simple Hill functions for the stimulatory and inhibitory effects the proteins P_1 and P_2 have on the production of protein one. Instead of using Hill functions one can also use “logical” functions switching genes “on” or “off” depending on their input signals (Alon, 2007). Models like this can obviously be extended to study the influence of many different proteins on the transcription of one of them. Writing ODEs or logical functions for all of the proteins, one obtains a model of a large gene network.

7.5 Summary

Models for mRNA and protein synthesis have a very simple general form. Positive feedback loops account for alternative stable steady states and hysteresis. Simple models for gene activity allow for complicated networks of regulatory interactions. The excellent book by Alon (2007) gives an exciting introduction of the structure of gene networks regulated by transcription factors, and uses simple mathematical models to illustrate the functioning of various interaction schemes. Highly recommended!

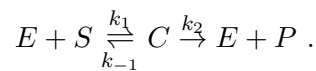
7.6 Exercises

Question 7.0. Read the chapter

- How can one system have various possible states under one and the same external circumstances? Can you give examples of such systems?
- What is a quasi steady state assumption?
- What is the difference between a quasi steady state and a steady state?
- When is it okay to treat the variable in $dx/dt = f(x)$ as a constant?
- Why is $1 - R = 1 - \frac{1}{1+A^n} = \frac{A^n}{1+A^n}$ in the Lac-operon model? Can you sketch $1 - R$ as a function of A ?
- Why are some bacteria fluorescent and others not in the Ozbudak experiments?

Question 7.1. Michaelis-Menten

The famous Michaelis-Menten term comes from a quasi steady state assumption in enzymatic reactions. Consider the following reaction for the formation of some product P from a substrate S . The enzyme E catalyzes the reaction, i.e.,



Because the enzyme is released when the complex dissociates one writes a conservation equation

$$E + C = E_0 .$$

- Write the differential equations for the product P and the complex C . Use the conservation equation!
- Assume that the formation of the complex is much faster than that of the product, i.e., make the quasi steady state assumption $dC/dt = 0$.
- Write the new model for the product. Simplify by defining new parameters.
- Sketch the rate at which the product is formed (dP/dt) as a function of the substrate concentration S .
- Write an ODE for the substrate, and note that you can add dC/dt to simplify dS/dt because $dC/dt = 0$.

Question 7.2. Positive feedback

Rewrite the mRNA protein model of Eq. (7.2) assuming that the protein is a transcription factor increasing its own transcription.

- Sketch the nullclines
- Determine the stability of the steady state(s). Can such a system with positive feedback be stable?
- Assume that the mRNA kinetics are much faster than those of the protein molecules, and write a model for dP/dt .

Question 7.3. Gene network

Consider a protein, P_1 , that is down-regulated by a transcription factor, P_2 . The transcription factor itself is up-regulated by P_1 :

$$\frac{dP_1}{dt} = \frac{c_1}{1 + P_2/h_2} - d_1 P_1 \quad \text{and} \quad \frac{dP_2}{dt} = \frac{c_2 P_1}{h_1 + P_1} - d_2 P_2$$

- What is the biological interpretation of h_1 ?
- What is the steady state of P_1 in the absence of its transcription factor?
- What is the steady state of P_2 in the absence of P_1 ?

- d. Sketch the nullclines, and determine the stability of all steady states.
- e. What is the expected behavior of this network?

Question 7.4. Lac-operon

The model for the Lac-operon has a positive feedback loop because an increased concentration of allolactose increases the expression of permease, which further increases the allolactose concentration. There is also a negative feedback loop because increasing allolactose levels increases the expression of β -galactosidase, which decreases the allolactose concentration by the hydrolysis of allolactose. To test which of these feedback loops is required for the hysteresis we remove the negative feedback loop by setting $v = 0$ in Eq. (7.4).

- a. Sketch the nullclines
- b. Determine the stability of the steady state(s)
- c. Assume that the mRNA kinetics is much faster than that of the allolactose, and write a model for dA/dt .
- d. What is the role of β -galactosidase in the hysteresis of the lac operon?

Question 7.5. Sahel

The Sahel zone is known for the desertification due to the interplay between low rainfall and local farmers exploiting the arid vegetation having herds of cattle. Cattle grazing in arid zones are known to have a sigmoid functional response: when there is too little vegetation the grazers stop searching for it. We write the following model for the vegetation in the Sahel zone:

$$\frac{dV}{dt} = rV(1 - V/K) - \frac{aHV^2}{h^2 + V^2},$$

where H is a “parameter” representing the herd size that is determined by the owner of the herd. For simplicity we write a logistic term for the growth of the vegetation.

- a. Plot the steady state vegetation obtained from solving $dV/dt = 0$ as a function of the herd size H (hint: remember the Noy-Meir (1975) construction method on Page 31).
- b. Sketch in this picture the following story. A herd owner has just a few cows, which graze on a relatively rich vegetation (i.e., $V \simeq K$). Because things go well, the herd owner buys another cow. The vegetation remains fairly rich, and the owner keeps on buying cattle, one at a time. This goes well for a long time, until at some unexpected moment the vegetation totally collapses. Due to the sparse vegetation the cows stop giving milk and the herd owner has to sell a few cows. Will the vegetation recover?
- c. The $dV/dt = 0$ nullcline plotted as a function of a parameter is basically a bifurcation diagram with saddle-node bifurcations (cf. Fig. 7.3b). How many saddle-node bifurcations are there in your picture?

Extra exercise for cool students:

- d. This problem has been published by May (1977): this is an excellent paper to read if you are interested.

Question 7.6. Catastrophic shifts in ecosystems

Read the paper by Scheffer et al. (2001) which gives a biological overview of catastrophic shifts between alternative stable states.

- a. Check that Eq. (1) in Box 1 of the paper indeed gives the hysteresis picture of Fig. 1c in the paper. Hint: use the graphical construction method introduced in the Noy-Meir exercise on Page 31, and split Eq. (1) into its positive part $dx/dt = a + f(x)$ and the negative part $dx/dt = -bx$.
- b. What data in the paper unequivocally support the conjecture of hysteresis? Hint: what data

truly require Fig. 1c, and cannot be explained with Fig. 1b.

c. For interested students: compare this paper with that of May (1977) on the same topic.

Chapter 8

Chronic viral infections and immune control

Viruses are the most common biological entities in the biosphere and outnumber their hosts by one to two orders of magnitude (Breitbart et al., 2002; Angly et al., 2006). Because they are so abundant they play a large role in regulating population densities, and they impose a very strong evolutionary selecting pressure on their hosts.

We consider the “epidemiology” of a chronic viral infection within one individual. Here a chronic viral infection consists of many viral generations where the virus infects target cells that produce novel virus particles. The damage caused by the virus occurs by lysis of the target cells (for so-called cytolytic viruses) or by the killing of infected cells by the host immune response (e.g., by $CD8^+$ cytotoxic T cells). Modeling work in virology has revealed a number of new insights into chronic viral infections like HIV infection, hepatitis, and human leukemia viruses like HTLV-1 (Ho et al., 1995; Wei et al., 1995; Nowak and Bangham, 1996; Nowak and May, 2000). Previously, it was thought that chronic viral infections were due to “slow viruses”, but thanks to this modeling work we now know that these chronic infections are a (quasi) steady state where a rapidly reproducing virus is controlled by the host (probably by the host immune response). HIV-1 and HTLV-1 have $CD4^+$ T cells as the major target cell, EBV infects B cells, and hepatitis viruses infect liver cells (hepatocytes). The availability of target cells may also play an important role in limiting both acute and chronic infections. A good example of the former is an influenza infection, where epithelial cells form the major target cell.

The mathematical mission in this chapter is to study models with so many differential equations that one can no longer use nullcline analysis. Only after simplifying the model by separating its slow and fast time scales we will again draw nullclines in the exercises.

8.1 Immune response

Virus infections typically evoke immune responses composed of antibodies and $CD8^+$ cytotoxic T cells. A natural model for target cells T , infected cells I , virus particles V , and a cellular immune response E , would be

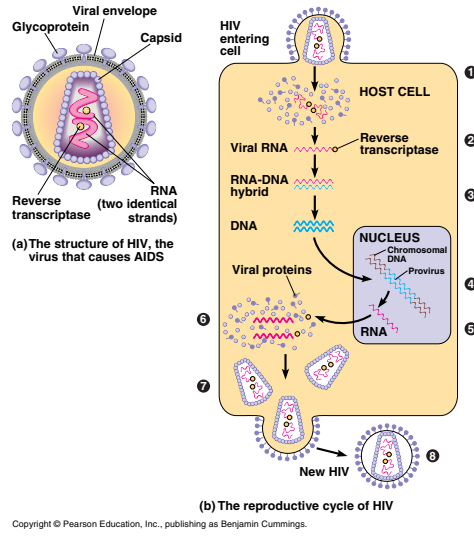


Figure 8.1: HIV-1 infection of a target cell. From: Campbell and Reece (2008).

$$\begin{aligned}
 \frac{dT}{dt} &= \sigma - \delta_T T - \beta TV, \\
 \frac{dI}{dt} &= \beta TV - \delta_I I - kEI, \\
 \frac{dV}{dt} &= pI - \delta_V V, \\
 \frac{dE}{dt} &= \alpha EI - \delta_E E,
 \end{aligned} \tag{8.1}$$

where σ is the daily production of target cells (in cells per day), uninfected target cells have a half life of $\ln[2]/\delta_T$ days, and infected cells have a half life of $\ln[2]/\delta_I$ days. One can set $\delta_I > \delta_T$ to allow for cytopathic effects of the virus. Uninfected cells can become infected by encountering virus particles at a rate β /day per virion. The kEI term reflects the killing of infected cells by the immune effectors E , and the αEI represents the clonal expansion of immune effectors in response to antigen.

The non-trivial steady states of this model should correspond to the situation of a chronic viral infection. These steady states are found by solving the equations from the simplest to the most complicated. Solving $dE/dt = 0$ yields the solutions $\bar{E} = 0$ or $\bar{I} = \delta_E/\alpha$. Proceeding with the latter, i.e., considering the case with an immune response, one solves $dV/dt = 0$ to find that $V = (p/\delta_V)I$. Next, one can solve $dT/dt = 0$ and finally one solves $dI/dt = 0$ to find:

$$\bar{I} = \frac{\delta_E}{\alpha}, \quad \bar{V} = \frac{p}{\delta_V} \bar{I} = \frac{p\delta_E}{\alpha\delta_V}, \quad \bar{T} = \frac{\sigma}{\delta_T + \beta\bar{V}} = \frac{\alpha\sigma\delta_V}{\alpha\delta_T\delta_V + p\beta\delta_E}, \tag{8.2}$$

and

$$\begin{aligned}
 \bar{E} &= \frac{p\beta}{k\delta_V} \bar{T} - \frac{\delta_I}{k} \\
 &= \frac{p\beta\alpha\sigma}{k(\alpha\delta_T\delta_V + p\beta\delta_E)} - \frac{\delta_I}{k},
 \end{aligned} \tag{8.3}$$

which is a saturation function of α (see Fig. 8.2c).

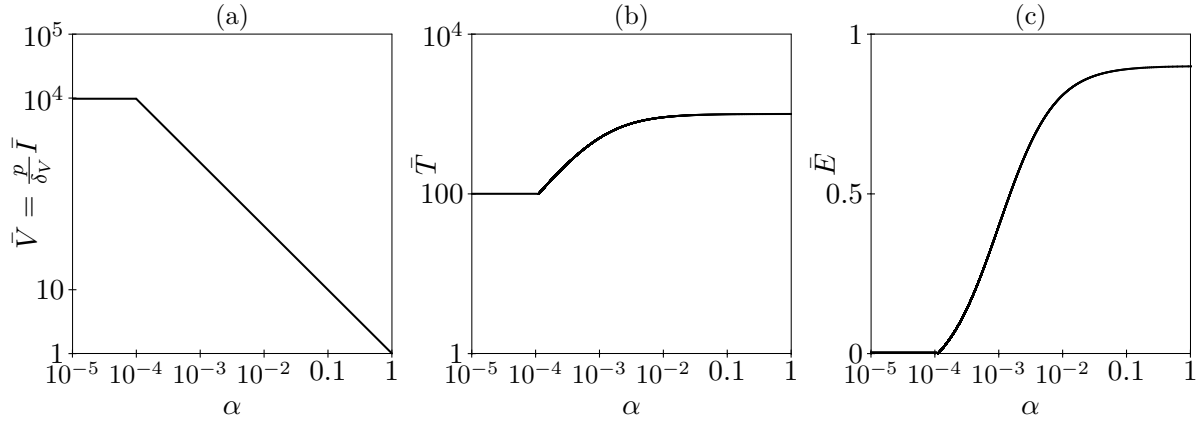


Figure 8.2: The steady state of Eq. (8.2) as a function of the immune activation parameter α . When α becomes too small the immune response cannot maintain itself, and the virus is controlled by target cell availability. This new steady state for low α can be computed by solving the steady state of Eq. (8.1) for $E = 0$, and is therefore independent of α . The model is parameterized to represent 1 μL of blood with a normal count of 1000 CD4^+ T cells: $\beta = 0.0001$ per virion per day, $\delta_T = \delta_E = \delta_I = 0.1$ per day, $\delta_V = 100$ per day, $k = 1$ per cell per day, $p = 1000$ per day and $\sigma = 100$ cells per day.

From these steady states one can read that the size of the target cell population declines with the viral load \bar{V} , i.e., the extend of liver damage, or of CD4^+ T cell depletion, increases with the viral load. Surprisingly, the steady state number of infected cells, $\bar{I} = \delta_E/\alpha$, only depends on immune response parameters (Nowak and Bangham, 1996), which suggests that target cell availability cannot have any contribution to the chronic viral load.

During the chronic phase HIV-1 infected patients have a quasi steady state viral load called the “set point” (see Fig. 8.3). Different patients have enormously different set points, i.e., there is more than a 1000-fold variation between patients. Patients with a high set point tend to have a much faster disease progression than patients with a low viral burden (Mellors et al., 1996). According to our model of Eq. (8.1) model the steady state number of infected cells $\bar{I} = \delta_E/\alpha$. Because the expected life span of effector cells, $1/\delta_E$, is not expected to vary much between people, 1000-fold variations in \bar{I} can only be explained by 1000-fold variations in α , see Fig. 8.2 (Nowak and Bangham, 1996; Müller et al., 2001; De Boer, 2012). The corresponding variation in the immune response \bar{E} is a saturation function of α , however. Patients differing 10-fold in the set point will therefore not differ 10-fold in the immune response \bar{E} (see the saturated regime in Fig. 8.2c). This provides an explanation for the paradoxical observation that patients with low and high viral loads of HIV-1 and HTLV-I tend to have the same level of the CD8^+ T cell response to most proteins of the virus (Nowak and Bangham, 1996; Nowak and May, 2000; Novitsky et al., 2003). Although the immune activation parameter, α , completely determines the steady state viral load, we now see that it has much less of an effect on the magnitude of the immune response.

8.2 Separation of time scales

For several viral infections it has been established that the kinetics of free viral particles is much faster than that of infected cells. For instance, for both HCV and HIV-1 infections we know that $\delta_V \gg \delta_I$ (Perelson et al., 1996; Neumann et al., 1998; De Boer et al., 2010). It is therefore quite reasonable to assume that the virus equation is at quasi steady state. Setting $dV/dt = 0$

we employ that $V = (p/\delta_V)I$, i.e., the viral load becomes proportional to the concentration of infected cells. Substituting $V = (p/\delta_V)I$ into the model yields

$$\begin{aligned}\frac{dT}{dt} &= \sigma - \delta_T T - \beta' T I, \\ \frac{dI}{dt} &= \beta' T I - \delta_I I - k E I, \\ \frac{dE}{dt} &= \alpha E I - \delta_E E,\end{aligned}\tag{8.4}$$

where $\beta' \equiv p\beta/\delta_V$. The technique by which we have simplified the 4-dimensional model into a 3-dimensional model is called “separation of time scales”. Here we have removed the fastest time scale by a quasi steady state assumption. Note that the virus concentration is not assumed to remain constant: rather it is assumed to be proportional to the infected cells.

There is another time scale in the model that we can eliminate under certain circumstances. After the immune response E has been established it probably changes on a rather slow time scale. For instance, during therapy of chronically infected patients, the stimulation of the immune effector cells will drop, because αI decreases, but due to immune memory effects (like life long immunity) the effector population may remain large for a long time. One could account for such memory effects by giving the immune effectors E a very long half-life $\ln[2]/\delta_E$, i.e., by making δ_E a small parameter. If the immune effector cells are long-lived, their decline during therapy should be negligible, and one can simplify the model during therapy by the approximation that E remains constant. This fixed value of E is given by Eq. (8.3). Thus, the simplified model where we have removed the fastest and the slowest time scale becomes

$$\frac{dT}{dt} = \sigma - \delta_T T - \beta' T I, \quad \frac{dI}{dt} = \beta' T I - \delta I, \tag{8.5}$$

where $\beta' \equiv p\beta/\delta_V$ and $\delta \equiv \delta_I + k\bar{E} = \frac{p\beta\alpha\sigma}{\alpha\delta_T\delta_V + p\beta\delta_E}$.

This is a model that you are familiar with. It is a host-parasite model with a fixed production term (see the “Malaria” exercise on Page 23). So you know the R_0 of the infection and its steady state:

$$R_0 = \frac{\beta'\sigma}{\delta_T\delta} \quad \text{such that} \quad \bar{T} = \frac{\sigma}{\delta_T R_0} = \frac{K}{R_0} \quad \text{and} \quad \bar{I} = \frac{\sigma}{\delta} \left(1 - \frac{1}{R_0}\right), \tag{8.6}$$

where K is the “carrying capacity” of the target cells. Since most viruses have rapid initial growth rates, i.e., typically $R_0 \gg 1$, this reveals that the steady state density of infected cells, $\bar{I} \approx \sigma/\delta$, and hence the viral load, remains fairly independent of β' (Bonhoeffer et al., 1997).

The 2-dimensional model of Eq. (8.5) can be used to fit the data from HIV-1 or HCV infected patients under anti-retroviral treatment. Current treatments consist of nucleoside analogs that block *de novo* infections, and of protease inhibitors blocking production of infectious virus particles. This basically means that the drugs reduce the infection parameter β . Thus the model for infected cells under treatment becomes $dI/dt = -\delta I$, which has the simple solution $I(t) = I(0)e^{-\delta t}$. By plotting the decline of the viral load during treatment on a logarithmic scale, and fitting the data by linear regression, one can therefore obtain estimates for the half life $\ln[2]/\delta$ of productively infected cells. For HIV-1 this has been done (Ho et al., 1995; Wei et al., 1995), and these now classical studies estimate half lives of 1–2 days for cells productively infected with HIV-1. Similar results have been obtained with HBV (Nowak and Bangham, 1996) and HCV (Neumann et al., 1998). Importantly, this means that chronic viral infections are not slow, but involve hundreds of viral generations over the host life time. This is a fine example where mathematical modeling has increased our understanding of chronic viral infections.

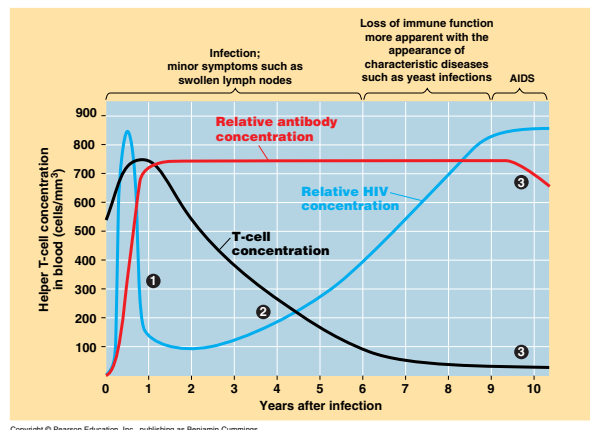


Figure 8.3: The time course of an HIV-1 infection. From: Campbell and Reece (2002).

8.3 Summary

Models of viral infections and immune reactions strongly resemble ecological models. Intuitively one cannot predict which parameters are most important in controlling the viral load. Here we had to solve I from $dE/dt = 0$ and large differences between patients with low and high viral loads can only be explained by large differences in immune response parameters, which need not result in very different magnitudes of the actual immune response. The fact that the viral generation time can be estimated by a simple linear regression proves that simple models sometimes allow for important new interpretations.

Nowak and May (2000) have published a very readable book on modeling viral infections using the same mass-action type models as we have used in this chapter.

8.4 Exercises

Question 8.0. Read the chapter

- How come that the steady state level of infected cells is not affected by the infectivity parameter β ?
- Check the R_0 of the infection in Eq. (8.6).
- How can one estimate the expected life span of productively infected $CD4^+$ T cells in patients infected with HIV?
- What is the discontinuity at $\alpha = 10^{-4}$ in Fig. 8.2?
- What is a separation of time scales?
- How can there be some much variation in the viral set-points of chronically infected individuals, while they all mount immune responses of similar magnitude?

Question 8.1. $CD4^+$ T cells

HIV-1 infected patients die from the immunodeficiency that is brought about by their low $CD4^+$ T cell counts. A form of treatment that has been tried is to give immunostimulatory medication to increase the $CD4^+$ T cell counts in infected people. Suppose that $CD4^+$ are the most important target cells of HIV-1.

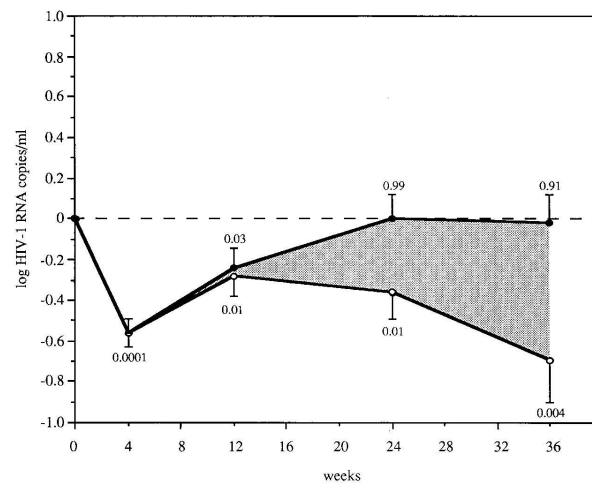


Figure 8.4: Mean changes from baseline (\pm SE) in the total HIV-1 RNA load (\bullet), and 70 wild-type HIV-1 RNA (\circ). Absolute copy numbers of 70 wild-type RNA were calculated from total serum HIV-1 RNA load by using the percentages of 70 wild-type RNA, as detected by the point mutation assay. Numbers above and underneath error bars indicate P values of the changes (paired two-tailed t test). The shaded area represents the contribution of 70 mutant HIV-1 RNA to changes in total HIV-1 RNA load. From: De Jong et al. (1996).

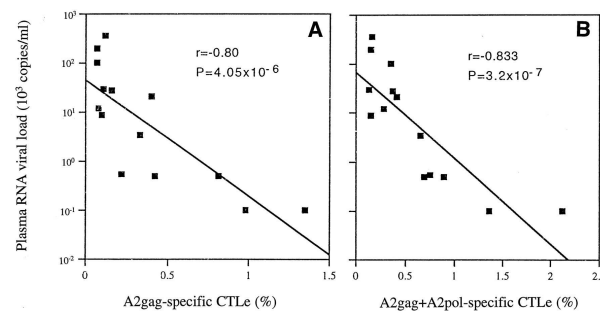


Figure 8.5: The viral load as a function of the size of the $CD8^+$ T cell immune response. There is a strong negative correlation for two different proteins of the virus (gag and pol). From: Ogg et al. (1998).

- Incorporate an immunostimulatory treatment in Eq. (8.5).
- What is the effect that you expect from this treatment?
- What alternative treatment is in fact suggested by the result in **b**?
- How would this alternative treatment affect the number of uninfected $CD4^+$ T cells?

Question 8.2. Rebound

Patients treated with anti-retroviral medication (i.e., reverse transcriptase inhibitors) sometimes have a rebound in their viral load even before the virus evolves drug resistance (see Fig. 8.4). In the models developed here this form of treatment can be modeled by reducing β . Investigate the expected effects of treatment by analyzing the phase space of Eq. (8.5).

- Sketch the nullclines before and after treatment in one phase space.
- Sketch the trajectory corresponding to this treatment in the same figure (also do this with Madonna or GRIND (see Chapter 12)).
- Sketch the same behavior as a function of time.
- Is drug resistance necessary for the observed viral rebound?

Question 8.3. Immune control

Consider anti-retroviral therapy in the immune control model defined by Eq. (8.1).

- What do you expect in the long run for the infected cell load I from a therapy that decreases β ?
- Would such a treatment have any positive effect for the patient?
- What would happen with the viral load in the model of Eq. (8.1) if the virus would evolve a mutation such that it is no longer detected by the immune response (i.e., such that $\alpha = k = 0$)?

Question 8.4. Ogg et al. (1998)

Ogg et al. (1998) found a negative correlation between the size of the CD8⁺ T cell immune response and the viral load depicted in Fig. 8.5. The same authors have also argued that the large variations in the viral set points between HIV-1 infected patients have to be due to differences in the immune reactivity parameter α (Nowak and Bangham, 1996). Study whether these two interpretations are consistent by analyzing the following model

$$\frac{dI}{dt} = \beta V - \delta_I I - \alpha k E I, \quad \frac{dV}{dt} = p I - \delta_V V, \quad \frac{dE}{dt} = \alpha E I - \delta_E E,$$

where we have omitted the target cells for simplicity.

- Remove the fastest time scale by a quasi steady state assumption.
- Sketch the nullclines of the simplified model.
- Write expressions for the non-trivial steady state of the model.
- Assume that patients differ in the immune reactivity parameter α , what kind of correlation do you expect between the viral load V and the immune response E ?

Question 8.5. Competitive exclusion

Reconsider the full model Eq. (8.4) and let there now be two immune responses to the infected cells, i.e.,

$$\frac{dT}{dt} = \sigma - \delta_T T - \beta T I, \quad \frac{dI}{dt} = \beta T I - \delta_I I - k_1 I E_1 - k_2 I E_2, \quad (8.7)$$

$$\frac{dE_1}{dt} = \alpha_1 E_1 I - \delta_{E_1} E_1 \quad \text{and} \quad \frac{dE_2}{dt} = \alpha_2 E_2 I - \delta_{E_2} E_2. \quad (8.8)$$

For the sake of the argument let E_1 be the clone with the highest binding affinity of this antigen, i.e., let $\alpha_1 > \alpha_2$.

- From which equation would you solve the steady state of E_1 ?
- What is the steady state solved from dE_1/dt ?
- What is the steady state solved from dE_2/dt ?
- Can both be true when $\alpha_1 > \alpha_2$?
- Substitute your answer of **b.** into dE_2/dt , and simplify. What do you expect for the second immune response when the first is at steady state?
- What would happen in this system if the virus escapes from the dominant immune response? Consider the case where the virus mutates such that it is no longer recognized by the first immune response, i.e., let $\alpha_1 = 0$.

This exercise illustrates a concept from ecology called “competitive exclusion” (see Chapter 5): two immune responses cannot co-exist on the same resource (antigen). Since one can have several co-existing immune responses to several epitopes of the same virus during chronic immune reactions, one would have to argue that there is intra-specific competition in the immune system (De Boer et al., 2001).

Chapter 9

The Hodgkin-Huxley model

9.1 Introduction

The term Systems Biology has only come into fashion in the last two decades. However, it stands for an approach that is much older, and whereby models are applied to understand biological phenomena. This approach has a long tradition, especially in ecology and physiology. In this Chapter we will discuss a model from physiology, the Hodgkin-Huxley model (1952), which describes how action potentials are generated in neurons. Hodgkin and Huxley were capable of formulating this model by combining careful experimentation, electrophysical theory and model simulation. As both measurement techniques and computation devices were not yet very sophisticated in the 1950s, measurements had to be performed on the giant axons of certain squid species, whereas model simulations had to be performed on very slow mechanical calculators. This makes their work even more impressive.

The model Hodgkin and Huxley came up with is relatively complex. We discuss it in this course for a number of reasons. First, it is one of the most famous models in Theoretical Biology. Hodgkin and Huxley were honored with the Nobel prize for this work. Second, it is a very nice example of how modeling work can help to get an understanding of a complex biological process, and even predict things that have not yet been discovered. Third, it will give you an idea of what a large realistic model can look like. Finally, the model is very powerful, it can predict the outcomes of new experiments not used to make the model.

First, we will explain the full model, and then we will show how simplification by separation of time scales can help to obtain a better understanding.

9.2 Background

Cell membranes are semi-permeable, meaning that some substances can easily pass through them, whereas others need to be transported through protein channels or transporters. The non-permeability to certain substances allows membranes to maintain concentration differences between the inside and outside of cells. Ions are among the substances that can not pass the cell membrane, unless transported through protein channels. In rest, Na^+ concentrations are higher outside cells and K^+ concentrations are higher inside cells. As a net result, there is

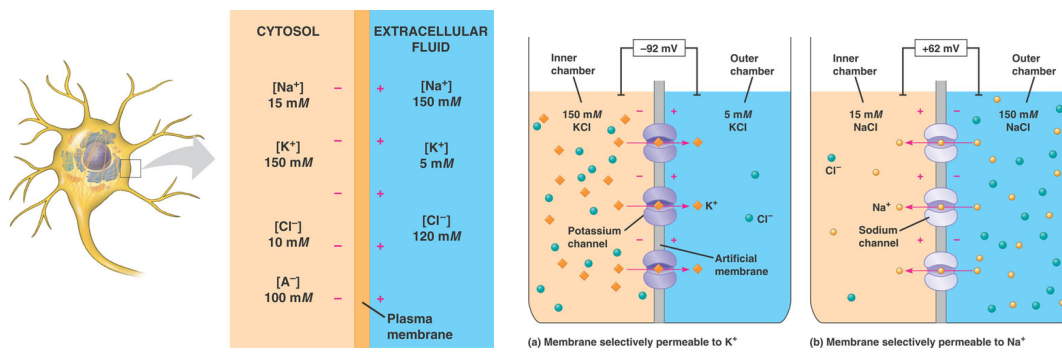


Figure 9.1: The resting membrane potential. Taken from Campbell and Reece.

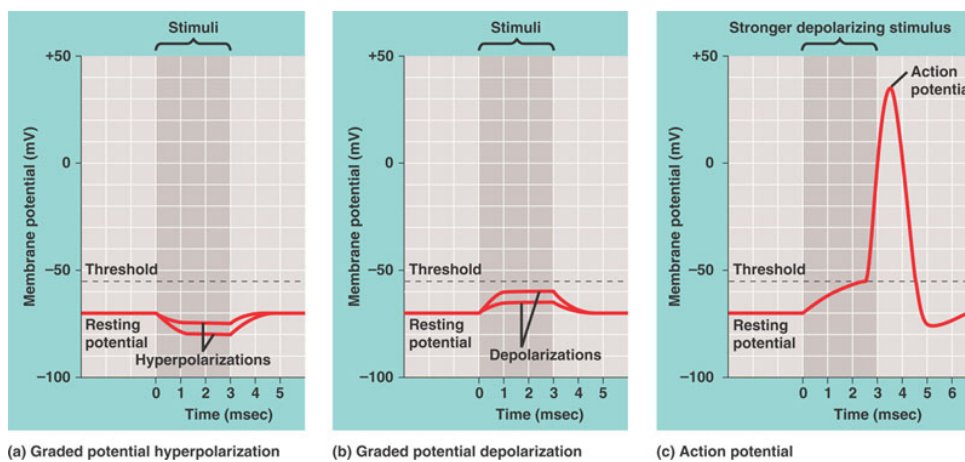


Figure 9.2: Membrane dynamics in response to perturbation. Only if a stimulus drives the membrane potential above a certain threshold, an active action potential is generated (right figure). Otherwise a passive return to the resting potential occurs (left and middle figures). Taken from Campbell and Reece.

more negative charge inside cells than outside cells, causing a charge difference that is called the **transmembrane potential** (Fig. 9.1).

Neurons, but also other cell types such as cardiac muscle cells, can generate a so called **action potential** (Fig. 9.2). During an action potential the transmembrane potential changes dramatically, first producing a strongly positive potential, and then reverting to the normal negative rest potential. These changes in membrane potential imply that the distribution of charges on both sides of the membrane change, and hence that ions are transported over the membrane, generating currents. At the time of Hodgkin and Huxley's research, voltage gated protein channels were not yet discovered, and the understanding in those days was that somehow the whole membrane changed its permeability to all ion species. How and why this happened, and how this led to the observed potential changes, was not understood.

To appreciate the major breakthrough made by Hodgkin and Huxley, let us first consider the following. Imagine that for some reason, a membrane becomes permeable to Na^+ ions. Because Na^+ ions are charged, their movement across the membrane will depend on two factors. First, movement depends on the difference in concentration of Na^+ ions between the inside and the outside of the cell. Movement across the membrane will tend to decrease this **concentration gradient**. Second, movement will depend on the total charge difference between the inside and the outside of a cell (irrespective of whether the charge is caused by Na^+ or other ions). Move-

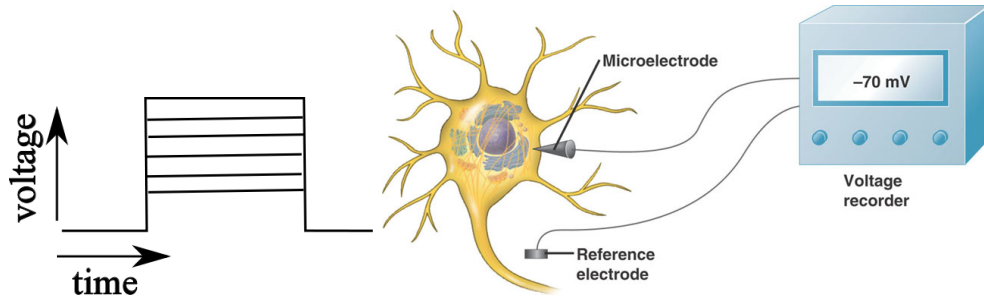


Figure 9.3: Illustration of a voltage clamp experiment. **Right:** The voltage clamp device measures the response current generated when a voltage step is applied, while at the same time maintaining the voltage at this level using two electrodes. **Left:** A series of superimposed voltage clamp experiments. Voltage is abruptly stepped up from a resting to a test level, and after a while returned to the resting level. A series of different test levels is applied.

ment of ions across the membrane will tend to decrease this **electrical gradient**. Together, these differences in concentration and charge across the cell membrane form the **electrochemical gradient** for Na^+ . For a given ion species, the so-called **Nernst potential** specifies the relation between its transmembrane voltage, and its inside and outside concentrations at equilibrium. In other words, the **Nernst equation** for Na^+ gives the conditions for which no net Na^+ transport takes place over the membrane (if Na^+ channels are open):

$$\overline{V_{Na}} = \frac{1}{z} \ln \frac{Na_o}{Na_i} \quad (9.1)$$

Here, $\overline{V_{Na}}$ is the equilibrium transmembrane potential (voltage) of Na^+ ions, Na_i and Na_o are the Na^+ concentrations inside and outside the membrane, and z is a constant that depends on ion valence. Using the Nernst equation, the current (I) of Na^+ ions across the membrane can be approximately described by:

$$I_{Na} = g_{Na}(\overline{V_{Na}} - V) \quad (9.2)$$

Here, V is the actual transmembrane potential (voltage) resulting from all ion-gradients (Na^+ , K^+ and some less frequent ion species), and g_{Na} is the ease with which Na^+ can diffuse across the membrane. This formula shows that the current can only be non-zero if the conductance of the membrane for Na^+ (g_{Na}) is non-zero. In addition it shows that the size of the Na^+ current depends on the difference between the actual membrane potential (V) and the Nernst potential for Na^+ ($\overline{V_{Na}}$). Likewise, for the K^+ current we can write $I_K = g_K(\overline{V_K} - V)$, and we can lump the contribution of all less frequent ion species into a rest current: $I_R = g_R(\overline{V_R} - V)$.

Back to Hodgkin and Huxley. From a careful look at the data, they observed that during the start of the action potential (the upshoot), the membrane potential approaches the equilibrium value for Na^+ , $\overline{V_{Na}}$ (± 50 mV) (see Fig. 9.2). To them, this suggested that at the start of an action potential, the membrane becomes mainly permeable to Na^+ , rather than to all ions at the same time. Moreover, during the end phase of the action potential (the undershoot), the potential approaches the equilibrium value for K^+ , $\overline{V_K}$ (± -80 mV), which suggested that the membrane becomes mainly permeable to K^+ . Based on this insight, they decided to measure Na^+ and K^+ currents independent of one another, and to study how the permeability of the membrane to Na^+ and K^+ depended on voltage and time.

The experiments through which this is measured are called voltage clamp experiments (Fig. 9.3). Such an experiment works as follows: First, you make sure that the currents that you are not interested in do not occur, by making sure that the ion species involved are not present.

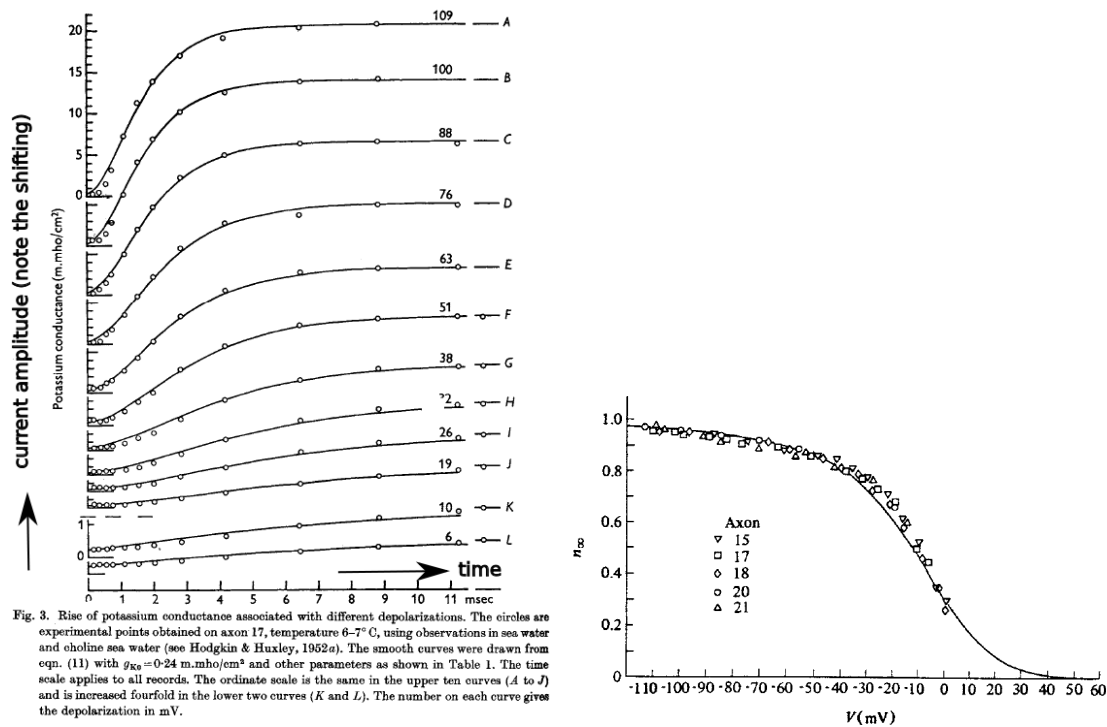


Fig. 3. Rise of potassium conductance associated with different depolarizations. The circles are experimental points obtained on axon 17, temperature 6–7°C, using observations in sea water and choline sea water (see Hodgkin & Huxley, 1952a). The smooth curves were drawn from eqn. (11) with $g_{K\infty} = 0.24$ m.mho/cm² and other parameters as shown in Table 1. The time scale applies to all records. The ordinate scale is the same in the upper ten curves (A to J) and is increased fourfold in the lower two curves (K and L). The number on each curve gives the depolarization in mV.

Figure 9.4: **a.** Current time-courses resulting from the voltage clamp experiments. **b.** Steady state values for the n gate as a function of voltage, as derived from the experimental data. Note that these are original figures from the Hodgkin and Huxley paper, in which the resting potential is defined as 0 mV, and the action potential produces a negative membrane depolarization, to around -100 mV.

Next, you test the time course and maximum amplitude of the current of interest at different test voltages (Fig. 9.3, on the left). As the current of interest itself will cause a voltage change, the voltage clamp device measures this current, and immediately sends back a counter-current to ensure that the voltage of the cell remains clamped at a particular level. By doing this for a whole range of voltages, the behaviour of the current can be characterized.

9.3 The Model

Before starting our discussion of the Hodgkin-Huxley model, one more thing needs to be said. Nowadays, it is conventional to depict a resting membrane potential as being negative (-80 to -90 mV), with an action potential causing the membrane potential to become positive (+20 mV). However, in the days of Hodgkin and Huxley's research these conventions did not yet exist, and they used a different, opposite normalisation. They normalised the rest potential at 0 mV, with an action potential producing a strong negative polarisation to -100 mV. Keep this in mind to avoid confusion!

The K^+ current

Fig. 9.4 (the left figure) shows the voltage clamp procedure and the resulting time-courses and amplitudes of the I_K current. We can make a number of observations:

1. As the voltage is stepped up, the I_K current switches on. When the voltage is stepped down again, the I_K current switches off (not shown in the figure). Hodgkin and Huxley therefore reasoned that there must be some gate for K^+ current in the membrane, that opens when the voltage increases and closes again when the voltage decreases. This gate was dubbed the n gate. For $n = 0$ the gate is closed, for $n = 1$ the gate is fully open.

2. The I_K current initially increases in a sigmoidal rather than a linear fashion. This implies a higher order gating process, i.e. that multiple *gates* need to open in a cooperative manner before the *channel* for K^+ is open. This led them to write the following equation for the K^+ current:

$$I_K = G_K n^4 (\bar{V}_K - V) \quad (9.3)$$

We see that the conductance g_k is replaced by the product $G_K n^4$. Here G_K is the maximum conductance if the channel would be fully open (if $n^4 = 1$, which is equivalent to saying $n = 1$), n is the openness of one gate in the channel, and n^4 is the openness of the total channel (which depends on a total of 4 n gates).

3. For higher voltage clamp levels, the maximum level of the I_K current increases, and the speed with which this maximum level is reached also increases. Thus if we call n_∞ the steady state 'openness' of the gate (varying between 0 and 1), n_∞ is a function of voltage. Furthermore if we call τ_n the time constant (the reverse of the speed) at which the gate opens, τ_n is also a function of time. Using n_∞ and τ_n , we can write the following equation for the dynamics of gate n :

$$\frac{dn}{dt} = \frac{n_\infty - n}{\tau_n} \quad (9.4)$$

This simply says that the value of n approaches its steady state value of n_∞ , with a time constant τ_n . Hodgkin and Huxley used their experimental data to determine equations for n_∞ and τ_n as a function of voltage. For example, from Fig. 9.4b we can find $I_{Kmax\infty}$, the highest steady state level of the current. This occurs at $n_\infty = 1$, so using Eq. 9.3 we can say $I_{Kmax\infty} = G_K (\bar{V}_K - V)$, and we can easily obtain the maximum conductance G_K if we know $I_{Kmax\infty}$: $G_K = I_{Kmax\infty} / (\bar{V}_K - V)$. Once we know G_K we can find a function for n_∞ from the steady state levels of I_K at different voltages: $I_{K\infty} = G_K n_\infty^4 (\bar{V}_K - V)$, so $n_\infty = (\frac{I_{K\infty}}{G_K (\bar{V}_K - V)})^{1/4}$ (Fig. 9.4b). A similar procedure was taken to determine τ_n as a function of voltage. The end result was the following equation for n :

$$\frac{dn}{dt} = 0.01(1 - n) \frac{V + 10}{e^{(V+10)/10} - 1} - 0.125ne^{V/80} \quad (9.5)$$

Note that this looks awful, but these numbers and the shape of the equation are merely the result of fitting experimental data. The only thing to remember here is the shape of the n_∞ curve as a function of voltage (Fig. 9.4b), and that τ_n also depends on voltage.

The Na^+ current

Fig. 9.5 shows the current traces obtained by Hodgkin and Huxley for the I_{Na} current when applying a similar voltage clamp protocol as for I_K . Again we can make a number of observations.

1. What happens when the voltage is increased, is similar to the K^+ current: the Na^+ current increases, the initial increase is non-linear, the maximum level reached increases with voltage level, and the speed at which it is reached also increases with voltage level. This led Hodgkin and Huxley to suggest that there is also a gate, dubbed m , that opens in response to an increase

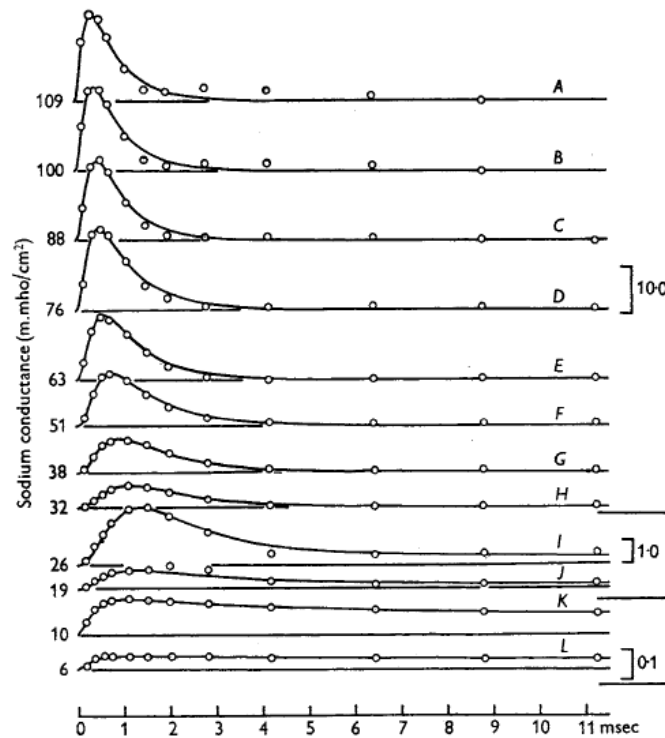


Fig. 6. Changes of sodium conductance associated with different depolarizations. The circles are experimental estimates of sodium conductance obtained on axon 17, temperature 6–7° C (cf. Fig. 3). The smooth curves are theoretical curves with parameters shown in Table 2; A to H drawn from eqn. 19, I to L from 14, 17, 18 with $\bar{g}_{Na} = 70.7$ m.mho/cm². The ordinate scales on the right are given in m.mho/cm². The numbers on the left show the depolarization in mV. The time scale applies to all curves.

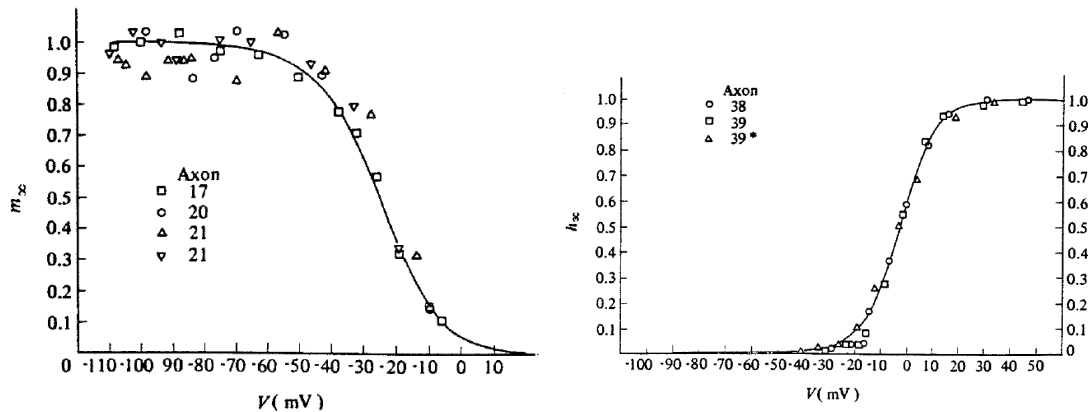


Figure 9.5: a. Current time-courses resulting from the voltage clamp experiments. b. Steady state values for the m gate as a function of voltage. c. Steady state values for the h gate as a function of voltage. Note that these are original figures from the Hodgkin and Huxley paper.

in voltage and allows transport of Na^+ ions. For the m gates they proposed that there were two gates that need to open cooperatively for the channel to be open.

2. What happens next is very different to what happens for the K^+ current. For the K^+ current we saw that after reaching a plateau, the current remained constant. Only after the voltage was stepped down again, the K^+ current decreased. This suggested that the K^+ current has a single type of gate that opens when voltage goes up and closes when voltage goes down. For the Na^+ current we see very different dynamics. We see that the Na^+ current decreases after some time, while the voltage is still at a high level. It would not be logical for the same gate to both open

and close as a response to increased voltage. Therefore, Hodgkin and Huxley postulated that the channel for Na^+ has two gates that behave differently. One is normally closed, and opens in response to an increase in voltage (the activation gate). The second gate is normally open, and closes in response to voltage (the inactivation gate). Obviously, this second gate, which they dubbed h , should respond more slowly to voltage than the first one, otherwise the Na^+ channels would never be effectively open. Together this led to the following equation for the Na^+ current:

$$I_{Na} = G_{Na} m^2 h (\overline{V}_{Na} - V) \quad (9.6)$$

Similar to the n gate, the dynamics of the m and h gates can be described once we know the functions describing m_∞ and τ_m and h_∞ and τ_h as a function of voltage. Fig. 9.5b and Fig. 9.5c illustrates the data for m_∞ and h_∞ derived from the voltage clamp experiments. From a fit to the data, the following functions for the dynamics of m and h were obtained:

$$\frac{dm}{dt} = 0.1(1 - m) \frac{V+25}{e^{(V+25)/10} - 1} - 4me^{V/18} \quad (9.7)$$

$$\frac{dh}{dt} = 0.07(1 - h)e^{V/20} - \frac{h}{e^{(V+30)/10} + 1} \quad (9.8)$$

9.4 Putting the model together

Once Hodgkin and Huxley had described in detail the behaviour of the Na^+ and K^+ currents and the rest current, a model for the action potential could be formulated.

First we write the sum of all transmembrane currents as:

$$I = G_{Na} m^2 h (\overline{V}_{Na} - V) + G_K n^2 (\overline{V}_K - V) + g_R (\overline{V}_R - V) \quad (9.9)$$

with $G_{Na} = 120$, $G_K = 36$, $G_R = 0.3$, $\overline{V}_{Na} = -115$, $\overline{V}_K = 12$, and $\overline{V}_R = -10.5989$.

The membrane acts as a capacitor, which means that the change in voltage V is related to the current I and the capacitance C :

$$\frac{dV}{dt} = \frac{I}{C} \quad (9.10)$$

We can use this to write an expression for the voltage:

$$\frac{dV}{dt} = \frac{1}{C} (G_{Na} m^2 h (\overline{V}_{Na} - V) + G_K n^2 (\overline{V}_K - V) + g_R (\overline{V}_R - V)) \quad (9.11)$$

Together with the equations for the dynamics of m , h and n :

$$\frac{dm}{dt} = 0.1(1 - m) \frac{V+25}{e^{(V+25)/10} - 1} - 4me^{V/18} \quad (9.12)$$

$$\frac{dh}{dt} = 0.07(1 - h)e^{V/20} - \frac{h}{e^{(V+30)/10} + 1} \quad (9.13)$$

$$\frac{dn}{dt} = 0.01(1 - n) \frac{V+10}{e^{(V+10)/10} - 1} - 0.125ne^{V/80} \quad (9.14)$$

we have a complete description of the voltage and gating dynamics during an action potential.

Fig. 9.6 shows an action potential simulated with the Hodgkin-Huxley model. We see that a sufficiently large decrease of the resting potential (note the y-axis, and remember that their voltage runs in the opposite direction to what is now conventional) results in a very realistically

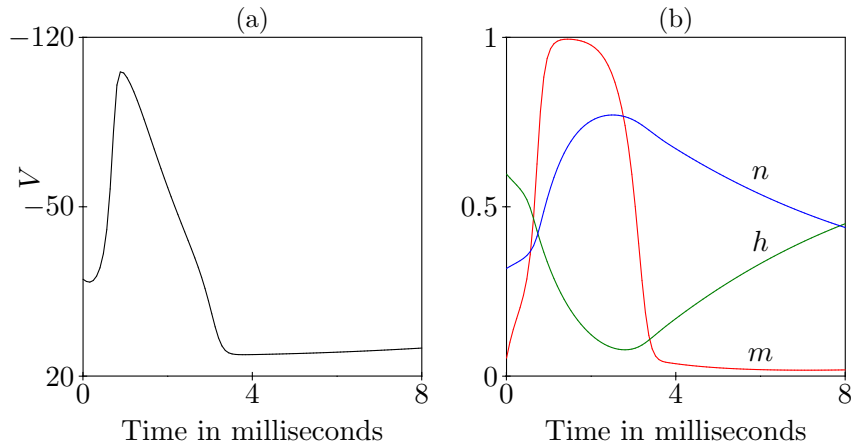


Figure 9.6: An action potential in the Hodgkin-Huxley model. **a.** Voltage dynamics. **b.** Gating dynamics. Note that the vertical axis in panel (a) runs from positive to negative, in order to get the picture of an action potential that we are now used to.

looking action potential. We also see that after the action potential, the model returns to a stable steady state at $V \simeq 0$, $m \simeq 0.05$, $h \simeq 0.6$ and $n \simeq 0.3$.

Looking at the dynamics of voltage and m , h and n gates we can now understand what happens during the generation of an action potential:

1. Due to the decrease in voltage, the m gate of the sodium channels open (see Fig. 9.5b and Fig. 9.6) and a small current of Na^+ ions starts leaking inwards. This causes the membrane potential to further decrease, and Na^+ current to further increase (positive feedback). As the conductance for Na^+ is now much larger than that for other ions, the voltage approaches the Nernst equilibrium potential for sodium, $\bar{V}_{Na} = -115$.
2. The continued decrease in voltage triggers the closing of the h gate of the sodium channels (see Fig. 9.5c and Fig. 9.6), causing the sodium channels to become closed again and stopping Na^+ influx.
3. In addition, the voltage decrease triggers the opening of the n gate of the potassium channel, allowing K^+ to leave the cell (see Fig. 9.4b and Fig. 9.6). As now positive charge is leaving rather than entering the cell, the membrane voltage starts to recover. Because now the membrane is almost exclusively permeable to K^+ ions, the membrane potential approaches the Nernst equilibrium potential for potassium, $\bar{V}_K = 12$, producing an “undershoot” of the voltage to well below the resting potential.
4. Finally, due to the decrease in voltage the m and n gates close, the h gates open and the voltage reverts to the resting potential.

Note how this sequence of events corresponds exactly to how the generation of an action potential is explained in current day textbooks such as Campbell (Fig. 9.7)! It was only much later that transmembrane protein channels specific for either Na^+ or K^+ ions were found to exist, which respond to voltage changes with conformational changes, influencing their permeability to ions. Hodgkin and Huxley were able to predict the existence of these channels based on their careful modeling work.

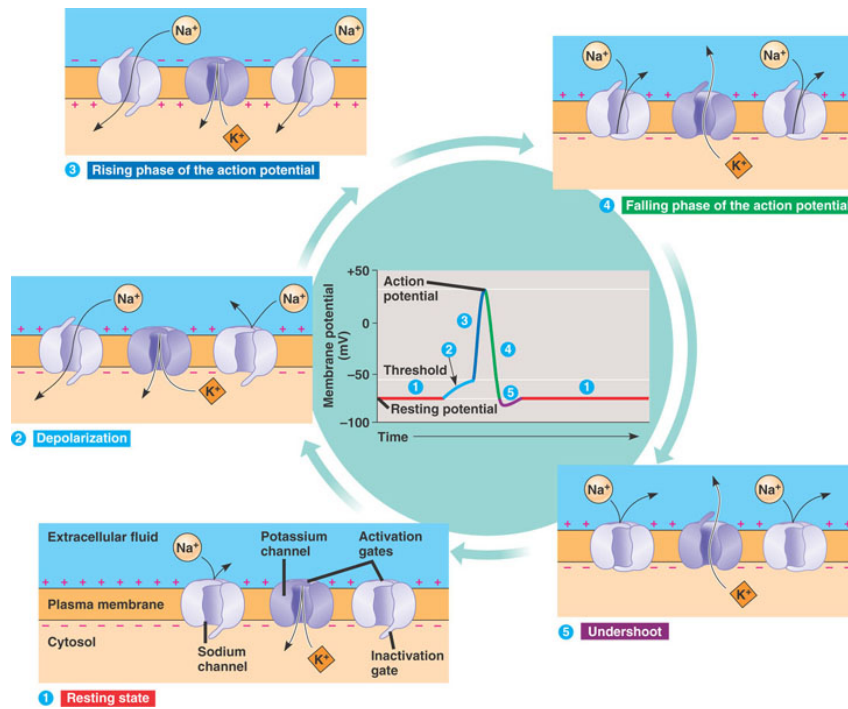


Figure 9.7: Textbook illustration of the events during an action potential. Taken from Campbell and Reece.

9.5 The Fitzhugh-Nagumo model

The Hodgkin-Huxley model is unpleasantly complex. As a consequence, even professional theoretical biologists can do little more than simulate the model on a computer to see its behavior in time. Several researchers have tried to simplify the model to obtain better insight into its behavior (and thus into the behavior of the neurons it models). Citing Fitzhugh (1960): “The usefulness of an equation to an experimental physiologist (...) depends on his understanding how it works.” Fitzhugh (1960) analyzed the Hodgkin-Huxley model to derive the a much simpler model, that is a phenomenological description of the Hodgkin-Huxley model. In the exercises you will work with this simpler Fitzhugh-Nagumo model.

One of the things Fitzhugh observed is that the variables have quite different time scales: the V and m variables change much more rapidly than h and n . For instance, during the first milli-second in Fig. 9.6, h and n have hardly changed. Because dm/dt is so much faster than the h and n variables, we do a so called **quasi steady state** (QSS) approximation: $dm/dt = 0$. This means that we assume that m is so fast relative to other variables, that when these other variables change, m immediately switches to the steady state value corresponding to these changed conditions. Hence, m is always in steady state, so we set $dm/dt = 0$, which gives us $m = m_\infty$ (check this yourself). This equation gives us a value for m for any value of V . By removing the equation $\frac{dm}{dt}$ from the model and replacing all occurrences of m with the algebraic expression for m_∞ , we simplify the Hodgkin-Huxley model from a full four-dimensional model to a three-dimensional QSS model.

There is another reasonable simplification that can be made. One can see in Fig. 9.6 that the behavior of the h and n variables is more or less complementary, i.e., $n + h \simeq 0.91$. This is called a **conservation equation**. One can therefore eliminate the dn/dt differential equation

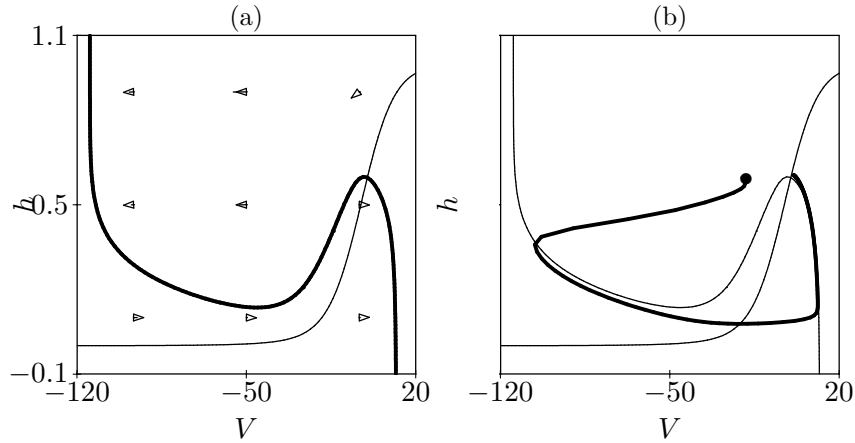


Figure 9.8: The nullclines of the Hodgkin-Huxley model for the QSS assumption $dm/dt = 0$ and the approximation $n = 0.91 - h$. The heavy line in (a) is the $dV/dt = 0$ nullcline and the heavy line in (b) is a trajectory of the complete 4-dimensional model. The trajectory of the full model appears to obey the nullclines of the simplified model.

by substituting $n = 0.91 - h$ in Eq. (9.9). This then delivers a two-dimensional model, which has the $dV/dt = 0$ and $dh/dt = 0$ nullclines depicted in Fig. 9.8. Fig. 9.8b depicts a trajectory of the full four-dimensional model projected into the two-dimensional phase space of the simplified model. One observes that the trajectory obeys the vector field and nullclines reasonably well, which shows that our simplification seems fair.

Now that we have arrived at a 2-dimensional model, we can use our earlier techniques of phase plane analysis to get an understanding of the behaviour of the model. From the vectorfield we can determine that both V and h have a negative feedback on themselves, which implies that the equilibrium -which corresponds to the resting state of a neuron- is stable.

Next we analyse what happens if we perturb the system from the stable equilibrium, by considering possible trajectories in the phase plane. To be able to do so, we take one more look at Fig. 9.6. This depicts the dynamics of V , m , h and n , of which only V and h are relevant for the simplified model that we are now working with. If we compare the dynamics of V and h , we see that h changes much slower than V . Thus, in the phase space of Fig. 9.8, if we would draw the vector field in a more quantitative way, arrows in the horizontal direction would be much larger than those in the vertical direction. This means that changes in the horizontal direction are very fast, and changes in the vertical directions are very slow.

If we decrease the voltage beyond the rising part of the V -nullcline, one enters an area where $dV/dt < 0$ and $dh/dt < 0$. As we discussed above, V dynamics are much faster than h dynamics, so the trajectory goes mostly to the left and only somewhat downward, until it approaches the downward oriented part of the $dV/dt = 0$ nullcline. After passing this nullcline, the vector field now dictates the trajectory to move to the right and further downward. However, now the trajectory can not go mostly to the right and only a little downward: it would immediately cross the $dV/dt = 0$ nullcline again, and there the vector field would force it back in the opposite direction again. Indeed, the dominant horizontal direction of the vector field forces the trajectory to stay on the $dV/dt = 0$ nullcline as it moves to the right and slowly downward. (Put differently, V is much faster than h . But as h now has to change, V is in steady state with it, so $dV/dt = 0$.) This continues until we meet the upward part of the $dV/dt = 0$ nullcline. The trajectory can no longer follow it, as this would conflict with what the vector field dictates. Thus now, due to the horizontal dynamics being dominant, the trajectory moves mostly to the right and slightly

downward, until we meet the second downward oriented part of the $dV/dt = 0$ nullcline. Here again a mostly horizontal trajectory is not possible, h has to change and the fast V dynamics cause the trajectory to follow the nullcline until finally the intersection point of the V and h nullclines is reached and the system returns to its stable equilibrium.

According to this description an action potential is a large excursion through phase space, that was triggered by a sufficiently large perturbation of the steady state. This particular nullcline configuration defines an “excitable” system. A small disturbance (excitation) is blown up into a large signal, that ultimately reverts back to its resting state. The shape of the $dV/dt = 0$ nullcline creates a threshold around the steady state that has to be breached to initiate the action potential. If a smaller stimulus is applied and the threshold is not passed, a direct return to the equilibrium occurs, as dictated by the vector field (see also Fig. 9.2).

During the final part of the action potential, i.e. when the trajectory moves upwards along the rightmost branch of the $dV/dt = 0$ nullcline, the system is refractory to new excitations. To excite the neuron within that time window, one has to give a much larger stimulus. This can be easily understood from the picture: because the distance to the threshold (i.e. to the upward part of the V -nullcline) is much larger, a larger decrease in the voltage is required for excitation.

Above we showed how the Hodgkin-Huxley model can be simplified using the QSS assumption $dm/dt = 0$ and a “conservation equation” $n + h \simeq 0.91$. An alternative approach would be to realize that the behaviour can be summarized using a two equation phenomenological model, describing the voltage and the recovery dynamics. This approach was followed by both FitzHugh and Nagumo, producing the famous FitzHugh-Nagumo model for action potentials that you will work with in the exercises.

Background to the material covered in this chapter can be found in the books of Edelstein-Keshet (1988) and Keener and Sneyd (1998).

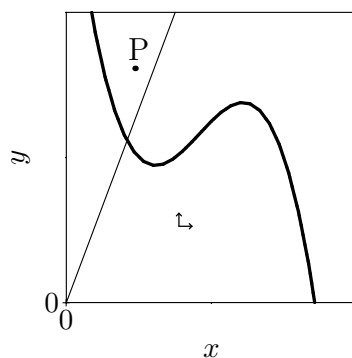
9.6 Exercises

Question 9.1. Time scales

Consider the following biochemical system

$$\frac{dx}{dt} = f(x, y) \quad \text{and} \quad \frac{dy}{dt} = \epsilon(ax - by) ,$$

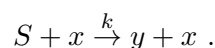
where $a, b > 0$ and $\epsilon \ll 1$ such that **the kinetics of y is much slower than that of x** . The phase space is:



where the heavy line represents the $dx/dt = 0$ nullcline, and the straight line is the $dy/dt = 0$ nullcline.

a. Sketch a trajectory from the point P.

Now consider a case where y is actively produced from a substrate S by a reaction that is catalyzed by x :



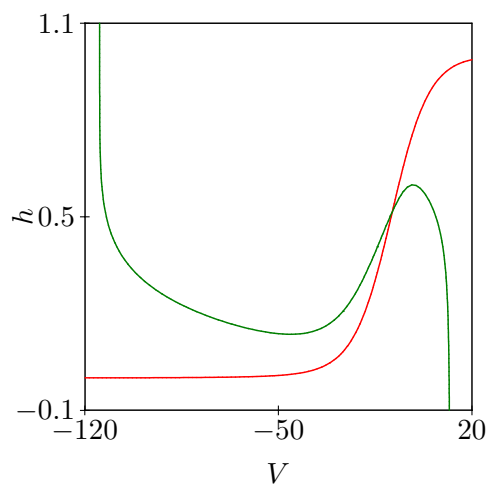
- b. Which parameter of the model above should be changed if S is decreased?
- c. How will the nullclines change?
- d. Sketch two qualitatively different nullcline configurations.
- e. Sketch trajectories for both of them.

Question 9.2. Inhibition

The sigmoid $dh/dt = 0$ nullcline in Fig. 9.8 closely resembles the h_∞ line in Fig. 9.5. How can this be?

Question 9.3. Hodgkin Huxley (Extra exercise for cool students)

We have simplified the Hodgkin-Huxley model and found the nullclines depicted in Fig. 9.8. Changing the parameters of the model, one can also obtain the following nullclines:



After this (minor) change of the parameters the h variable has remained much slower than the V variable (like it is in Fig. 9.8).

- a. Determine the stability of the steady state.
- b. Sketch a trajectory and let it approach the final behavior of the system.
- c. Sketch the behavior in time.
- d. Give a biological interpretation of a neuron with these parameters.

Question 9.4. FitzHugh-Nagumo model (Extra exercise for cool students)

Instead of deriving a reasonable simplification of the Hodgkin-Huxley model, one can also define a “phenomenological” model that has essentially the same behavior. A famous phenomenological model is the FitzHugh-Nagumo model,

$$\frac{dV}{dt} = -V(V - a)(V - 1) - W \quad \text{and} \quad \frac{dW}{dt} = \epsilon(V - bW) ,$$

where V is some arbitrary variable representing the voltage, and W is a slow variable basically following V . The steady state of W is $W = V/b$ and the small ϵ parameter makes dW/dt a slow equation. Note that one can easily express the $dV/dt = 0$ nullcline as $W = -V(V - a)(V - 1)$, which is zero at three values of V . Because the model should resemble the Hodgkin-Huxley model, make sure that the nullclines intersect in only one steady state.

- a. Sketch the nullclines of the model assuming that $a < 1$.
- b. Determine the stability of the steady state.
- c. Sketch a trajectory corresponding to an excitatory perturbation of this steady state.
- d. Does this resemble the action potential of the Hodgkin-Huxley model?
- e. Is this a good model for the action potential?
- f. Now add an external input, e.g., from a dendrite, $dV/dt = i - V(V - a)(V - 1) - W$ and sketch the nullclines for all qualitatively different possibilities.
- g. Determine the stability of all steady states.
- h. Sketch for each situation a representative trajectory.

Chapter 10

Introduction in Spatial Patterns

10.1 Introduction

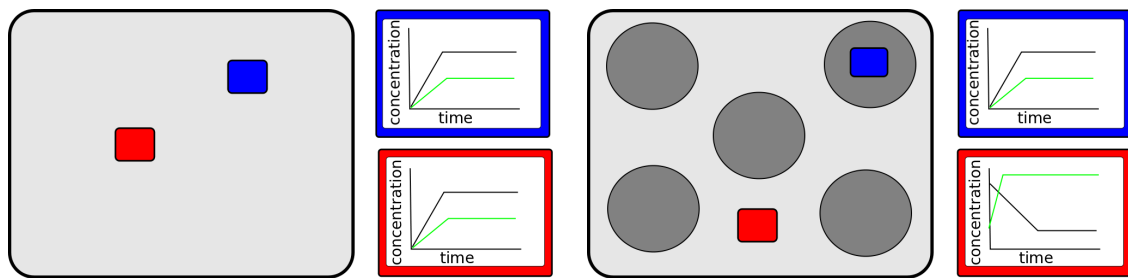


Figure 10.1: **A.** On the left, a field with homogeneous conditions: at different places (red and blue) the same things happen at the same time. **B.** On the right, a field with heterogeneous conditions: at different places, different things happen at the same time.

Up until now, we have assumed that the variables that we studied only changed as a function of time. We assumed that the value of variables did not depend on their location in space. This situation is depicted in Fig. 10.1A. Everywhere on this field, the same things occur at the same time. In other words, the dynamics of two variables in different locations will be the same, this system is **homogeneous** (or “*well-mixed*”) over space. This also means that we do not need to take space into account: the behaviour of a variable anywhere in this space can simply be described by the behaviour of a variable in a single point. So if we want to model two variables in such a *spatially homogeneous system*, we can just write a system of two differential equations, as we have done so far.

In Fig. 10.1B we see a different situation. Here the behaviour of a variable will depend on its location in space. For two variables in different locations, the dynamics may be different. We call such a system **heterogeneous** with regard to space. In other words, in this system there are **spatial patterns**. As a consequence, we cannot approximate such a system by just describing the dynamics in a single point.

Note that if there is no “communication” between different points in space, we can describe the dynamics of the variables in this field by writing down an independent set of differential equations for each of the points in the field. However, this is rarely the case. More often,

there is some form of communication between variables in different points in space. Examples of such “communication” include the diffusion of chemicals, migration of animals, dispersal of seeds, etcetera. This means that changes in variables at one location will depend not only on other variables in that location, but also on variables in surrounding locations. For instance, the number of animals in a location can change due to local birth and death, as we have seen. But it can also change due to immigration from and emigration to other locations. If we want to model this, we need a model that describes the change of variables not just as a function of time, but as *a function of both space and time*. We will discuss these types of models in this last part of the course.

Spatial patterns occur in a lot of biological systems, and over a wide range of different spatial- and timescales. Examples include the stripes on a zebra’s skin, the patterns of vegetation in desert ecosystems and a cell becoming polar just before division, in order to give rise to two different daughter cells. How can we know when to expect a (more or less) homogeneous situation, and when to expect spatial patterns in a system? Put very simply, if the “communication” between points in space is *strong and fast*, differences between different points in space will tend to even out quickly over time, and the system will be (approximately) homogeneous or “well-mixed”. If, in contrast, the communication is *weak and slow*, differences between different points in space may persist for a long time, and spatial patterns can arise.

However, there are exceptions to the general rule described above. For instance, in particular systems known as *Turing systems*, spatial patterns arise due to strong diffusion. So in such systems, strong communication leads to patterns in space, which is not what you would intuitively expect. Such particular mechanisms however, are outside the scope of this course.

We can distinguish two types of spatial patterns. Firstly, **dynamic patterns** are spatial patterns that continuously keep changing over time. We will discuss some examples in the next chapter. Secondly, **stationary patterns** are formed during a dynamic initial phase, after which they become constant. Such patterns are common for instance in developmental biology. However, we will not extensively discuss stationary patterns in this course. Dynamic patterns often occur in the form of waves and spirals, whereas static patterns may occur in the form of spots and stripes, but also as more complicated patterns.

10.2 Including space in models: PDEs and Diffusion

How can we make models in which variables vary both over time and space? To achieve this, our models need to do two things: **1.** they need to model the dynamics of variables *in each individual point* in space, and **2.** they need to include the *coupling with variables in nearby points* in space. The simplest process by which variables in different positions can influence each other, is by diffusion. In its literal sense, diffusion means the net transport of particles from a region of high concentration to a region of low concentration. However, we can also approximate the migration of animals or the dispersal of seeds as a diffusion-like process.

How can we model a diffusion process? For simplicity, let us study diffusion in a one-dimensional cylinder or cable. In Fig. 10.2 we zoom in on three points somewhere on this cable, $i - 1$, i and $i + 1$, each having a concentration c of some particle. We know that the net flux J between two neighbouring locations increases with the *concentration difference* between the two points, decreases with the *distance* Δx between the points, and depends on the *diffusion constant* D , which describes how easily this type of particle diffuses. Thus for the fluxes between the three

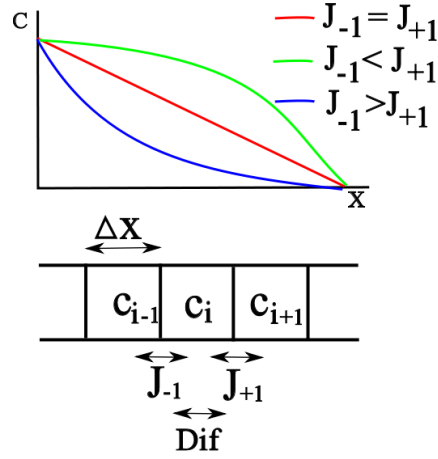


Figure 10.2: **Top:** Different spatial concentration profiles. **Bottom:** Fluxes arising from concentration differences between nearby cells.

points in Fig. 10.2 we can write:

$$J_{-1} = D \frac{c_{i-1} - c_i}{\Delta x} = D \frac{\Delta c}{\Delta x} \quad (10.1)$$

$$J_{+1} = D \frac{c_i - c_{i+1}}{\Delta x} = D \frac{\Delta c}{\Delta x} \quad (10.2)$$

If we want to know the net change in concentration in the middle point i , due to fluxes with its two neighbouring points $i - 1$ and $i + 1$, we can write:

$$F = \frac{J_{-1} - J_{+1}}{\Delta x} = \frac{\Delta J}{\Delta x} = \frac{\Delta \frac{D \Delta c}{\Delta x}}{\Delta x} = D \frac{\Delta^2 c}{\Delta x^2} \quad (10.3)$$

Note that J_{-1} , J_{+1} and F are formulated such that if $F > 0$, the concentration in i increases and if $F < 0$ the concentration in i decreases.

If we now assume that the points are infinitely close together we can write the above as:

$$F = D \frac{\partial^2 c}{\partial x^2} \quad (10.4)$$

So, apparently, we can model the change in concentration due to diffusion as a second order derivative to x (the variable that describes space). We can also understand this in a more intuitive manner. For this, take a look at the three different spatial concentration profiles shown in Fig. 10.2. First consider the straight line. For the straight line, the concentration differences between cells $i - 1$ and i and between cells i and $i + 1$ are equal. As a consequence the influx from cell $i - 1$ (J_{-1}) on the left and the efflux to cell $i + 1$ ($-J_1$) on the right are equal, and hence there is *no net change* in the concentration of cell i ! Second, look at the lower line that first declines steeply and then less steeply. In this case the concentration difference between $i - 1$ and i on the left is larger than between i and $i + 1$ on the right. So, the influx from $i - 1$ is larger than the efflux to $i + 1$, and hence the concentration in cell i will *increase* due to diffusion. Finally, look at the third, upper line. Here, the concentration difference between $i - 1$ and i on

the left is smaller than between i and $i + 1$ on the right. So, the influx from $i - 1$ is smaller than the efflux to $i + 1$, and hence the concentration in cell i will *decrease* due to diffusion. So clearly, diffusion only causes concentration changes if the concentration profile is non-linear: if it has a non-zero second order derivative. Furthermore, diffusion will cause an increase in concentration if the second order derivative is positive, and a decrease if it is negative.

Up until now we have worked with equations that are known as **ordinary differential equations** (ODEs). These equations only contain the derivative of N to time:

$$\frac{dN}{dt} = f(N) \quad (10.5)$$

If we now want to write a spatial model, where N depends on both time and space, we write:

$$\frac{\partial N}{\partial t} = f(N) + D \frac{\partial^2 N}{\partial x^2} \quad (10.6)$$

We call this a **partial differential equation** (PDE), as it contains partial derivatives of N with respect to both time t and space x . Note that we need to apply this equation at each point x in space, and that the coupling between the variable N at different locations here is through a local diffusion process.

Using such an equation, we can model for example predators and prey that both move around in space as:

$$\begin{aligned} \frac{\partial R}{\partial t} &= rR(1 - \frac{R}{K}) - bRP + D_R \frac{\partial^2 R}{\partial x^2} \\ \frac{\partial P}{\partial t} &= cbRP - dP + D_P \frac{\partial^2 P}{\partial x^2} \end{aligned}$$

Using this model we can investigate the influence of prey diffusion (D_R) and predator diffusion (D_P), or how fast they move relative to one another, on the ecosystem dynamics.

We can also model the propagation of an action potential along an axon as:

$$\begin{aligned} \frac{\partial V}{\partial t} &= -V(V - a)(V - 1) - W + D \frac{\partial^2 V}{\partial x^2} \\ \frac{\partial W}{\partial t} &= c(V - bW) \end{aligned}$$

This is a spatial extension of the FitzHugh-Nagumo model we discussed in chapter 9. Note that only the voltage V spreads out through diffusion (of course it is actually the ions that displace), whereas refractoriness W is a local membrane bound process. In chapter 11 we will discuss the type of patterns that can be generated by such a model in one and two dimensions.

10.3 Inherently spatial models: CAs and IBMs

As explained in chapter 6 Cellular Automata (CAs) and Individual Based Models (IBMs) allow us to model variables (individuals, molecules) in a discrete manner, thus avoiding unrealistic situations such as 0.3 rabbits or 0.01 molecule occurring in the model. In addition, these model formalisms explicitly incorporate space, making them very suitable for studying spatial pattern formation processes.

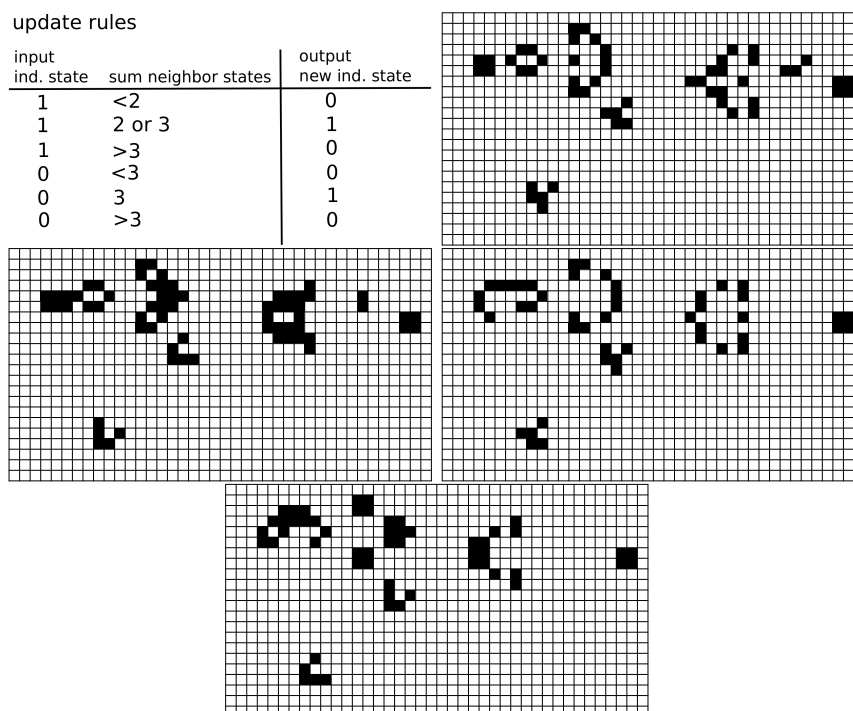


Figure 10.3: A Glider gun in the Game of Life. Four consecutive time steps are shown in a, b, c and d.

However, the fact that space is incorporated in a model, be it a PDE, CA, or IBM does not mean that spatial patterns necessarily will arise. Whether or not a spatial pattern arises depends on the rules of the model. In general, if individuals or molecules move around fast and random this will cause a mixing over space and spatial patterns will be prevented, whereas if movement is more local and / or more directed spatial patterns are expected to arise.

A very famous example of a simple CA model generating life-like spatial patterns is the so-called “Game of Life”, invented in 1970 by John Conway. In this model each grid point is either “dead” (state zero) or “alive” (state one). Each time step, all the automata (grid points) count their eight immediate neighbors. A cell dies if it has too many or too few neighbors. The simple rule of the “game” is that a cell can only stay alive when it has two or three neighbors. In addition, a dead cell can become alive when it has exactly three neighbors (see Fig. 10.3). This extremely simple CA can be easily studied with a computer, and has become famous for its very complex behavior, despite its simple rules. Although the Game of Life is completely deterministic, its long term behavior is unpredictable. It can have replicating structures and “gliders”, which are structures that propagate through space (see Fig. 10.3). Complex behaviour occurs everywhere in biology, and the Game of Life CA model is a good reminder of the fact that complexity can arise even from very simple rules.

Another example of a simple CA with only two states, that produces nice spatial patterns, is the “Majority Voting” CA (see Fig. 10.4). In this CA, the grid cells count the states in their 3×3 immediate neighborhood (including their own state), and simply adopt the state of the majority in their neighborhood. Thus if more than four cells are alive, a cell becomes alive. The cell dies if less than five cells in the immediate neighborhood are alive. It turns out that this “doing what the majority around you does” produces a patchy spatial pattern, which resembles certain vegetation patterns in which plants need each other to more effectively store and harness water from the soil.

update rules

input ind. state	sum neighbor states	output new ind. state
1	≤ 3	0
1	> 3	1
0	≤ 4	0
0	> 4	1
i.e. if sum ≤ 4		0
i.e. if sum > 4		1

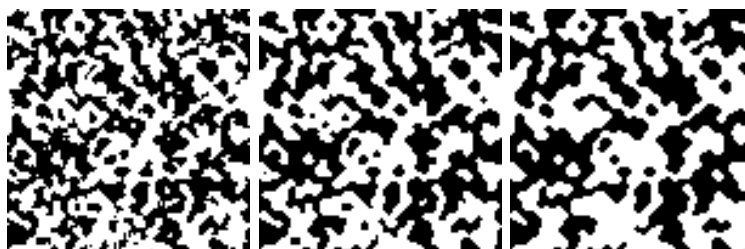
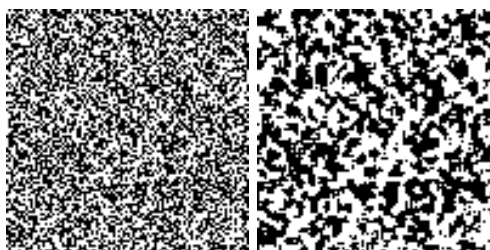


Figure 10.4: Majority voting: from an initial random distribution a stable pattern is attained. First the update rules are shown. Then from left to right and top to bottom time steps 0, 1, 2, 4 and 8 are depicted. Note how a patchy spatial pattern arises.

variable states update rules

	input ind. state	neighbor states	output new ind. state
□ 0 empty	0	at least one 1	0/1 (random movement)
■ 1 moving	0	no 1	0
■ 2 frozen	1	at least one 2	2
	1	no 2	0/1 (random movement)
	2	irrelevant	2

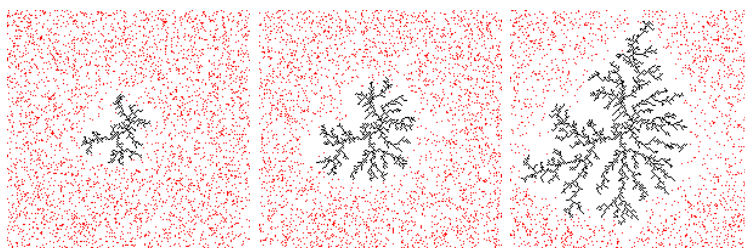
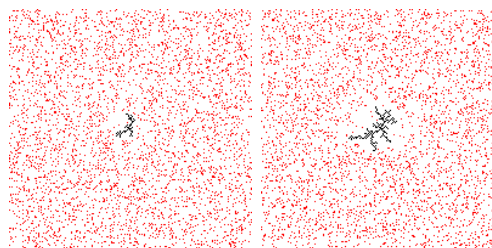


Figure 10.5: Diffusion limited aggregation. From left to right, time steps 100, 200, 400, 800, and 1600 are depicted. Note the growth of a finely structured, fractal-like structure, which resembles a frozen water crystal.

Yet another example is the so-called “Diffusion Limited Aggregation” (DLA) CA. This CA is a model for water molecules that are diffusing in space, and that will freeze whenever they touch another frozen water particle. The CA thus has three possible states for each grid point: empty, moving water and frozen water. One rule of the DLA model is that the water molecules follow a Brownian motion. The second rule is that a moving particle becomes a frozen particle, whenever there is a frozen particle in their immediate 3×3 neighborhood. The simulation depicted in Fig. 10.5 started with a random distribution of water molecules and one frozen particle in the middle. This simple rule generates branching structures that are known as **fractals**, and that are pleasingly similar to ice crystals, branching trees, or branching structures in small arteries.

In chapter 6 we also discussed IBM models. As an example we discussed the model by Hemelrijk

and co-workers on sterling flocking behavior. This example nicely illustrated the use of IBM models both for modeling discrete individuals as well as for modeling complex spatiotemporal patterns. In one of the exercises of the next chapter we will further demonstrate the usefulness of IBM type models for studying dynamical spatial processes.

10.4 Exercises

Question 10.1. Diffusion

In the chapter we derived the diffusion equation as

$$\partial c / \partial t = D \partial^2 c / \partial x^2$$

, which states that the rate of change of a concentration c at a specific time and location can be found from the product of the diffusion rate and the second order space derivative of the concentration c . We also saw that for a discrete space and timestep (as opposed to $\Delta t \rightarrow 0$ and $\Delta x \rightarrow 0$) this can be written as

$$\Delta c / \Delta t = D \frac{\frac{c_{i-1} - c_i}{\Delta x} - \frac{c_i - c_{i+1}}{\Delta x}}{\Delta x}$$

Give an intuitive explanation for why we need the second order derivative to space to describe diffusion using the terms concentration gradient, fluxes and net change of concentration.

Question 10.2. Rabbit populations

Below we list a number of different situations, in which two rabbit populations can occur. Explain what type of modeling formalism (ODE, PDE, CA) you would use to describe these situations, and why.

- Two large rabbit populations separated by a mountain range
- Two large rabbit populations with in between them a medium size forest
- Two tiny rabbit populations with in between them a medium size forest

Question 10.3. Game of Life

Determine the next two spatial configurations of these two initial conditions in the Game of Life cellular automaton:

.....
.....
..xxx..	..xx..
.....	..xx..
.....

Question 10.4. Majority Voting and plants in the desert

Explain why majority voting gives patterns similar to those of vegetation patterns in arid (desert-like) areas. (Hint: the major problem to survive for plants in such areas is to hold on to water in the soil.)

Chapter 11

Dynamic Patterns: Excitable Media

11.1 Introduction

In Chapter 9, we treated the typical behaviour of neuron cells. Characteristic properties of this system are that, in response to a below-threshold stimulus, only a passive return to the equilibrium occurs: the neuron doesn't fire. An above-threshold stimulus on the other hand, produces a large excursion through phase space, which in the case of a neuron is called an action potential. This type of behaviour is called an *all-or-none response*. Furthermore, after a response has been generated, a so-called refractory period occurs. In its refractory state, the system is recovering, and it is not (or less) sensitive to subsequent stimulation.

Another characteristic property of neurons is that action potentials propagate through nerve tissue (i.e. along an axon). If at a certain location an action potential is generated, passive diffusion of ions causes an elevation of membrane potential in nearby locations, causing them to exceed their threshold and generate their own action potential. As a consequence, waves of action potentials can travel through nerve tissue. Due to refractoriness, some time occurs (and has to occur) in between subsequent activation waves. This refractoriness also prevents waves from traveling in the backward direction.

The general properties of activity-waves followed by a refractory period are in fact not unique for nerve cells, but also hold for a number of other biological, chemical and physical systems. Such systems are generally referred to as **excitable media**.

The easiest way to model a spatial excitable medium with wave propagation, is to add diffusion of voltage to the the FitzHugh-Nagumo (FHN) model, described in chapter 9 (see the last question of that chapter):

$$\frac{\partial V}{\partial t} = -V(V - a)(V - 1) - W + D\left(\frac{\partial^2 V}{\partial x^2} + \frac{\partial^2 V}{\partial y^2}\right) \quad (11.1)$$

$$\frac{\partial W}{\partial t} = c(V - bW) \quad (11.2)$$

Note that this describes a two-dimensional spatial system: equation 11.1 has two diffusion terms, denoting diffusion of voltage in two directions (x and y).

11.2 Wave patterns

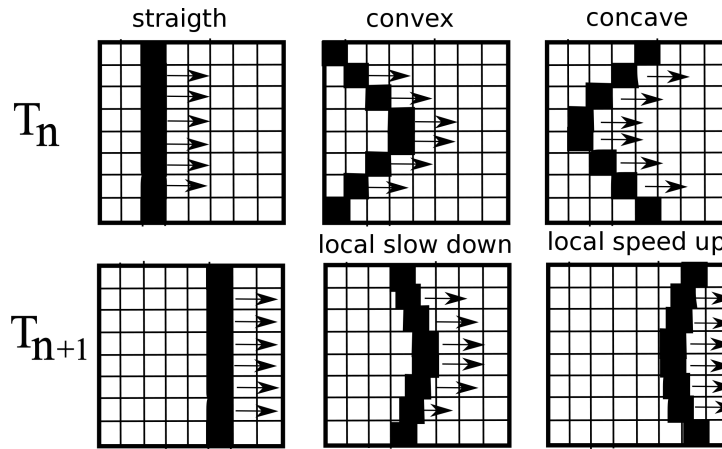


Figure 11.1: **Top:** Straight, convex and concave waves at time T_n . **Bottom:** The same waves at the next time step T_{n+1} . All waves propagate from the left to the right across the tissue. The straight wave maintains the same shape. The convex and concave waves become less convex and concave. Over time they will straighten out.

Now let us consider two-dimensional (2D) excitable media. In 2D, a wave takes the shape of a line on a surface. It turns out that curvature (non-straightness) of this line affects its local propagation speed. To see why this is the case, consider Fig. 11.1.

First consider the convex wave, and look at the part of the wave furthest to the right. At this point the curvature of the wave is largest, and this point of the wave is furthest ahead of the rest. Because the rest of the wave is lagging behind, the excitation (voltage) in this point not only diffuses to points right in front of it, but also to points to the side and back. The flow of excitation to neighbouring points is thus divided over more points, causing it to be less per point. Therefore it will take longer for these neighbouring points to reach the threshold level for which they generate their own excitation response, causing a delay in the propagation of the wave. The more curved the wavefront locally is, the more points will need to be excited by the local point, and the larger the delay is. As a consequence, the points in the wave that are furthest ahead get the largest delay, causing the curved wavefront to straighten out over time.

For a concave wavefront, exactly the opposite applies. Here, consider the most leftward part of the wave, that is most curved and lags behind the most. Because the rest of the wave is ahead of it, not only does this part of the wave only have to excite the points to the right (in front of it), but also part of its job has already been done by other parts of the wave. As a consequence, this part of the wave can excite its neighbours faster than normal, causing a speedup in wave propagation. The more curved the wave is (the further it is lagging behind), the more of its job has already been done, and hence the larger the speedup is. So, also in this case the curved wave will tend to straighten out.

In Fig. 11.2 we show what happens when a wave meets an obstacle. An obstacle is a part of the field that can not be excited, that is, it does not conduct the wave. In nerve or cardiac tissue it can be formed by scar tissue. It can also be formed by a part of the tissue that has different properties due to disease, and is still refractory.

If a wave runs into an obstacle, it locally becomes blocked (at the site of the obstacle), and

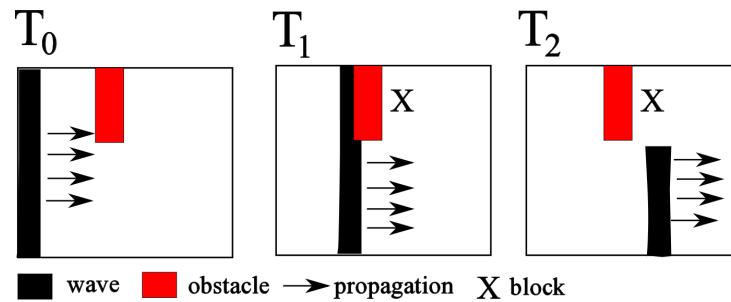


Figure 11.2: **Left:** A wave is initiated on the left side of the 2D tissue (black). In the middle of the tissue is an obstacle (red), that does not conduct the wave. **Middle:** As the wave propagates to the right, its upper half runs into the obstacle, whereas its lower half does not. **Right:** As the wave propagates further to the right, the upper half of the wave that was blocked by the obstacle has disappeared and only the lower half remains.

subsequently disappears. The reason for this is simple. First, because the obstacle does not conduct the wave, the wave can not proceed into and through the obstacle. Second, because there is also no diffusion of the excitation signal through the obstacle, the wave can also not jump across it to excite the normal tissue on the other side. So, at the site of the obstacle, the wave simply comes to a halt and dies out, as locally the end of the excitation is reached. In Fig. 11.2 we see that if the size of the wave is larger than the size of the obstacle, only part of the wave is blocked and disappears. The other part of the wave can still propagate. As a consequence, the remaining wave will no longer span the entire tissue height, and a free wave end or wave-break is formed.

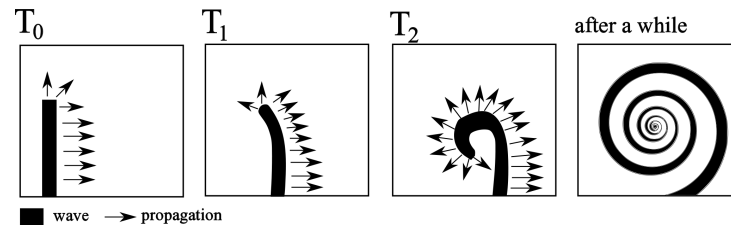


Figure 11.3: From left to right we display how the presence of a wave with a free wave end (far left) over time transforms into a spiral shaped wave (far right).

What happens if, due to an obstacle, a wave with a free wave end is formed? Due to the curvature of such a free wave end, propagation will locally slow down. As a consequence, the wave end will lag behind, curvature will increase, causing even more lagging behind, etcetera. The end-result is that the free wave end will curl back on itself, leading to the formation of a **spiral wave** (Fig. 11.3). (Note that in the case of a free end, curvature of the wave front increases, whereas in the absence of a free end the opposite occurs: curvature decreases.)

Spiral waves are a special type of waves. Because they rotate, they come back to tissue that has already been excited (i.e. has produced an action potential) and has recovered again (i.e. is no longer refractory), to re-excite it. Spiral waves are thus self-perpetuating. This is in contrast with a wave that is initiated by stimulating the tissue once. Such a wave will simply propagate over the tissue, until it reaches the tissues borders, and then disappear, leaving the tissue behind in its resting state.

It turns out that we can have three different types of patterns in 2D tissue. First, **target wave**

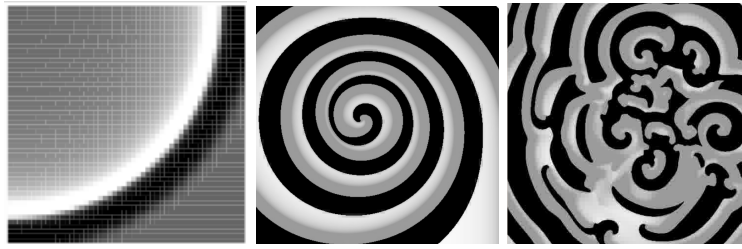


Figure 11.4: **Left:** Target wave pattern **Middle:** Spiral wave pattern **Right:** Turbulent multi-spiral pattern.

patterns arise if the tissue is stimulated normally: a single stimulus produces a single wave (Fig. 11.2, left). Second, we saw that a **spiral wave pattern** can be produced from a target wave pattern if a wave break occurs (Fig. 11.2, middle). Furthermore, it turns out that some spiral waves are unstable, and fragment into a pattern of multiple spiral waves, a self-maintaining **turbulent wave pattern** (Fig. 11.2, right).

11.3 Cardiac tissue and Arrhythmias

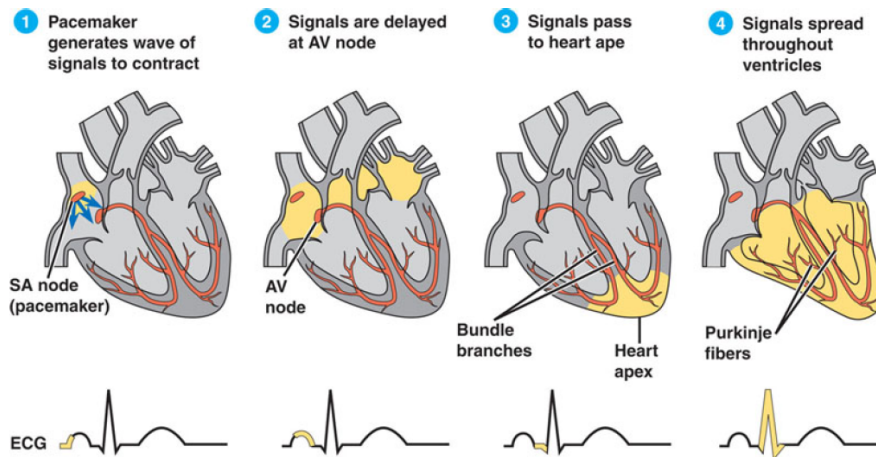


Figure 11.5: Sequence of events during a single normal heart beat, and the corresponding ECG (electrocardiogram) phase. **1.** The heart's pacemaker, the sinus node, generates an electrical signal. **2.** The electrical wave spreads fast across the atria, but can only cross from the atria to the ventricles via the atrioventricular node, where it is delayed. This delay is needed to allow contraction of the atria to occur before contraction of the ventricles. **3.** The His-Purkinje system first conducts the electrical signal from the AV node to the apex of the heart. **4.** From the apex, the electrical wave spreads over the ventricles in a bottom-to-top direction. This direction of wave-spread and contraction is needed, as the arteries through which the blood is pushed out of the heart, are located at the top of the ventricles.

The cells in the heart behave both like nerve cells (they generate and conduct action potentials), and like muscle cells (they contract to produce force). These two properties are connected, the action potential signals the cardiac cells when to contract. Under normal conditions, the natural pacemaker of the heart (the sinus node) produces action potentials at a regular frequency. These

action potentials then quickly spread over the heart, causing the coordinated contraction of first the atria, and then the ventricles. This regular electrical activity is reflected in a regular ECG pattern (Fig. 11.5).

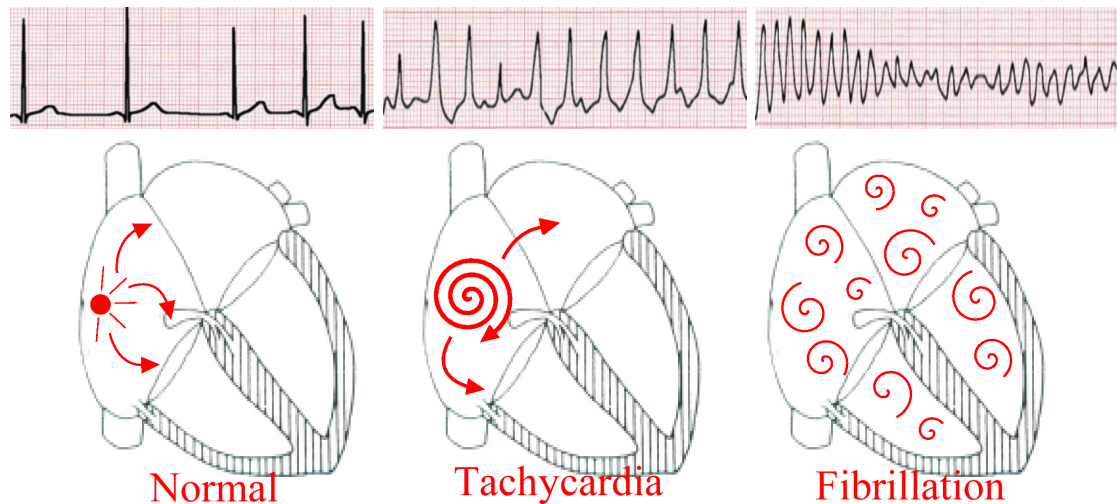


Figure 11.6: **Left:** ECG and excitation pattern during normal heart beats. **Middle:** ECG and hypothesized excitation pattern during tachycardia. **Right:** ECG and hypothesized excitation pattern during fibrillation.

During cardiac arrhythmias, the normal rhythm and coordination of contraction is disturbed. Cardiac arrhythmias are usually caused by abnormalities in action potential generation and propagation, and are reflected by abnormal ECG patterns. In Fig. 11.6 we show ECG patterns of the normal sinus rhythm, tachycardia and fibrillation. During tachycardia, the heart rate is increased, but contraction is still quite coordinated. As a consequence, the pumping of blood is less efficient, but still more or less sufficient. During fibrillation, the heart rate is even further increased, and in addition the coordination of contraction is lost. As a consequence, no effective pumping of blood occurs, so this is lethal within a few minutes. Theoreticians hypothesized that while normal sinus rhythm would correspond to a target wave pattern, tachycardia would correspond to a single spiral wave, and fibrillation would correspond to a multi-spiral turbulent wave pattern (Fig. 11.6).

The idea behind this hypothesis is that for example an infarction scar can act as an obstacle that generates a spiral wave in the heart. Spiral waves typically maximize their rotation frequency: they return to a patch as soon as the action potential and refractory period are over. In contrast, the sinus node will typically operate at a safe frequency, lower than the maximally possible one. Thus the spiral wave emits waves faster than the sinus node. As a consequence, cells will receive an excitation signal from the spiral wave earlier than from the sinus node and hence will respond to the spiral wave signal, and be refractory to the sinus node signal. Therefore the spiral wave takes over control, and it will produce a higher heart rate. If instead of a single spiral, multiple spirals are present, each of these spirals will be in control of its own piece of heart tissue, and these different pieces of tissue will become uncoordinated, causing fibrillation.

Experimental studies in both animal and human hearts have confirmed that the presence of single spiral waves in the heart lead to tachycardia, whereas the presence of multi-spiral turbulence gives rise to fibrillation. Therapies are aimed at preventing spiral waves from occurring, or preventing their fragmentation, or, if they do occur, eliminating them as fast as possible. We will discuss some possible interventions in the exercises.

11.4 Other excitable media

Thus far we have discussed nerve cells and cardiac muscle cells as examples of biological excitable media. However, there are many more types of excitable media in biology.

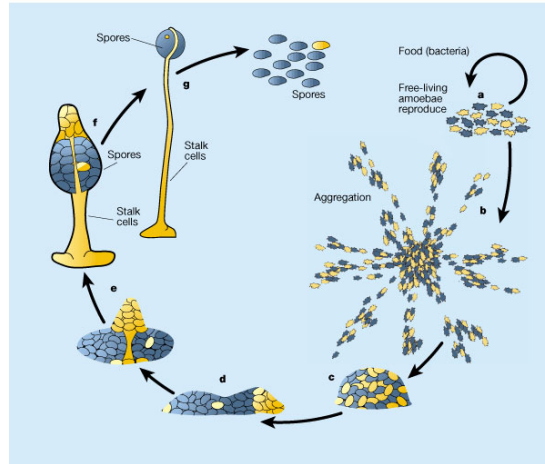


Figure 11.7: Life cycle of the slime mold *Dictyostelium discoideum*. If food and light are sufficiently available, these slime molds live and reproduce as single celled amoebae. However, if food and light become scarce, the single amoebae aggregate into a pile, and this pile changes into a kind of slug. This multi-cellular slug moves in a coordinated manner toward light and heat. If a suitable location is reached, the slug halts and transforms into a stalk with a fruiting body on top. From the fruiting body, spores are released. Upon germination, the spores become single celled amoebae again.

One interesting example is the slime mold *Dictyostelium discoideum* (Fig. 11.7). Slime molds normally occur as single celled amoeba, living in soil. However, when food or light become scarce, these single cells aggregate into a multicellular slug that crawls through the soil to the surface, where it forms a fruiting body. This fruiting body emits single-celled spores, which hopefully spread to locations with better conditions. In order for the cells to aggregate and to coordinately move once they form a multicellular “super-organism”, they communicate with each other through the signaling molecule c-AMP. c-AMP is produced by the cells under stress (too little light or food), and acts as a chemo-attractant to other cells. In addition, these other cells will respond by producing more c-AMP. Finally, after having produced c-AMP the cells become refractory: for a while they can not produce c-AMP or respond to it.

Other interesting examples are the dynamics in certain spatial predator-prey or virus-host systems. We will discuss these in the exercises.

11.5 Exercises

Question 11.1. Fibrillation

- Explain how a heart attack may increase the risk of fibrillation.
- Fibrillation is treated with electrical shocks. How would this stop the fibrillation?

- c. Can you think of an alternative way to end fibrillation?

Question 11.2. Epidemic

The population of a large island has been suffering from an unpleasant infectious disease for decades. The disease tends to spread over the island from village to village, returning each year. The main reason for the persistence of the epidemic is that the immunity to this disease only lasts for a few months. These observations suggest that the epidemic is a wave traveling through an excitable medium.

- What happens when a wave walks into a village that was recently infected by another wave? Someone suggests to eradicate the disease from the island by bringing all susceptible individuals together to infect them all at the same time.
- Would this work?
- A small number of susceptibles defects and stays at home. How would that affect this idea?
- What happens if tourists from non-vaccinated countries visit?

Question 11.3. Spiral formation

Go to <http://www-binf.bio.uu.nl/khwjtuss/SystemsBiology/Movies>

On this website you find movies of spiral wave formation.

- Watch movie 1 and then sketch the primary steps of how a spiral is formed. Why does a wave break curl backwards and form a spiral?
- Compare movies 1, 2 and 3 where spirals are formed in fields of different sizes. What do you observe? Explain why athletes with an enlarged sports heart run a relatively higher risk for arrhythmias?
- Explain how a drug that prolongs action potential duration and hence increases the size of a spiral wave influences arrhythmia risk.
- Play movie 4. Sketch an ECG of the electrical activity you see in the movie.

Question 11.4. Fire spread

Let us consider two NetLogo models for fire spread through a vegetation.

- For the first model, we can use the NetLogo program installed on the local computers. The model can be found under:

File → Models Library → Earth Science → Fire

The model contains trees and fire. Trees can have several different states: normal, on fire, or have been burned. If a tree is not on fire but its near neighbors are it will also catch fire. If trees have been on fire for a while they will stop burning and can not be set on fire again for a while. The fire is started all along the left edge of the forest. Vary the density of trees. What do you observe? Can you explain why this is so?

- Next let us consider another NetLogo model not part of the installed NetLogo version. For this model you should go to:

modelingcommons.org/browse/one/model/3479#model_tabs_browse_applet

This model also contains vegetation and fire. In this model, after the vegetation has burned down, it takes a certain amount of time before it has regrown and can easily catch fire again. Put differently, the probability of flammability, that the fire spreads to the next tree, (*pfs*) is a function of the time since the last fire happened for that particular tree (*tsf*). The amount of time this recovery takes can be varied using the **log-alpha** and **tp-max** parameters. In this model, rather than initiating the fire at one edge of the vegetation, at each timestep fire is set at a number of random locations, this number, the **ignition rate**, can also be varied in the model. Play around with the number of fires per timestep and the log-alpha

and tp_{\max} values influencing how flammability depends on time of last fire. What do you observe? Explain.

Question 11.5. Evolution of Virulence and Contagiousness

A host and its virus pathogen co-evolve. The host tries to prevent infection, the virus tries to optimize infection. For most viruses, this evolution does not lead to maximum virulence (pathogenicity, how sick you get of a given pathogen) and contagiousness (“besmettelijkheid”), as one at first sight may naively expect. Explain why, keeping the knowledge you gained in this chapter in mind.

Chapter 12

GRIND

The phase portraits in this book were made with a computer program called GRIND, for GReat INtegrator Differential equations. The user interface of GRIND is not as fancy as that of similar programs (like Berkeley Madonna), but GRIND has phase plane analysis as its major additional feature. GRIND allows you to study differential equation models by means of numerical integration, steady state analysis, and phase space analysis (e.g., nullclines and separatrices). The model equations are defined in a very natural formalism, and one can easily change parameters and initial conditions. The user interface to GRIND is based upon a simple command language. The best way to learn more about GRIND is to walk through the example listed below. Table 12.1 lists the most important GRIND commands, and the full manual is available from theory.bio.uu.nl/rdb/grind.pdf. GRIND commands have a help function to remind you of their syntax.

The best way to get started is to download a GRIND model, e.g., `lotka.grd`, from the website theory.bio.uu.nl/rdb/tb/models. On the Utrecht University computers it is best to save that file on the U-drive, and then double-click the file. This opens a black “command line” window in which you see the equations of the model. The prompt `GRIND>` asks you to type commands into GRIND. Models can be changed by opening them with a Windows texteditor, e.g, Wordpad.

On Windows computers it should be easy to install GRIND on your own computer. GRIND is publicly available from theory.bio.uu.nl/rdb/grind.html, and can best be installed with the installer (Method 1). Grind also operates under Apple Unix, and Linux (see the same web page).

12.1 Lotka Volterra model

A Lotka Volterra model with a density dependent growth rate of the prey can be studied with GRIND by downloading the file `lotka.grd` from the theory.bio.uu.nl/rdb/tb/models website, and then double-clicking it. Alternatively, you can type the following text file, and save it under the name `lotka.grd`. Note that models have to be saved on the U-drive. The file `lotka.grd` contains the following:

```
R ' = r*R*(1-R/k) - a*R*N;
N ' = c*a*R*N - d*N;
```

The model has two differential equations, $R' =$ and $N' =$, and five parameters a , c , d , k , and r . Note that r is different from R !

After firing up GRIND, by clicking the `lotka.grd` file in Windows, or typing `grind lotka` in Linux, you start typing commands and parameter values as soon as you get the `GRIND>` prompt. For example:

```
display lotka.grd
a=1
c=1
d=.5
r=1;k=1
R=0.01;N=0
par lotka.txt
```

This first displays the model equations of the `lotka.grd` file. The following lines set the parameters, and then gives an initial condition with a little bit of prey and no predators. The last line lists all parameter values, and saves them to a file `lotka.txt` that you can re-use in a later session by reading the file. Working with a model called `lotka` GRIND will read the file `lotka.txt` when you type `read`. Note again that GRIND is case sensitive.

Now you are ready to go. To obtain a numerical solution say that you want twenty time steps and give the `run` command:

```
finish 20
run
timeplot
where
```

On your screen you get a listing of the predator and prey values obtained by “running” the model and solving the differential equations numerically. Timeplot makes a nice graph on your screen. The `where` command gives the final state.

The curve on the screen depicts the logistic growth of the prey.

Next we become interested in the predator:

```
N=0.01
run
ti
fin 50 50
run
ti
```

Which first sets the initial condition of the predator, runs, and makes a new timeplot. Then the integration time is changed to 50 time steps asking for all 50 time points. The model is solved and timeplot is called.

The main feature of GRIND is phase plane analysis:

```
2d
nullcline
vector
run
ti
d=0.9
2d;nu
```

Which depicts a 2-dimensional phase space, draws nullclines, shows the vector field, and the trajectory. Finally, the phase space is redrawn for $d = 0.9$.

GRIND can do local stability analysis for you:

2d	make a 2-dimensional phase space
axis	define the identity and scaling of an axis
bye	leave GRIND
bifurcate	make a series of Poincaré sections
continue	follow a steady state as a function of a parameter
cursor	ask for a mouse click to set the initial condition
display filename	show the contents of a text file
eigen	compute eigenvalues
export	export a picture to a file
finish	set the time span and number of points reported
grid	start many trajectories
help	get help
keepvar	copy the final state into the initial state
newton	approach a close-by equilibrium point
noise	set Gaussian or uniform noise on a parameter
nullcline	draw nullclines
parameter	list parameter setting and/or save them into a file
poincare	make a poincaré section
read filename	read a file with parameters and/or commands
run	solve the model numerically
timeplot	depict the solutions
vector	show the vector field
where	where am I?

Table 12.1: A sample of the most important GRIND commands. Note that GRIND commands can be abbreviated to the first two letters.

```
axis x R 0 0.9
d=0.5
parameter lotka.txt
2d
nu
cursor
newton
eigen
```

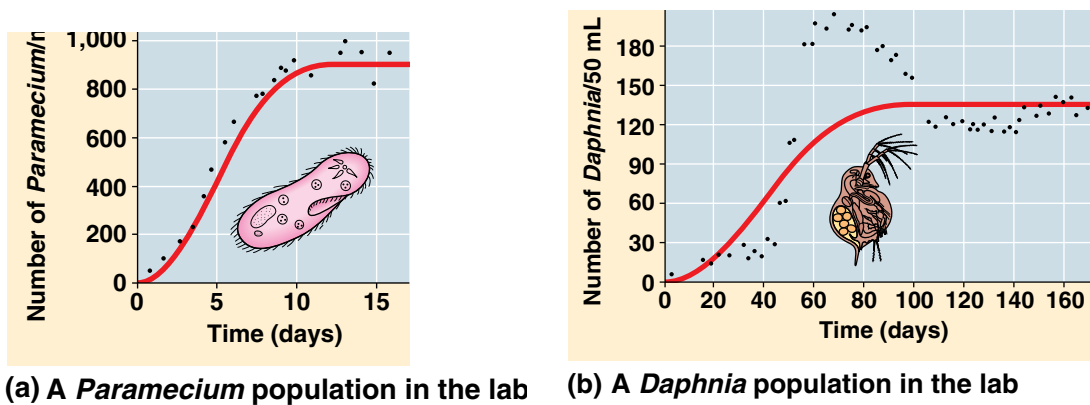
Illustrates the usage of the `axis` command. Parameter values are listed and saved into a file `lotka.txt`. Such a file can later be read with the `read` command. Redraw the nullclines for $d = 0.5$ and click with the mouse close to the non-trivial intersection point of the two nullclines. Then do a “Newton Raphson” iteration to approach a nearby equilibrium point, and display the eigenvalues.

To set Gaussian variation on a parameter:

```
noise k 1 0.2
run
fin 100 100
run
ti
bye
```

Noise draws new values for k every time step from a Gaussian distribution with mean 1 and standard deviation 0.2. The model is solved. The time length is increased, the model is run, and the solution is plotted.

12.2 Exercises



Copyright © Pearson Education, Inc., publishing as Benjamin Cummings.

Figure 12.1: Logistic growth of *Paramecium* and non-logistic growth of *Daphnia*. From: Campbell and Reece (2008).

Question 12.1. Tutorial

Here is a set of questions to test if you understood the tutorial you just did:

- When you called `run;timeplot` you got a nice graph on your screen. What is the meaning of this graph?
- How is the system of ODEs defining this graphs?
- When you called `2d>nullcline` you also got nice graphs on your screen. What do these mean?
- With the Newton Raphson command you just jump to a nearby steady state, whether it is stable or unstable. After issuing the `eigen` command, GRIND responds with eigenvalues. What do these values tell you?

Question 12.2. The Monod functional response

In Chapter 4 we analyzed the following predator prey model with a saturated functional response:

$$F = R/(h + R);$$

$$R' = rR*(1-R/K) - b*N*F;$$

$$N' = b*N*F - d*N;$$

The algebraic expression F defines the functional response, and is used in the differential equations $R' =$ and $N' =$.

This model is available from `theory.bio.uu.nl/rdb/tb/models` as the file `monod.grd` with the corresponding parameter file `monod.txt`.

- Double click the monod model and start with `read monod.txt`. Check the equations (`display`) and its parameter values (`par`).
- Make a time plot showing the logistic growth of the prey by starting with zero predators and few prey. Explain in words what this curve represents.
- Now study the 2-dimensional system by making a phase space. List the parameter values and make qualitatively different phase spaces. Sketch trajectories for each of these systems.
- When is the non-trivial steady state stable and when is it unstable? What is the behavior when it is unstable?
- What is the effect of changing the carrying capacity of the prey? Can you repeat Rosenzweig's paradox of enrichment?
- Which population increases most when you increase the carrying capacity of the prey?
- In Fig. 12.1 the growth of *Daphnia* is compared with logistic growth of *Paramecium* (see Fig. 12.1). A striking difference is that *Paramecium* asymptotically approaches its carrying capacity, whereas *Daphnia* has an oscillatory approach to its steady state. As *Daphnia* feeds on algae you can use this Monod saturated predator prey model to see if you can understand *Daphnia*'s

growth curve depicted in Fig. 12.1b. Simulate the experimental curves in Fig. 12.1 by adding a few predators to a prey population at carrying capacity. Can you obtain the oscillatory approach of *Daphnia*?

h. Can you also obtain the asymptotic approach of *Paramecium* with the same model for other parameter values?

Question 12.3. Cattle in the Sahel

In the last exercise of Chapter 7 you repeated the classical work of Noy-Meir (1975) and obtained catastrophic saddle-node bifurcations using sigmoid functional responses of cattle feeding on a sparse vegetation. We here ask you study a more recent alternative model that emphasizes the dynamics of water uptake in arid zones (Rietkerk and Van de Koppel, 1997; HilleRisLambers et al., 2001). The main idea of this new model is that in arid areas without any vegetation coverage, most of the water that falls on the soil by the sometimes heavy rainfall fails to penetrate into the soil. Instead the water is rapidly washed off into rivers and disappears. Thus, the vegetation cover increases the penetration of water into the soil. Additionally, models for vegetation growth in arid areas can remain simple because the availability of water in the soil is typically the major limiting factor for vegetation growth. This main idea is translated into the following model:

$$\begin{aligned}\frac{dW}{dt} &= R\left(w_0 + \frac{V}{k_2 + V}\right) - r_W W - \frac{gVW}{k_1 + W}, \\ \frac{dV}{dt} &= i + \frac{cgVW}{k_1 + W} - dV,\end{aligned}$$

where R is the rainfall (in mm d⁻¹), V is the vegetation biomass (in g m⁻²), and W is the amount of water in the soil (mm). The model has two saturation constants, k_1 (mm) defines the amount of water at which the vegetation grows at half its maximal rate, and k_2 (g m⁻²) is the vegetation cover at which the penetration of water into the soil is $R(w_0 + 1/2) = 1.4$ mm d⁻¹. Parameters of this model have been estimated by Rietkerk and Van de Koppel (1997) and HilleRisLambers et al. (2001) and are:

Name	interpretation	value	dimension
R	rainfall	2	mm d ⁻¹
c	conversion of water to plant biomass	10	g mm ⁻¹ m ⁻²
d	death rate of vegetation	0.25	d ⁻¹
g	maximum water uptake	0.05	mm g ⁻¹ m ² d ⁻¹
k_1	half saturation constant	5	mm
k_2	half saturation constant	5	g m ⁻²
r_W	soil water loss due to evaporation	0.2	d ⁻¹
w_0	water infiltration in absence of vegetation	0.2	—
i	immigration of seeds/plants	0.01	g m ⁻² d ⁻¹

The death rate of the vegetation is partly due to normal turnover and partly due to grazing by cattle. In the absence of cattle the vegetation turnover is about $d = 0.05$ d⁻¹, and the vegetation reaches a carrying capacity of approximately 450 g m⁻². A single cow per farm corresponds to a grazing rate of 0.025 d⁻¹. In the absence of a vegetation there is about 2 mm water in the soil. The model and its parameter file are available on the website under the names `sahel.grd` and `sahel.txt`, respectively. The latter file defines three macros, one for clicking in the phase space to determine the stability of a steady state, one for buying a cow, i.e., setting $d = d + 0.025$ d⁻¹, and one for selling a cow, i.e., setting $d = d - 0.025$ d⁻¹ and running the corresponding

trajectory. The `sahel.txt` file defines a logarithmic axis for the vegetation because the vegetation grows exponentially and covers a wide range of densities.

- Check the dimensions of all terms. Why is there 2 mm of water in the soil if there is no vegetation?
- Compute the approximate location of the $dV/dt = 0$ nullcline by ignoring the immigration term i . How much water do you expect in the soil if there is a rich vegetation?
- Use Grind to draw the nullclines if the average herd size is 8 cows per farm, i.e., set $d = 0.05 + 8 \times 0.025 = 0.25 \text{ d}^{-1}$.
- Identify the stability of all steady states and give each of them a biological interpretation.
- Make a phase portrait by running the Grind `grid` command. Which of the two variables has the fastest time scale, and is that reasonable?
- Study the effect of increasing and decreasing the herd size by buying and selling cows (use the two macros). Make a sketch of the expected vegetation cover as a function of the death and grazing rate d .
- Perform a similar analysis for the effect of the rainfall. What is the effect on the vegetation of a few years of low, or high, rainfall, and how does this depend on the herd size?
- You can try to use GRIND for making a bifurcation diagram (Warning: GRIND is not so good at this and may crash, so save your work first). For instance, use the `click` macro to select the saddle point as an initial point, select d as a bifurcation parameter by defining the horizontal axis as `axis x d 0.05 0.35`, and issue the `continue x 1` to follow this steady state for different values of d .

Question 12.4. Several immune responses to HIV

It is not well understood why some people infected with the AIDS virus survive much longer than others. One of the prevailing ideas is that individuals who survive better mount more immune response to HIV than those with fast disease progression. You will be asked to study the effect of the diversity of the immune response during a chronic viral infection. Shortly after sexual transmission HIV migrates into lymphoid tissues where the viral particles infect activated $CD4^+$ T cells, which after about two days burst and produce tens of thousands new virions. The new virions infect new $CD4^+$ T cells in the lymphoid tissues. Over a time course of the first few weeks infected individuals develop several $CD8^+$ cytotoxic T cell (CTL) immune responses. CTL kill virus infected cells. The death rate of infected cells has been measured in hundreds of patients, and surprisingly it was found that in almost all individuals the expected life span of productively infected $CD4^+$ T cells is one to two days, and that this life span hardly depends on the virus load, or the immune response in these patients (Bonhoeffer et al., 2003). Thanks to collaborative work between immunologists, virologists and mathematical modelers many parameters of this viral infection have been quantified. We know that the virus replicates at a rate of approximately $r = 1.5 \text{ d}^{-1}$ before the number of $CD4^+$ target cells and/or the immune responses become limiting, and we know that the maximum effective population size is about $K = 10^5$ infected cells. Activated CTL divide at a maximum rate of approximately $p = 1 \text{ d}^{-1}$ and have an expected life span of about ten days ($d = 0.1 \text{ d}^{-1}$). Every infected individual mounts several CTL responses, that seem to co-exist despite differences in their affinity, a_i , for the epitopes expressed by infected cells. This can be summarized by the following model:

$$\delta = k \sum_{i=1}^n a_i E_i \quad , \quad \frac{dI}{dt} = rI(1 - I/K) - \delta I \quad , \quad \frac{dE_i}{dt} = \frac{pE_i a_i I}{h + E_i + a_i I} - dE_i \quad ,$$

where $i = 1, 2, \dots, n$ defines the number of immune responses. Here δ is the death rate as determined by the total cytotoxic response, I is the number of infected cells, and E_i is the number of killer cells in each immune response. The proliferation rate of the immune responses is determined by a competitive saturation function allowing a maximum division rate $p \text{ d}^{-1}$ when $a_i I \gg h + E_i$, and requiring more infected cells $a_i I$ at higher cell numbers (i.e., E_i in

the denominator basically increases the saturation constant h). Since CTL require few infected cells to become fully stimulated, we set $h = 100$ cells. The parameter $0 \leq a_i \leq 1$ measures the affinity of each response for the epitopes expressed by infected cells. A CTL with an affinity $a_i = 1$ requires the lowest amount of infected cells to become stimulated, i.e., will divide at its half maximal rate when $I = h$ cells. This model, with $n = 3$ immune responses, and its parameter file are available on the website under the names `ctl.grd` and `ctl.txt`, respectively. The affinity is set to $a_1 = 1, a_2 = 0.5$ and $a_3 = 0.1$, and the mass-action killing rate to $k = 10^{-4}$ per CTL per day, i.e., about 10^4 CTL are required to achieve a killing rate of $\delta = 1 \text{ d}^{-1}$. The parameter file defines logarithmic axes because all populations grow exponentially and cover wide ranges of densities.

- a. Study a simple infection by starting with one infected cell, $I = 1$ cell, and one excellent CTL, $E_1 = 1$ cell, and by simulating the model for about three months, e.g., `finish 100 100` days. What is the set-point level of infected cells, what is the steady state immune response, and what is the killing rate at that steady state (`value delta`)?
- b. What would the set-point be in the absence of any immune response? What is then limiting the infection and is this realistic?
- c. What would the set-point be if the affinity of E_1 were 2-fold lower? What would the size of the immune response and the killing rate be?
- d. Note that for $h \ll E_i + a_i I$ the steady state expression of the equation for the immune response simplifies to

$$pE_i a_i I / (E_i + a_i I) - dE_i = 0 ,$$

which after division by E_i delivers a simple relation between the expected number of killer cells per infected cell. Derive this relation and check in Grind whether it is approximately correct for $h = 100$ cells.

- e. Now study a diverse immune reaction by allowing $n = 3$ CTL responses, i.e., set $a_1 = 1, a_2 = 0.5$ and $a_3 = 0.1$ and initialize I, E_1, E_2 , and E_3 as one cell. Study the first three months of the infection. What is now the viral load at set point and what are the densities of the three immune responses?
- f. What is the expected killing rate of infected cells? How can it be that this does not depend on the diversity of the immune response?
- g. What would this killing rate be if all three immune responses were of high affinity? Can you explain this? (Hint: check the steady state expression of $dI/dt = 0$ for the case that the immune responses collectively keep $I \ll K$).
- h. What is your expectation for the life span of infected cells in patients with very different immune responses? What is the effect of the diversity of the immune response in the viral set point on 1) number of infected cells, 2) the size of the immune response, and 3) the killing rate.
- i. The proliferation term of this model is fairly complicated. What would have happened with the diversity of the immune response at steady state, if we had written a conventional saturation function $pE_i a_i I / (h + a_i I)$?
- j. Simplify the proliferation term for the cases where there are very many infected cells, i.e., $a_i I \gg h + E_i$, and where there are very many killer cells, $E_i \gg h + a_i I$. Do you get reasonable proliferation terms in each of these two cases?
- k. How was the death rate of productively infected cells actually measured in Chapter 8?

Chapter 13

Examples of exam questions

The true exam will be in Dutch and the Glossary of Chapter 14 will be provided.

Question 13.1. Larvae and adults

Consider an insect population where there is competition between the larvae and the adults. The larvae L therefore suffer from density dependent death imposed by the adults A :

$$\frac{dL}{dt} = aA - bL(1 + A/k) - cL \quad \text{and} \quad \frac{dA}{dt} = cL - dA .$$

- Sketch (!) the nullclines for all qualitatively different possibilities.
- Determine the vector field.
- Determine the stability of the non-trivial steady state.
- Simplify the model into one differential equation by assuming that the kinetics of the larvae is much faster than that of the adults.

Question 13.2. Eider down

Eider ducks make their nest on the ground with a very rich down that on Iceland is being harvested for the highest quality sleeping bags and coats. Some populations of the Common Eider, *Somateria mollissima*, are infected with parasitic worms that are transmitted directly between healthy and infected eiders. Thus, the most important enemies of the eiders are (1) people ruining their nests for collecting eider down, and (2) this lethal worm. Consider the following model for healthy eiders, E , and dying infected eiders, D , where we assume that healthy eiders suffer from a density dependent death (the infected eiders die rapidly anyway):

$$\frac{dE}{dt} = E(fb - d(1 + cE) - \beta D) \quad \text{and} \quad \frac{dD}{dt} = D(\beta E - \delta) ,$$

where b is the normal birth rate, β is an infection rate, and f is the fraction of nests that is not harvested for eider down. The d and δ parameters are death rates.

- What is the carrying capacity of the eiders in the absence of harvesting and worms (i.e., for $f = 1$ and $D = 0$)?
- What is the R_0 of the ducks, and what is the R_0 of the infection?
- Express the steady state from **a** in terms of the R_0 of the ducks.
- What would be the steady state of the ducks if half of the nests were destructed ($f = 1/2$) in the absence of the infection ($D = 0$)?

- e. What is the steady state of the healthy ducks, \bar{E} , in the presence of the infection?
- f. What would be the effect on the steady state number of healthy ducks, \bar{E} , if one would forbid the harvesting of down in infected eider populations?
- g. Sketch the nullclines for $f = 1$ and $f = 1/2$ for an area with infected ducks.

Question 13.3. Immunity

A natural model for a virus infection has target cell T , infected cells I , virus particles V , and immune effector cells E that clean up the infected cells:

$$\begin{aligned}\frac{dT}{dt} &= \sigma - \delta_T T - \beta TV, & \frac{dI}{dt} &= \beta TV - \delta_I I - kEI, \\ \frac{dV}{dt} &= pI - \delta_V V, & \frac{dE}{dt} &= aEI - \delta_E E,\end{aligned}$$

where σ is the production of new target cells, β determines the infection rate, k is the killing rate of infected cells by effector cells, p the production of virus particles, a the growth and activation of effector cells, and the various δ parameters determine the life spans of the cells and virus particles.

- a. Modify the model such that the virus is no longer limited by the availability of target cells.
- b. Simplify this new model by assuming that the turnover of virus particles is much faster than that of the other entities.
- c. Sketch the nullclines.
- d. Provide a biological interpretation of all steady states.

Chapter 14

Glossary

A dictionary translating some technical terms from English to Dutch:

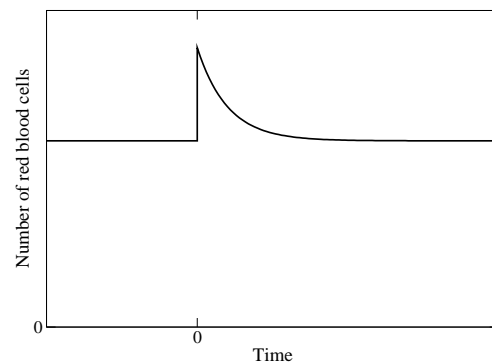
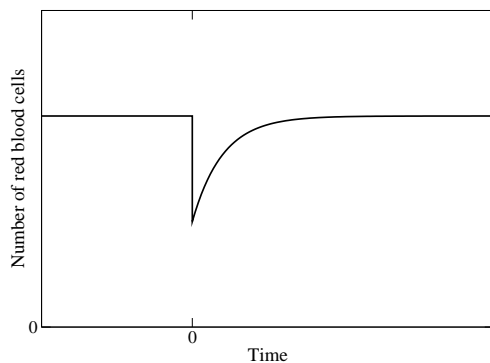
Brownian motion	diffuse beweging van partikels
CA	cellulaire automaat
decay	verval
deterministic	niet stochastisch; zonder kansproces
efflux	uitstroom
equilibrium point	evenwichtspunt
limit cycle	limiet cyclus
half life	halfwaardetijd
nitrogen	stikstof
nullcline	0-isocline
ODE	normale differentiaalvergelijking
<i>per capita</i>	per hoofd
PDE	partiële differentiaalvergelijking
phase space	toestandruimte
pineal gland	epifyse of pijnappelklier (producent van melatonine)
potassium	kalium
quasi steady state	quasi evenwichtspunt
sodium	natrium
solution	oplossing
stochastic	stochastisch: met kansproces
steady state	evenwichtspunt
susceptible	vatbaar
tangent	raaklijn
viral load	virus concentratie in het bloed
viral setpoint	karakteristieke virus concentratie in het bloed

Chapter 15

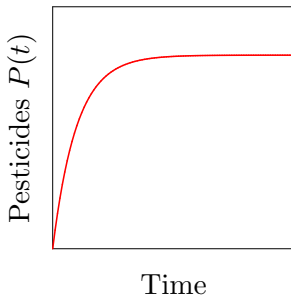
Answers to the exercises

Question 1.1. Red blood cells

A possible good answer has the following sketches:



- a. $dN/dt = m - dN$, so similar to equation 1.3
- b. For this let us first study whether the equation has an equilibrium, so let us solve $m - dN = 0$ which results in $N = m/d$.
If we would draw $f(N) = m - dN$ this would be a descending straight line with an intersection point of $(0, m)$ with the y axis and of $(m/d, 0)$ with the x-axis, so left of m/d the graph lies above zero and arrows in the phase portrait point to the right, whereas right of m/d the graph lies below zero and arrows in the phase portrait point to the left: the equilibrium point m/d is stable. Alternatively, this stability can be derived from the solution equation 1.4.
Now, consider donating blood, which results in a reduction in your blood content. Because the equilibrium is a stable attractor, over time your blood content will return to the level m/d : See the sketch in Panel (a)
- c. Receiving blood temporarily increases your blood content, again the stable equilibrium will cause a return of your blood levels to the m/d level: See the sketch in Panel (b)

Question 1.2. Pesticides on apples

- a. To do this note that $\sigma - \delta P = 0$ results in an equilibrium pesticide level of $P = \sigma/\delta$. As in the previous exercise (exact same shape of the differential equation and hence of the solution) this equilibrium is stable. Assuming you start out with zero pesticide levels at birth you will over time approach the stable equilibrium: See the sketch.
- b. $\bar{P} = \sigma/\delta$.
- c. By stopping your apple intake the model for pesticide dynamics now becomes $dP/dt = -\delta P$ with the initial condition $P(0) = \sigma/\delta$. For an equation of the shape $dP/dt = -\delta P$ we now that the general solution is $P(t) = P(0)e^{-\delta t}$. To find the time at which we reach $P(0)/2$ we thus can solve $P(0)/2 = P(0)e^{-\delta t}$ which yields $t_{1/2} = \ln[2]/\delta$.
- d. From $dP/dt = 2\sigma - \delta P$ with $\bar{P} = 2\sigma/\delta$, one obtains the same $\ln 2/\delta$ days for the half life. In other words, as decay time of the pesticide stays the same so does the half-life in which half of it disappears. The only difference is in the absolute amount, which will be higher.
- e. For this we solve $50 = \ln 2/\delta$ from which we obtain $\delta = 0.014$ per day.

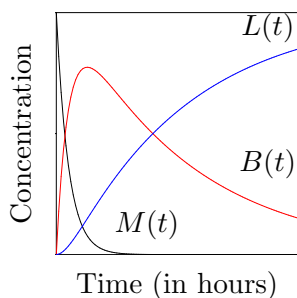
Question 1.3. Bacterial growth

- a. $t = \ln[2]/r$.
- b. $dB/dt = rB - kNB = (r - kN)B$ has as a solution $B(t) = B(0)e^{(r-kN)t}$. So, if $r - kN < 0$ we have exponential decrease of the bacteria, whereas for $r - kN > 0$ we have exponential growth of the bacteria. Thus it should hold that $N > r/k$. Alternatively, from a phase portrait analysis we find that if $N > r/k$ $rB - kNB$ is a decreasing line, so the equilibrium $N = r/k, B = 0$ is stable whereas for $N < r/k$ the line is increasing, causing the equilibrium to be unstable resulting in a persistent increase of the amount of bacteria.
- c. $\frac{dB}{dt}$ has the dimension “nr of bacteria per ml per hour”, so the terms rB and $-kNB$ should have these same dimensions. In rB the B takes care of the “nr of bacteria per ml” part, so r has the dimension per hour. The same holds for the B in the kNB term, this means that kN has the dimension per hour, and hence k has the dimension “per neutrophil per hour”. This can also be checked from the expression $N = r/k$ that should be “neutrophils per ml” on both the left- and right-hand side.
- d. Again the whole term $\frac{kNB}{h+B}$ should be in “nr of bacteria per ml per hour”. The $\frac{B}{h+B}$ part is dimensionless. Thus kN should also have the dimension “nr of bacteria per ml per hour”. Given that N represents the nr of neutrophils per ml this means that k has the dimension “bacteria per neutrophil per hour”. Note that this is the maximum number of bacteria that one neutrophil can encounter and kill per hour.
- e. From $rB - kNB/(h+B) = 0$ we neglect the trivial $B = 0$ and obtain $N = (r/k)(h+B)$ as an equilibrium. Given $B(t) = B(0)e^{(r-(kN/(h+B)))t}$ we derive that for $N < (r/k)(h+B)$ there is exponential growth, while for $N > (r/k)(h+B)$ there will be exponential decay. Alternatively, from a phase portrait analysis we find that for $N < (r/k)(h+B)$ we have an increasing function ($dB/dt > 0$) so the equilibrium is unstable and bacteria keep growing indefinitely, while for $N > (r/k)(h+B)$ we have a decreasing function ($dB/dt < 0$) and the equilibrium is stable, keeping the bacteria in check. Note that in this case the number of neutrophils needed to control bacteria is actually dependent on the number of bacteria, which makes more sense.
- f. h needs to have the same dimension as B , number of bacteria per ml. When $B = h$ the model is $dB/dt = rB - kN/2$ saying the neutrophils are killing at a rate $k/2$, i.e., half their

maximal killing rate.

Question 1.4. Injecting anesthesia

- Note that in the muscle there is only exponential decay, whereas in the blood and liver there is a combination of an exponential growth and decay process. See the sketch.
- $t_{1/2} = \ln 2/e$ hours.
- During the whole operation one would like the highest possible amounts of anesthesia in the blood. As can be seen from the figure, anesthesia levels in the blood first increase and then decrease. The moment at which increase switches to decrease depends on the rate of efflux from muscle to blood e and the rate of clearance from the blood c : when cB exceeds eM this switch occurs. For lower values of c it will take longer for cB to exceed eM and hence anesthesia levels in the blood will keep increasing longer, reaching higher levels. Thus, given e , the optimal operation time depends on the clearance rate from the blood c , and also on how long the operation takes (ideally switch from increase to decrease should be somewhere midway operation so throughout operation you have quite high levels).
- For $\delta = 0$ everything ends up in the liver: $L(\infty) = M(0)$.



Question 1.5. SARS

- Let us count the total number of infected patients $I(t)$. $R_0 = 3$ in two weeks means that $\beta = 1.5$ per week. Also the number of weeks an individual survives was $1/d = 2$ weeks so $d = 0.5$. For a time scale of weeks the model therefore is $dI/dt = 1.5I - 0.5I = I$. The equation to solve is $3 \times 10^9 = I(0)e^{rt}$, where $r = (\beta - \delta) = 1$, and where one starts with one infected individual, i.e., $I(0) = 1$. Solving $3 \times 10^9 = e^t$ yields $t = 22$ weeks for the time required to have $I(t) = 3 \times 10^9$.
- To answer the more difficult question when half of world population is still uninfected one should also keep track of the total number of dead individuals $dD/dt = \delta I$ and solve $I(t) + D(t) = 3 \times 10^9$ (which for $\beta = 1.5$ and $\delta = 0.5$ per week gives a total time of $t = 21$ weeks [not shown]). The difference remains small because the epidemic is growing exponentially.
- No, it will go slower because the epidemic will limit itself by depleting the number of susceptibles. A better model is to add an ODE for the susceptibles, S , where $S(0) = 6 \times 10^9$ is the initial population size. By redefining β as the chance to meet and infect a susceptible person the model then becomes:

$$\frac{dI}{dt} = \beta IS - \delta I \quad \text{and} \quad \frac{dS}{dt} = -\beta IS.$$

Another improvement of the model that would slow down the epidemic is to allow for an incubation period, i.e., to introduce a time lag at the beginning of the two week period during which patients are not yet infective.

Question 1.6. Chemical reactions

$$\begin{aligned} \frac{dA}{dt} &= k_1 AS - k_2 AB - 2k_3 E_1 A^2 \\ \frac{dB}{dt} &= k_2 AB - k_4 BE_2 \end{aligned}$$

Please note that you need powers, like A^2 terms, to account for the correct collision rates (i.e. one A needs to bump into another A for this reaction so the probability and hence rate

of such an event is proportional to the concentration of A to the power 2), and stoichiometry constraints, like the $2k_3$ terms, to account for the conservation (i.e. in this reaction 2 A molecules disappeared).

Question 1.7. Physics

- The dimension of v is m/s and that of a is m/s².
- The derivative of the $v(t)$ solution is $dv/dt = a$ and that of the $x(t)$ solution is $dx/dt = at + v(0)$.

Question 2.1. Heck cattle

- The population will be at steady state when the *per capita* birth rate equals the death rate, which happens at a density of about 330 animals (intersection point of the birth and death lines).
- The maximum birth rate $b = 0.4$ per year and the minimum death rate is 0.03 per year. Since we now that at 400 animals the birthrate is approximately 0.2 we can solve $0.4(1 - 400/k_1) \simeq 0.2$ and estimate that $k_1 = 800$ animals. Since we now that at 500 animals the death rate is approximately 0.33 we can solve $0.03(1 + 500/k_2) \simeq 0.33$ we can estimate that $k_2 = 50$ animals. When $N = k_1$ the birth rate is zero and when $N = k_2$ the death rate has doubled.
- The full model becomes

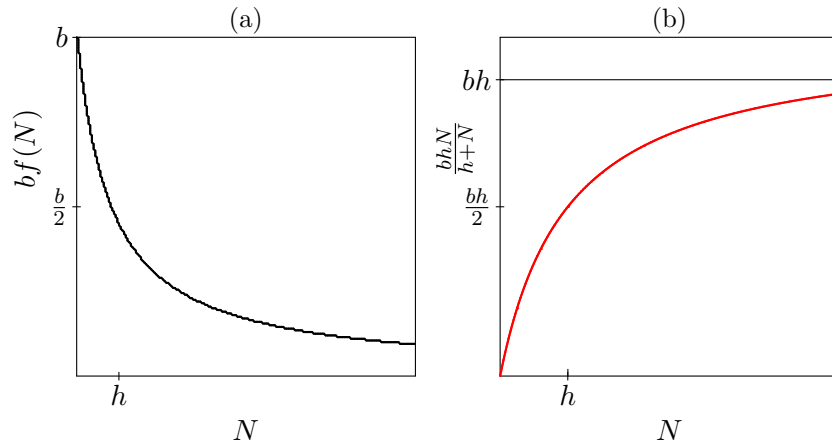
$$\frac{dN}{dt} = [\beta(N) - \delta(N)]N = [0.4(1 - N/800) - 0.03(1 + N/50)]N.$$

Setting $dN/dt = 0$ gives $\bar{N} = 0$ or $0.4(1 - N/800) - 0.03(1 + N/50) = 0$. This can be rewritten as $0.4 - (0.4N/800) - 0.03 + (0.03N/50) = 0$ and then $0.4 - 0.03 = (0.4/800 + 0.03/50)N$ which finally gives us $\bar{N} = \frac{0.4-0.03}{0.4/800+0.03/50} = 336$ animals.

- The death rate is $\delta(N) = 0.03(1 + 336/50) = 0.23$ per year (23% per year), which amounts to $0.23 \times 336 = 78$ starving animals per year.
- The $R_0 = b/d = 0.4/0.03 \simeq 13$ offspring per generation. This is normal logistic growth model because there is a positive linear growth term initially causing exponential growth and a negative quadratic term causing saturation of the growth to a steady state population level.
- The number of animals dying from starvation is lowest when about $s = 30$ animals are shot per year, but the total number of animals dying at this hunting rate is 60 animals per year (so still 30 from starvation), which is not that much lower than the 78 animals dying per year in the absence of hunting. Furthermore overall population level has decreased from 336 to 200 animals and as a consequence birth rates are also lower.
- For $s = 31$ the parabola has been shifted downward so much that it touches the x axis, resulting in an equilibrium with one stable and one unstable direction. For $s > 31$ the parabola lies entirely below the x axis, and the population will go extinct. In the abc-formula this is reflected by the term under the square root becoming negative, i.e. there are no longer any equilibrium solutions.
- Starting below the unstable equilibrium leads to extinction of the population.
- GRIND simulations closely mimic the time courses shown in the article.

Question 2.2. Density dependent growth

A possible good answer has the following sketches:



- Per capita birth rate is $\frac{b}{1+N/h}$: See the sketch in Panel (a).
- The population birth rate is $\frac{bN}{1+N/h} = \frac{bhN}{h+N}$, which approaches the horizontal asymptote bh for N going to ∞ . See the sketch in Panel (b).
- Solving $dtN = (\frac{b}{1+N/h} - d)N = 0$ gives $N = 0$ and $\frac{b}{1+N/h} - d$. From the latter we obtain $N = h(b-d)/d$.
- $R_0 = b/d$ and $N = h(b-d)/d = hb/d - hd/d = hR_0 - h = h(R_0 - 1)$.
- Yes: $1/(1+N/h)$ is the same as $h/(h+N)$ which is a declining Hill function with steepness parameter $n = 1$.

Question 2.3. Freitas

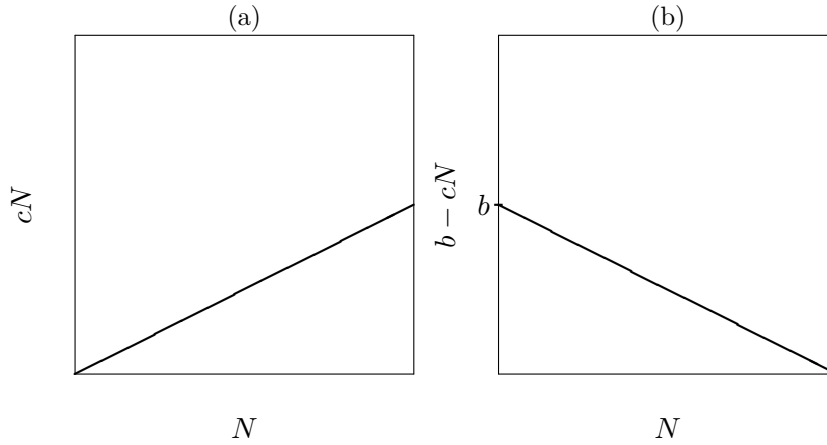
- No, the steady state of $dB/dt = m - dB$ is $\bar{B} = m/d$. In such a model the number of peripheral B cells is proportional to the number of bone marrow precursors (which determines m), whereas in the data the number of B cells is a saturating function of the number of bone marrow precursors.
- For instance with density dependent death, $dB/dt = m - dB(1 + eB)$ (resulting in $\bar{B} = \frac{-d \pm \sqrt{d^2 - 4edm}}{2ed}$), or with density dependent production, $dB/dt = m/(1 + eB) - dB$ (also resulting in $\bar{B} = \frac{-d \pm \sqrt{d^2 - 4edm}}{2ed}$).
- Yes clearly, given that the data show that for increasing number of precursor cells a steady state number of naive B cells is produced. (see a).
- No, it is accounting for a steady state, but not for any feedback mechanism resulting in density dependent population regulation.

Question 2.4. Stem cells

- The differentiation of stem cells introduces an additional loss term: $dS/dt = rS(1 - S/k) - mS$
- Apart from their production from stem cells we assume that differentiated cells have a limited life span: $dD/dt = mS - \delta D$
- Solving $dS/dt = rS(1 - S/k) - mS = 0$ results in $S = 0$ and $r(1 - S/k) - m = 0$. From the latter we obtain $r - (r/k)S = m$ $r - m = (r/k)S$ and finally $\bar{S} = k(r - m)/r$, which is independent of D . The $dD/dt = 0$ equation delivers $\bar{D} = (m/\delta)S$, which following the substitution of \bar{S} becomes $\bar{D} = (m/\delta)(k(r - m)/r) = \frac{mk}{r\delta}(r - m)$.

Question 2.5. Density dependent death

A possible good answer has the following sketches:



- The per capita death rate is cN : See the sketch in Panel (a)
- The per capita net growth rate is $b - cN$: See the sketch in Panel (b)
- $dN/dt = (b - cN)N = 0$ gives $N = 0$ or $b - cN = 0$. The latter results in $\bar{N} = b/c$.
- Because there is no generation time.
- For $f(N) = (b - cN)N$ the derivative $f'(N) = b - 2cN$. Substituting the non-trivial equilibrium $N = b/c$ yields $\lambda = -b < 0$. Thus the return time $T_R = 1/b$ is fully determined by the birth rate and is independent of the density dependent death rate c .

Question 2.6. Logistic growth of a tumor

- Tumor cells need oxygen and nutrients to grow. Initially, in a small tumor all cells have access to these resources, but as the tumor grows inside cells die do to limited resources while cells at the surface are still dividing. As the tumor grows further and further the surface to volume ratio of the tumor decreases (volume $4/3\pi r^3$, surface $4\pi r^2$), causing a smaller and smaller percentage of cells to reside at the surface where division is possible, and hence a per capita birth rate that decreases with the tumor size. Apparently, at the size of 1000 mm^3 these death and birth processes balance each other exactly. Tumors can overcome this limitation by angiogenesis: growing new blood vessels providing internal tumor cells with oxygen and nutrients.
- k is the volume at which the division rate becomes zero.
In general, for model fitting the number of data points available is relevant. If limited data is available, it is hard to constrain a large number of parameters to their relevant values. However, here we have another problem at hand. For this note that the extended model is mathematically identical to the logistic growth model, i.e.,

$$\frac{dN}{dt} = bN(1 - N/k) - dN = (b - d)N - bN^2/k = rN(1 - N/K)$$

where $K = k(1 - d/b)$ and $r = b - d$. From the data we can identify the net growth rate r , the overall carrying capacity K and the initial condition $N(0)$. However, independent of the number of data points available, it is not possible to determine b , d and k . The reason is that while there is a unique set of values for r , K and $N(0)$ giving the best fit to the data, there is no such unique set for b , d and k as multiple combinations of b , d and k values can produce the same r and K values.

- Substituting $N = 10^{-3}$ in the formula $T = 25 + 2.5 \log_{10}[N]$ used to fit the cell cycle data reveals that $T \simeq 17.5\text{h}$. At day 50 the tumor is about 1000 mm^3 , substituting this value in the same formula gives $T = 32.5\text{h}$. Note that at day 40 one would obtain a very similar cell cycle time since one would fill in a similar tumor volume.
- For tumors larger than 0.001 mm^3 we derived the following equation for the cell cycle time

$T(N) \simeq 25 + 2.5 \log_{10}[N]$. The division rate is the inverse of the cell cycle time, i.e.,

$$B(N) = \frac{1}{T(N)} = \frac{1}{25 + 2.5 \log_{10}[N]} = \frac{b}{1 + \log_{10}[N]/h},$$

where $b = 1/25 = 0.04$ per hour, and $h = 25/2.5 = 10$ (i.e. the division rate halves when $\log_{10}[N] = h = 10$, i.e., when $[N] = 10^{10}$). Here b is the division rate of a tumor of 1 mm^3 (because $\log_{10}[1] = 0$), so it is not a maximum “birth rate”. Indeed, based on the figure, the maximum growth rate occurs around a tumor size of 10^{-3} mm^3 , and would be $b_{\max} = 0.04/(1 - 3/10) \simeq 0.057$ per hour (indeed $1/b_{\max} \simeq 17.5\text{h}$).

e. The new model would be

$$\frac{dN}{dt} = \frac{bN}{1 + \log_{10}[N]/h} - dN,$$

and one solves the steady state from $\frac{bN}{1 + \log_{10}[N]/h} - dN = 0$ so $\frac{bN}{1 + \log_{10}[N]/h} = dN$, so $N = 0$ or $\frac{b}{1 + \log_{10}[N]/h} = d$. The latter can be rewritten as $b = d + d \log_{10}[N]/h$ so, $b - d = d \log_{10}[N]/h$ so $\frac{h(b-d)}{d} = \log_{10}[N]$ or $\log_{10}[N] = h[b/d - 1]$. So finally, $N = (h[b/d - 1])^{10}$. Note that this model is only valid when $\log_{10}[N]/h > -1$, which for our estimate of $h = 10$ means that the tumor should be larger than 10^{-10} mm^3 . Since the smallest tumors in Fig. 2.5 are larger than 10^{-3} mm^3 this seems a safe range.

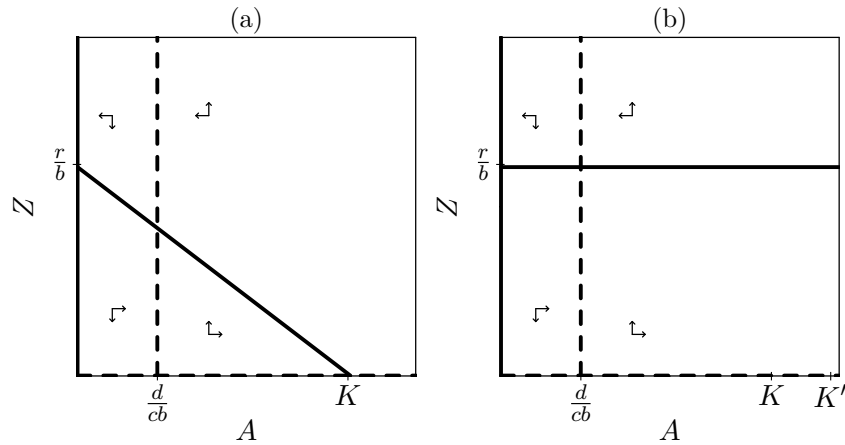
- f. Knowing that the steady state should be $K = 1027 \text{ mm}^3$, and with $h = 10$ and $b = 0.04$ we solve d from $\log_{10}[N] = h[b/d - 1]$, i.e., $\log_{10}[1027] \simeq 3 = 10[0.04/d - 1]$, to obtain that $d = 0.03$ per hour. Although this obviously gives the correct carrying capacity, the dynamics of this model is not entirely correct (you can check this with the program GRIND later on in the course). For instance, at a tumor size of 1 mm^3 the new model has a net replication rate of $r = b - d = 0.01$ per hour. At the same tumor size of 1 mm^3 the logistic model is in its exponential growth phase (see the Figure), with a net growth rate of $r = 0.37$ per day, or $r = 0.015$ per hour, which is 50% faster than the predicted growth rate of the new model. Indeed the authors argue that the death rate increases with the density, and that this density dependent death is a major contributor to the regulation of the tumor growth (Zobl et al., 1975). This makes perfect sense since as the tumor grows more and more cells in the middle will become deprived of oxygen. Apparently, the constant density independent death rate we now derived underestimates the actual density dependent death rate for low tumor sizes. The next step would therefore be to allow for a density dependent death rate, but unfortunately we have no data to estimate the parameters of such a function.
- g. Because we have added more data, i.e., we added how the division rate depends on the tumor volume.

Question 2.7. Negative birth

There are at least two approaches to answer this. First, one can argue that, if there is a non-zero death rate and a steady state, there has to be a positive birth rate balancing the death in the steady state. Second, in the text we derived that the non-trivial steady state is located at $\bar{N} = k(1 - 1/R_0)$ which is less than k . At the equilibrium point we therefore have a positive birth rate.

Question 3.1. Algae and zooplankton

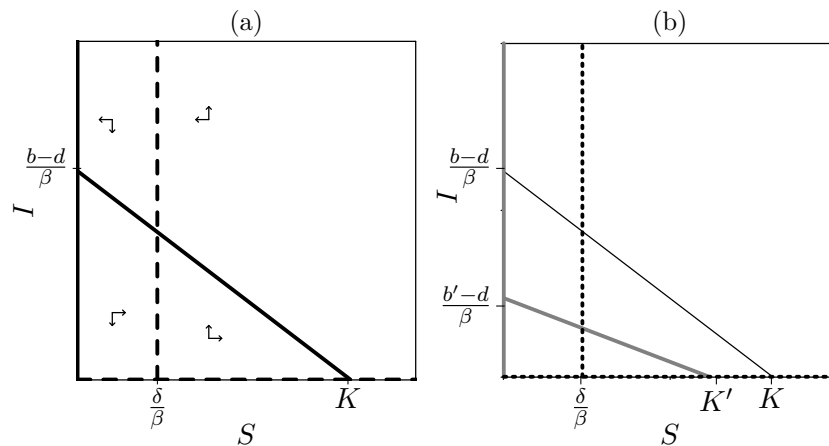
A possible good answer has the following sketches:



- Equations are those of the Lotka-Volterra model, so nullclines and stability of equilibria is the same as shown in Figure 3.2, left panel. See the sketch in Panel (a)
- The heavy gray line in Panel (b) is the new $dA/dt = 0$ nullcline.
- Only the zooplankton increases; the algae stay at $A = \frac{d}{cb}$.

Question 3.2. Seals

Note that this is again basically a Lotka-Volterra model with an explicit parameter for the non-virus induced death of the seals. A possible good answer has the following sketches:



- In the absence of infection $I = 0$, so we can skip the second equation and fill in $I = 0$ in the first equation, resulting in $dS/dt = bS(1 - S/k) - dS$. Solving $dS/dt = 0$ results in $S = 0$ and $b(1 - S/k) - d = 0$, which results in $S = k(1 - d/b)$ the term $k(1 - d/b)$ can be interpreted as the K of the classical Lotka-Volterra model.
- For seals, maximal reproduction means absence of infection so $R_0 = b/d$. For the infection, maximum reproduction requires highest number of seals possible, which is K so $R_0 = \beta K/\delta$ where $K = k(1 - d/b)$ is the carrying capacity of the seals.
- Given $S = k(1 - d/b)$ and $R_0 = b/d$ we obtain $S = k(1 - 1/R_0)$
- Let us call the new birth rate b' then $b' = b/2$ so $S = k(1 - d/b')$ is the new steady state.
- In this case we no longer have $I = 0$, so we need to consider both equations. Note that S now can only be solved from $dI/dt = \beta SI - \delta I = 0$, giving $S = \delta/\beta$. (Solving $dS/dt = 0$ only gives us $S = 0$ and I as a function of S , but not a concrete value of S).
- This is not changed: b' is not influencing $S = \delta/\beta$! Apparently, the reduced birth rate now only affects the number of infected individuals.
- The situation with a chronic infection is sketched in Panel (a). Note that these are simply

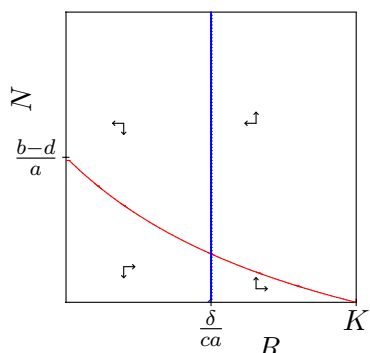
the Lotka-Volterra nullclines and vectorfield, thus the stability of the equilibria is the same as in the Lotka-Volterra model. For the non-trivial equilibrium S has a negative feedback onto itself and I has a zero feedback on itself, thus the equilibrium is stable.

- h. To do this we need to consider how the S nullcline changes when b is halved to b' . From $dS/dt = 0$ we obtain $S = 0$ and $I = (b/\beta)(1 - S/k) - (d/\beta)$ which can be rewritten as $I = (b - d/\beta) - (b/\beta k)S$, which is a decreasing line with intercept $(b - d/\beta)$ with the y axis. From this it follows that if b changes to $b' = b/2$ the intercept with the y axis is lowered with an unknown amount, while the slope of the line is halved. The question now is whether this combination of changes results in a line intersecting the x axis at a K' that is higher or lower than the original K , since a lower intercept tends to decrease, while a lower slope tends to increase the intercept with the x axis. To figure this out note that we know that $K = k(1 - d/b)$ and hence that $K' = k(1 - d/b')$ which should be lower than K as b' is lower than b . The nullclines in the presence and absence of PCBs are sketched in Panel (b).

Question 3.3. Solving the steady state

First find the equation from which one can solve B most easily. This is $dC/dt = 0 = eBC - fC$ yielding $\bar{B} = f/e$.

Question 3.4. Density dependent birth



- a. The predator nullcline stays the same. We need to find the new prey nullcline from $dR/dt = \frac{bR}{1+R/k} - dR - aNR = 0$ from which it follows that $R = 0$ or $\frac{b}{1+R/k} - d - aN = 0$. The latter can be rewritten into $N = \frac{b/a}{1+R/k} - d/a$. The latter has a horizontal asymptote at $N = -d/a$ (For R going to ∞ $\frac{b/a}{1+R/k}$ goes to zero), and a vertical asymptote at $R = -k$ (for $R = -k$ a division by zero causes N to go to ∞). The intersect with the vertical N -axis is $N = (b - d)/a$ (fill in $R = 0$). The intersect with the horizontal R axis is $R = k(b/d - 1) = K$ (solve R from $\frac{b/a}{1+R/k} - d/a = 0$).

- b. The carrying capacity is $R = K = k(b/d - 1) = k(R_0 - 1)$,

where R_0 is the fitness of the prey.

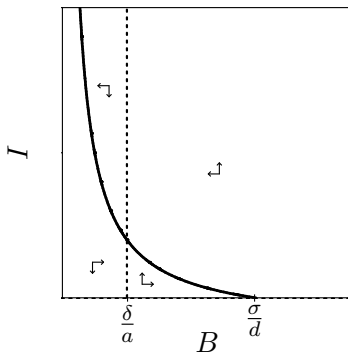
- c. The fitness of the predator is $R'_0 = \frac{caK}{\delta}$.

- d. Since $R'_0 = \frac{caK}{\delta}$, and the predator nullcline is located at $\bar{N} = \delta/(ca)$, one can write $\bar{R} = K/R'_0$.

- e. $(0,0)$ unstable (saddle), $(K,0)$ unstable (saddle). The non-trivial steady state is stable because R has a negative feedback on itself and N has zero feedback on itself.

- f. No, the only (minor) difference is that the nullcline has a curvature.

Question 3.5. Malaria



a. The $dI/dt = 0$ nullcline is $I = 0$ and $B = \delta/a$. The $dB/dt = 0$ nullcline is given by $\sigma - dB - aBI = 0$ which first can be rewritten into $aBI = \sigma - dB$ and then $I = \frac{\sigma}{aB} - \frac{d}{a}$. For $B = 0$ there is a division by zero and I goes to ∞ so $B = 0$, the I -axis is a vertical asymptote. For $B \rightarrow \infty$ the fraction $\frac{\sigma}{aB}$ goes to zero and the nullcline approaches the horizontal asymptote $I = -d/a$.

b. Carrying capacity means the maximum number of red blood cells supported by the system in absence of infection. Setting $I = 0$ results in $B = \sigma/d$ so $K = \sigma/d$

c. Now $I \neq 0$ and \bar{B} follows from dtI and is $\bar{B} = \delta/a$

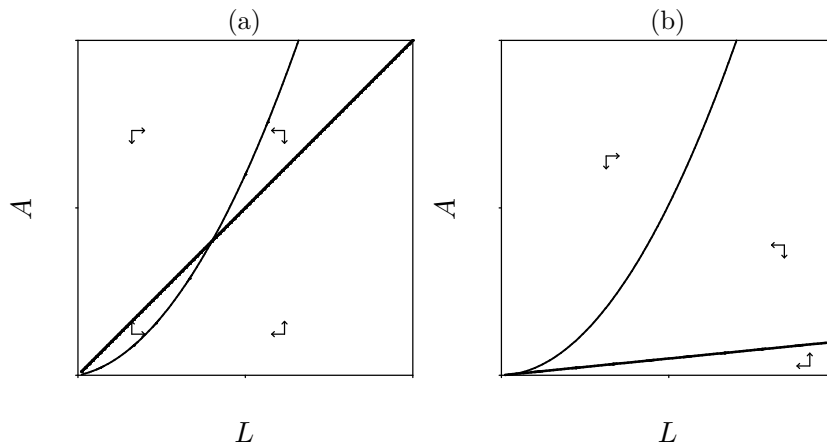
d. The R_0 for the infection occurs for B at its carrying capacity $K = \sigma/d$, so $R_0 = aB_{max}/\delta = aK/\delta$. From $R_0 = aK/\delta$ and $\bar{B} = \delta/a$ one obtains $\bar{B} = K/R_0$. This is a famous result from epidemiology: the depletion of the susceptibles (relative to their steady state in absence of an infection) is proportional to the R_0 of the epidemic.

e. $(K, 0)$: unstable (saddle); the non-trivial equilibrium is stable because B has a negative feedback on itself and I has zero feedback on itself.

f. There is a carrying capacity in the absence of density dependence. The origin $(0, 0)$ is not a steady state.

Question 3.6. Growth of insects

A possible good answer has the following sketches:



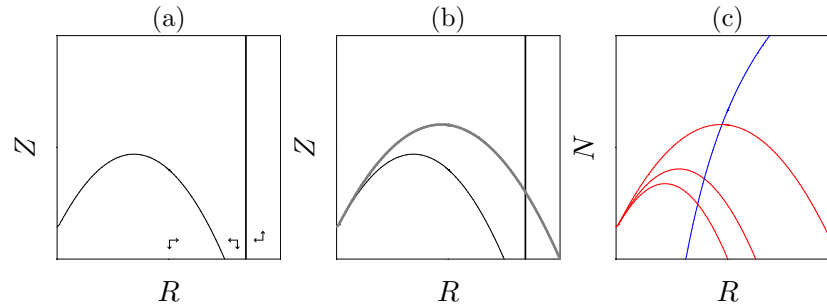
a. aA : adults (A) reproducing (a) generate new larvae, $dL(1 + eL)$: density dependent ($1 + eL$) death (d) of the larvae (L), cL : larvae (L) mature (c) into adults, δA : death (δ) of the adults (A).

b. $dL/dt = aA - dL(1 + eL) - cL = 0$ gives $aA = dL(1 + eL) + cL = dL + deL^2 + cL$ and finally $A = \frac{d+c}{a}L + \frac{de}{a}L^2$, which describes a parabola; $dA/dt = cL - \delta A = 0$ gives the straight line $A = (c/\delta)L$. There are two possibilities; see Panels (a) and (b). To determine the vectorfield, assume that A is small and L is large, putting us in the lower right corner of the phase plane. Filling in a small A and large L in dL/dt causes the negative L terms to dominate so $dL/dt < 0$ so a leftward pointing arrow. Similarly, filling in a small A and large L results in $dA/dt > 0$ and hence an upward pointing arrow. The other arrows follow from flipping the horizontal vector when passing the L nullcline and flipping the vertical vector when passing the A nullcline.

c. In Panel(a) the equilibrium at the origin $(0,0)$ is unstable, and the non-trivial steady state is a stable node. In Panel (b) the origin $(0,0)$ is the only steady state and is stable.

Question 4.1. Paradox of enrichment

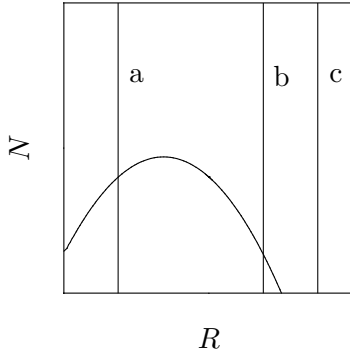
A possible good answer has the following sketches:



- No, McAllister findings perfectly agree with the model which predicts that as nutrients and hence the carrying capacity increases the algal density should not increase while the zooplankton population should increase significantly (see e.g. Fig. 4.3).
- The new predator equation is: $dN/dt = \frac{caNR}{h+R} - dN - eN^2$. From $\frac{caNR}{h+R} - dN - eN^2 = 0$ we obtain $N = 0$ or $\frac{caR}{h+R} = d - eN$. The latter can be rewritten into $\frac{caR}{h+R} - d = eN$ and finally we obtain $N = \frac{(ca/e)R}{h+R} - \frac{d}{e}$. The nullclines thus are $N = 0$ and $N = \frac{(ca/e)R}{h+R} - \frac{d}{e}$, which is a saturation function starting at $N = -d/e$ when $R = 0$ and intersecting the horizontal axis at the same point $R = h/(R_0 - 1)$ at which the earlier vertical nullcline intersected the x axis. See the sketch in Panel (c).
- We now see that as nutrients are added and the carrying capacity increases most increase is still in the zooplankton population, but now there is some increase also in the algae population. The latter is due to the non-straight shape of the predator nullcline which in turn is caused by the density dependent death of predators. By increasing predator death as predator density is increasing, predator increase is limited and some of the increase actually ends up in the algae population. Note that this small increase in algae only occurs if e is small enough and hence the isocline is non-straight enough. Still, the increase in algae is considerably more when zooplankton is not present as then the amount of algae is entirely determined by the carrying capacity and hence the amount of nutrients in the system: $\bar{R} = K$.

Question 4.2. Enriching oligotrophic lakes

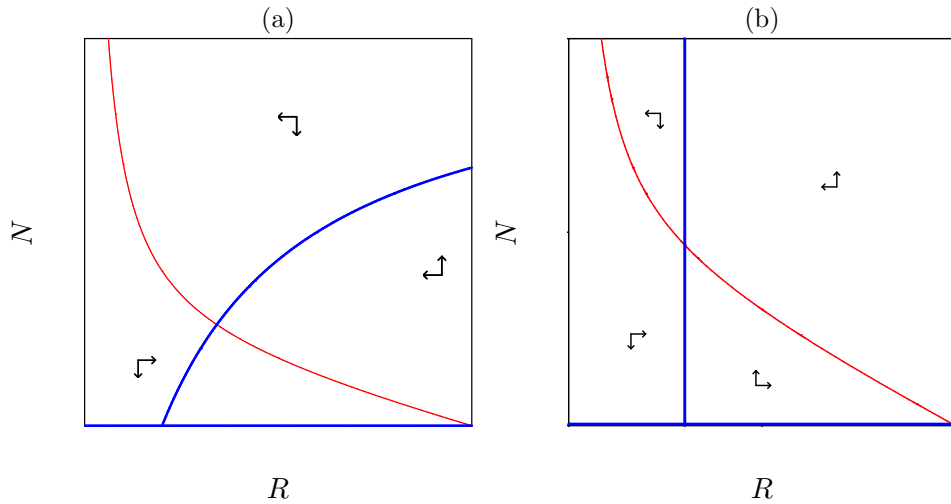
- The N nullcline lies right of the R parabola nullcline, as a consequence there is no non-trivial equilibrium: See the sketch in Panel (a).
- The equation for the R parabola nullcline is $N = (r/a)(h + R)(1 - R/K)$ so the rightmost intersection point with the x axis is $N = K$. The equation for the N nullcline is $R = \frac{h}{\frac{R_0}{1} - 1}$, so $\frac{h}{\frac{R_0}{1} - 1} > K$.
- Adding nutrients means increasing the carrying capacity, and hence the rightmost intersection point of the N nullcline shifts to the right also causing the top of the parabola to ly higher: The heavy gray line in Panel (b) is the algae nullcline after eutrophication.
- No, here eutrophication leads to an increase of the diversity since it allows the zooplankton to survive.

Question 4.3. Ditch

- a. The death rate d of the zooplankton increases.
- b. Assuming that we start with a zooplankton nullcline intersecting the algae parabola nullcline at the left hand side of the top, we go from (a) to (b) in the sketch, i.e., pollution would have a stabilizing effect by transforming limitcycle dynamics to a stable steady state. Alternatively, we could start with an intersection point of the nullclines at the right hand side of the top, in which case we go from (b) to (c) and expect that the zooplankton dies out.

Question 4.4. Bacterial oscillations

A possible good answer has the following sketches:

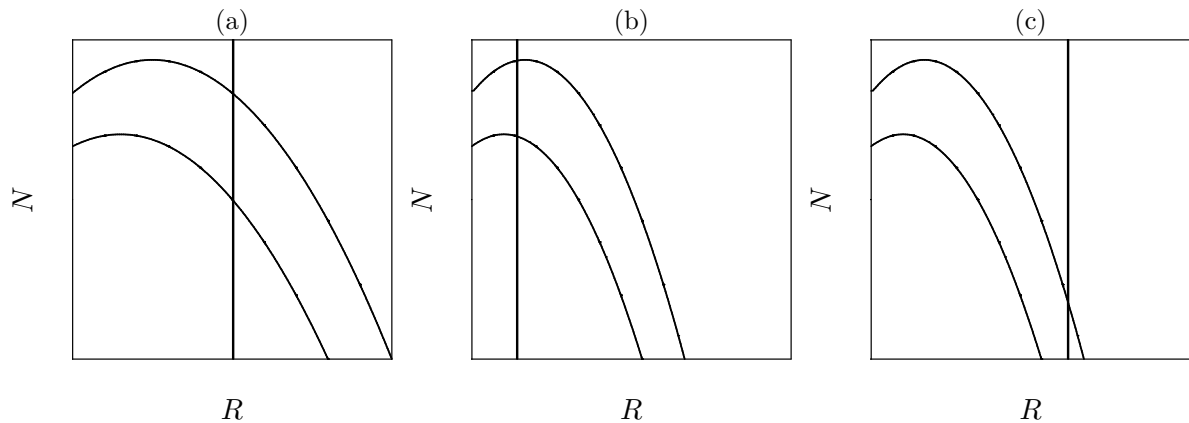


- a. All populations disappear at the efflux, or “wash out” rate, of the chemostat.
- b. xNT represents the effect of the toxin. It is a mass-action term, bacteria die at a rate proportional to the toxin concentration.
- c. The resource equation stays the same since it does not contain a term with T in it. The new equation for the bacteria becomes $dN/dt = \frac{bNR}{h+R} - wN - x'N^2$, where $x' = xp/w$. (Note that this quasi steady state assumption is in fact not so reasonable because all populations have the same turnover rate w , so the toxin does not have a much faster time scale than the two other populations (see Chapter 7)).
- d. The nullcline of the resource is solved from $dR/dt = s - wR - \frac{aNR}{h+R} = 0$. This gives us $s - wR = \frac{aNR}{h+R} = 0$, which can be rewritten as $(s - wR)(h + R) = aNR$ and hence as $N = \frac{1}{aR}(h + R)(s - wR)$. Since $(h + R)(s - wR) = hs + sR - whR - wR^2$ this can also be written as $N = \frac{s-wh}{a} + \frac{hs}{aR} - \frac{w}{a}R$. Note that this equation is of the form $y = a + \frac{b}{x} - cx$. For $R = 0$ N approaches ∞ so this nullcline has the vertical axis ($R = 0$) as a vertical asymptote. The intersection point with the horizontal axis can be found from solving $\frac{s-wh}{a} + \frac{hs}{aR} - \frac{w}{a}R = 0$. By dividing over a and multiplying by R we obtain $(s - wh)R + hs - wR^2 = 0$. Reordering this gives us $-wR^2 + (s - wh)R + hs = 0$ which can be solved using the abc-formula: $R = \frac{-(s-wh) \pm \sqrt{(s-wh)^2 - 4(-w)hs}}{-2w}$. This can be rewritten as $R = \frac{(wh-s) \pm \sqrt{s^2 - 2swh + w^2h^2 + 4whs}}{-2w}$ and thus $R = \frac{(wh-s) \pm \sqrt{s^2 + 2swh + w^2h^2}}{-2w}$ and thus $R = \frac{(wh-s) \pm \sqrt{(s+wh)^2}}{-2w}$ and finally $R = \frac{(wh-s) \pm (s+wh)}{-2w}$. From this we can find $R_+ = \frac{(wh-s) + (s+wh)}{-2w} = \frac{wh-s+s+wh}{-2w} = \frac{2wh}{-2w} = -h$, which is biologically

- irrelevant, and $R_- = \frac{(wh-s)-(s+wh)}{-2w} = \frac{wh-s-s-wh}{-2w} = \frac{-2s}{-2w} = \frac{s}{w}$. See the sketch in Panel (a). The nullcline of the bacteria is solved from $dN/dt = \frac{bNR}{h+R} - wN - x'N^2 = 0$, where $x' = xp/w$. This gives $N = 0$ and $\frac{bR}{h+R} - w - x'N = 0$. From the latter we obtain $N = \frac{1}{x'} \left(\frac{bR}{h+R} - w \right)$, which is a saturation function. The intersection point with the vertical axis can be obtained from filling in $R = 0$, resulting in $N = -w/x'$. The intersection point with the horizontal axis can be obtained from solving $\frac{1}{x'} \left(\frac{bR}{h+R} - w \right) = 0$ which gives us $\frac{bR}{h+R} - w = 0$ so $\frac{bR}{h+R} = w$ and hence $bR = wh + wR$, and thus $(b-w)R = h$ and finally $R = \frac{wh}{b-w}$. Finally, for R going to ∞ the function has a horizontal asymptote at $N = (b-w)/x'$. See the sketch in Panel (a).
- e. No, R and N both have a negative feedback on themselves thus the equilibrium is stable.
- f. The model now becomes $dR/dt = s - dR - \frac{aRN}{h+R}$ and $dN/dt = \frac{caRN}{h+R} - \delta N$. The bacteria nullcline now can be found from $\frac{caRN}{h+R} - \delta N = 0$, resulting in $N = 0$ or $\frac{caR}{h+R} = \delta$. This can be rewritten as $caR = \delta h + \delta R$ and hence as $(ca - \delta)R = \delta h$ and finally as $R = \frac{\delta h}{ca - \delta}$ or $R = h/(R_0 - 1)$ (where $R_0 = ac/\delta$). So instead of a single saturating line we now have a horizontal line at the x axis and a vertical line at $h/(R_0 - 1)$. The resource nullcline is the same as before: See the sketch in Panel (b). No, like in Panel (a) the steady state is always stable (R negative and N zero feedback on itself). Apparently we need logistic growth of the prey to have predator-prey oscillations.
- g. Grind exercise.

Question 4.5. Pump

A possible good answer has the following sketches:

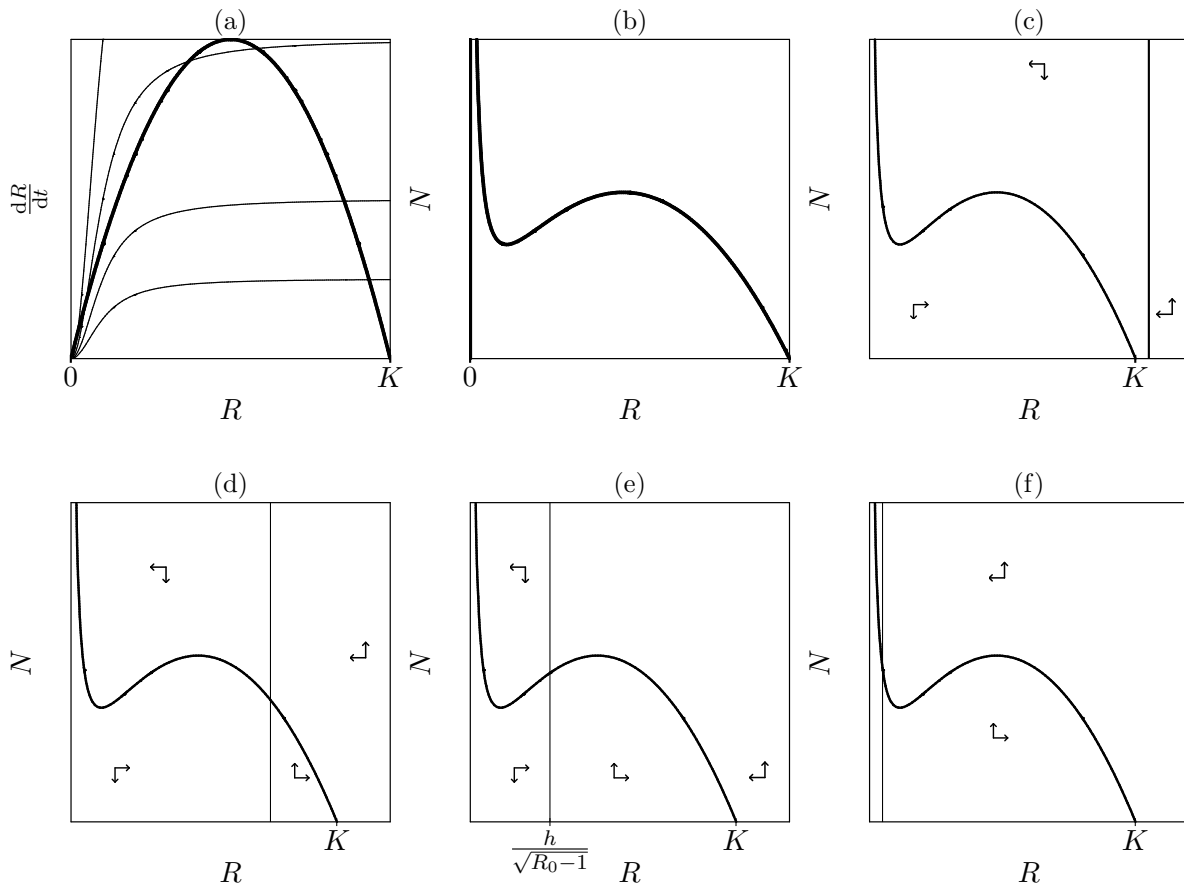


- a. $dR/dt = rR(1 - R/K) - \frac{aNR}{h+R} - pR$ and $dN/dt = \frac{caNR}{h+R} - dN$
- b. The predator nullcline is the same as for the model of Eq. 4.3, so $N = 0$ and $R = \frac{dh}{ca-d}$. The prey nullcline now needs to be solved from $rR(1 - R/K) - \frac{aNR}{h+R} - pR = 0$, which gives us $R = 0$ and $r(1 - R/K) - \frac{aN}{h+R} - p = 0$. The latter can be written as $\frac{aN}{h+R} = r(1 - R/k) - p$ and hence as $N = \frac{r}{a}(1 - R/k)(h+R) - \frac{p}{a}(h+R)$ or $N = \frac{r}{a}(1 - R/k - p/r)(h+R)$. For $p = 0$ this is a parabola intersecting the x-axis at $R = k$ and $R = -h$. For $p > 0$ this changes into a parabola intersecting the x-axis at $R = -h$ and $R = K' = K(1 - p/r)$ (obtained from solving $1 - R/k - p/r = 0$). Thus, the larger p the smaller the new carrying capacity K' .

There are three interesting situations. The parabola at the top is always the lake without the pump. The bottom parabola is obtained with $p > 0$ (the total area in phase space where the algae increase should become smaller whenever $p > 0$). See Panels (a)–(c). In (a) the steady state remains stable, the zooplankton density decreases, and the algae density remains the same. In (b) limit cycles turn into a stable steady state. Again, the average amount of algae stays the same, and the average zooplankton density decreases. In (c) the zooplankton goes extinct, and the algae density goes to carrying capacity. (c) is the only situation where the lake becomes less dirty and green (but we have lost the zooplankton)!

Question 4.6. Sigmoid functional response

A possible good answer has the following sketches:



a.

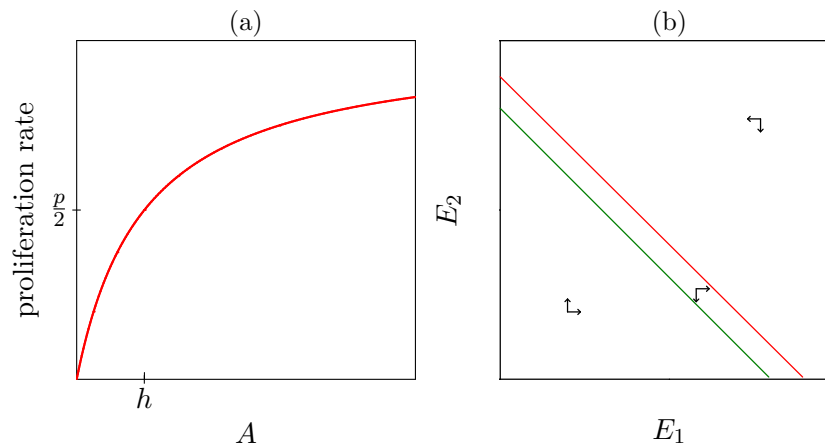
$$\frac{dR}{dt} = rR(1 - R/K) - \frac{aNR^2}{h^2 + R^2} \quad \text{and} \quad \frac{dN}{dt} = \frac{caNR^2}{h^2 + R^2} - dN$$

- b. Solving $\frac{caNR^2}{h^2 + R^2} - dN = 0$ gives us $N = 0$ and $\frac{caR^2}{h^2 + R^2} - d = 0$, which can be rewritten as $caR^2 = dh^2 + dR^2$ and hence as $(ca - d)R^2 = dh^2$ and hence as $R^2 = \frac{dh^2}{ca-d}$ which finally gives us $R = \sqrt{\frac{dh^2}{ca-d}}$ or $R = h\sqrt{\frac{d}{ca-d}}$. The R_0 of the predator is $R_0 = ca/d$. From this we obtain $ca = R_0d$, so we can write $R = h\sqrt{\frac{d}{R_0d-d}}$ and hence finally $R = h\sqrt{\frac{1}{R_0-1}}$, which is very similar to the $R = \frac{h}{R_0-1}$ of the model with the non-sigmoid saturating response.
- c. The heavy parabola in Panel (a) is $rR(1 - R/K)$ part and the sigmoid curves are the $\frac{aNR^2}{h^2 + R^2}$ part for several values of N .
- d. This yields the nullclines depicted in Panel(b).

- e. There are four possible configurations, which are depicted in Panels (c–f). The non-trivial steady state is stable when the nullclines intersect in either of the declining parts of the R nullcline (Panels d and f), as then R has a negative and N has zero feedback on itself. The non-trivial steady state is unstable when the nullclines intersect in the rising part (Panel e), as then R has a positive and N zero feedback on itself. In Panel c there is no non-trivial equilibrium present.

Question 5.1. Saturated proliferation

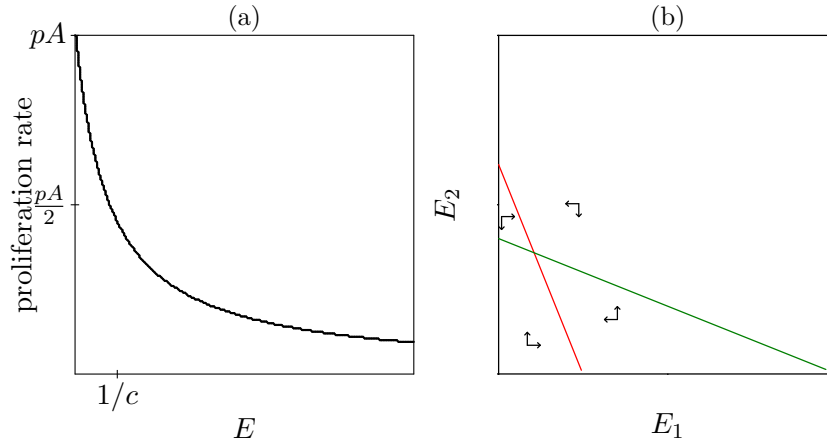
A possible good answer has the following sketches:



- We need to draw functions of the shape $\frac{pA}{h+A}$. See Panel (a). Note that if we would draw these functions for E_1 and E_2 in the same picture, the function for E_2 would have a more shallow slope due to its larger h_2 value, and hence approaches its maximum value slower.
- $dE_1/dt = \frac{pE_1A}{h_1+A} - dE_1 = 0$ yields $E_1 = 0$ and $\frac{pA}{h_1+A} = d$ so $pA = dh_1 + dA$ so $(p-d)A = dh_1$ and finally $A = \frac{dh_1}{p-d}$. Note that also holds $A = 1 - kE_1 - kE_2$. So to express E_2 as a function of E_1 we can rewrite $\frac{dh_1}{p-d} = 1 - kE_1 - kE_2$ into $1 - \frac{dh_1}{p-d} - kE_1 = kE_2$ and hence $E_2 = 1/k - \frac{dh_1}{k(p-d)} - E_1$. Repeating this for $dE_2/dt = 0$ yields first $E_2 = 0$ and $\frac{pA}{h_2+A} = d$ and hence $A = \frac{dh_2}{p-d}$. Again we can write $\frac{dh_2}{p-d} = 1 - kE_1 - kE_2$. Thus we obtain in a similar manner $E_2 = 1/k - \frac{dh_2}{k(p-d)} - E_1$. (Remember that both times you should write E_2 as a function of E_1 in order to be able to draw both functions in the same phase space). Thus, both nullclines have a slope of -1 in the phase space depicted in the sketch. Since $h_2 > h_1$ the E_2 nullcline is the lowermost nullcline.
- No, parallel nullclines cannot intersect
- Hardly any difference: competitive exclusion

Question 5.2. Competitive proliferation

A possible good answer has the following sketches:



- a. We need to draw the function $\frac{pA}{1+cE}$, which is a decreasing function of E . For E going to ∞ this function approaches zero so the x axis is a horizontal asymptot of the function. For $E = -1/c$ the function goes to ∞ so $-1/c$ is a vertical asymptot of the function. See Panel (a). Note that if we draw the functions for E_1 and E_2 in the same Panel, the graph for E_2 would have a vertical asymptot at a more negative value (more leftward), and would be approaching zero faster.
- b. Solving $dE_1/dt = \frac{pE_1A}{1+c_1E_1} - dE_1 = 0$ yields $E_1 = 0$ and $\frac{pA}{1+c_1E_1} - d = 0$. The latter we can rewrite into $\frac{pA}{1+c_1E_1} = d$ and hence $pA = d + dc_1E_1$ and finally $A = \frac{d}{p} + \frac{dc_1}{p}E_1$. Since we also know that $A = 1 - kE_1 - kE_2$ we can write $1 - kE_1 - kE_2 = \frac{d}{p} + \frac{dc_1}{p}E_1$. Now we can write $1 - \frac{d}{p} - (k + \frac{dc_1}{p})E_1 = kE_2$ and finally $E_2 = \frac{p-d}{pk} - (1 + \frac{dc_1}{pk})E_1$. Solving $dE_2/dt = \frac{pE_2A}{1+c_2E_2} - dE_2 = 0$ yields $E_2 = 0$ and $\frac{pA}{1+c_2E_2} - d = 0$. So we can write $1 - kE_1 - kE_2 = \frac{d}{p} + \frac{dc_2}{p}E_2$ and rewrite this as $1 - \frac{d}{p} - kE_1 = (k + \frac{dc_2}{p})E_2$ or $\frac{p-d}{d} - kE_1 = \frac{kp+dc_2}{p}E_2$ and $E_2 = \frac{p-d}{pk+dc_2} - \frac{pk}{pk+dc_2}E_1$. In a phase space with E_2 on the vertical axis, the nullclines are straight lines with different slopes and intercepts, with the E_2 nullcline having a lower intercept and slope. (see the Figure).
- c. Yes, the nullclines can intersect in a stable node.
- d. Due to the intra-specific competition coexistence is now possible.

Question 5.3. Virus competition experiments

- a. When $\rho(t) \equiv V_2(t)/V_1(t)$, the derivative $d\rho/dt \equiv \rho'$ obeyes

$$\begin{aligned}
 \frac{d\rho}{dt} &= \frac{V_2'V_1 - V_1'V_2}{V_1^2}, \\
 &= \frac{r(1+s)V_2V_1 - rV_1V_2}{V_1^2}, \\
 &= r(1+s)\rho - r\rho, \\
 &= r\rho + rs\rho - r\rho, \\
 &= rs\rho.
 \end{aligned}$$

- b. Since $d\rho/dt = rs\rho$ has the solution $\rho(t) = \rho(0)e^{rst}$, the natural logarithm of the ratio plotted in time should be a straight line with slope rs . Note that this slope is not reflecting the relative fitness, s , but the difference in the growth rate, rs (Marée et al., *J. Virol.*, 2001).

Question 6.1. Exponential Population Growth

As discussed, in CA models space is discrete and a single grid point can typically only be occupied by one or a few entities (individuals, molecules). Indeed for reproduction entities need

an empty grid point to reproduce in. Therefore, in CAs there is an implicit competition for space that will get worse as population size increases and space is more occupied, thus a CA always has density dependence and is not suited for modeling non-density dependent, unbounded exponential growth.

In IBM models space is not necessarily discrete and there is not necessarily a limit to the amount of entities per unit of area, so here it is perfectly possible to simulate exponential growth.

Thus a CA model has a carrying capacity that is equal to the number of grid points (times the number of maximum entities a grid point can contain, usually 1).

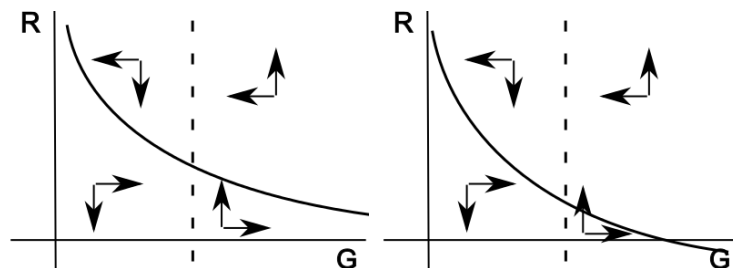
Question 6.2. Two populations

- No, since we use a CA model, there is implicit competition for space. So the two populations do compete for a resource, space.
- If we would have a single population, there would initially be exponential growth until the space is filled up and we enter a saturated growth regime. With two populations, and one with a substantial head start, this population can become much bigger before space is filled up and the saturated growth regime starts. So at the end of the simulation the big population will probably be much more than a factor of 10 bigger than the small population (growth amplification). Furthermore, the small population may even go extinct.

Question 6.3. Rabbits and Grass

- It is easy to get stable coexistence. Only for extreme parameter values you can get the rabbits to go extinct.
- Let us denote the grass by G and the rabbits by R we then can write the following system of ODEs:

$$\begin{aligned}\frac{dG}{dt} &= a - bGR \\ \frac{dR}{dt} &= cR - d\frac{R}{G}\end{aligned}$$



For the grass we incorporated constant growth and predation by the rabbits. For the rabbits, we ignored for simplicity the dependence of reproduction on grass consumption and focused on the dependence of death on grass consumption: the more grass there is to be eaten the lower the death rate. The grass nullcline is given by $R = \frac{a}{b} \frac{1}{G}$ which is a decreasing function of the amount of grass. The rabbit nullcline is given by $G = \frac{d}{c}$. See figure, left panel. For large G and R we get $dG/dt < 0$ and $dR/dt > 0$, from which the rest of the vectorfield follows. The vectorfield shows rotating dynamics. Looking at the feedback of the variables on to themselves we see negative feedback of G on itself and zero feedback of R on itself, hence the equilibrium is stable. Note that, given that the grass grows in a CA-like manner

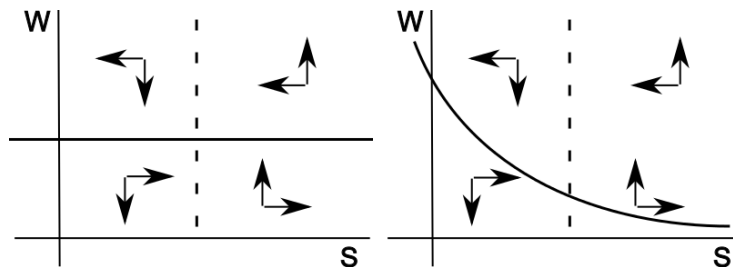
one could argue that since there is a competition for space grass grows in a density dependent manner and the equation should like like: $dG/dt = a(1 - \frac{G}{K}) - bGR$. This would result in the following equation for the grass nullcline $R = \frac{a}{b} \frac{1}{G} - \frac{a}{bK}$. Note that this nullcline has the same shape as before, just shifted by $\frac{a}{bK}$ downward. Thus, the vectorfield and equilibrium type are the same. See figure, right panel.

- c. For the ODE model we expect the system to go to and stay on the stable equilibrium, resulting in a constant amount of grass and a constant number of rabbits. For the IBM model, in which there is stochastic dynamics, the grass and rabbits will coexist and maintain *on average* constant numbers, but the numbers will fluctuate over time.
- d. The IBM model, as in nature birth, death etcetera are also probabilistic rather than deterministic processes.

Question 6.4. Wolves, Sheep and Grass

- a. No, this is not possible. On the long term you always get very high amplitude oscillations. These oscillations then lead to either one of two scenario's 1) the sheep go extinct after which the wolves also go extinct, or 2) the wolves go extinct after which the sheep population explodes.
- b. Denoting sheep by S and wolves by W we can write:

$$\begin{aligned}\frac{dS}{dt} &= aS - bSW \\ \frac{dW}{dt} &= cW - d\frac{W}{S}\end{aligned}$$



As for the model in the previous exercise, for the wolves we ignore the dependence of reproduction on sheep, and only incorporate the dependence of death on sheep: the more sheep there are the lower the death rate. The sheep nullcline is given by $W = \frac{a}{b}$, while the wolves nullcline is given by $S = \frac{d}{c}$. Thus, similar to the previous exercise the predator nullcline is a vertical line. However, in contrast to the previous exercise, now the prey nullcline is not a decreasing line but a horizontal line (see figure, left panel). Filling in large S and W results in $dS/dt < 0$ and $dW/dt > 0$, and again we obtain rotating dynamics for the vectorfield. However, in this case both S and W have zero feedback on themselves. Indeed, in case of perfectly horizontal and vertical nullclines we have a center point equilibrium type which is neither stable nor unstable, but neutral. As a consequence, the system neither converges to nor diverges from the equilibrium but keeps rotating around the equilibrium at a constant distance determined by the initial conditions.

- c. In the computer model individuals are discrete, rather than being modeled by continuous valued variables. Also, the dynamics is stochastic rather than deterministic. Over time, random fluctuations cause the system to move from small to large amplitude oscillations. On the large amplitude oscillations very low numbers of individuals occur, which by chance may lead to extinction to one of the two populations. If sheep go extinct first, the wolves follow.

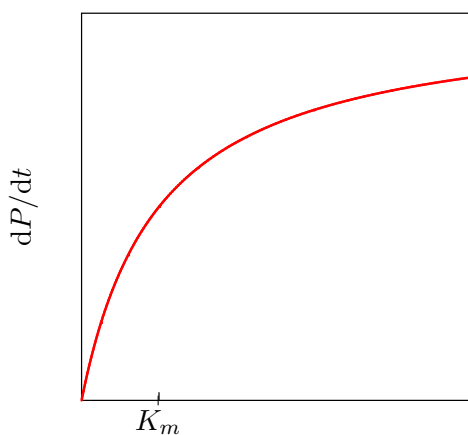
If wolves go extinct first, the constant growth of sheep (no density dependence) allows for exponential growth and hence an explosion of the population.

- d. The system now allows easily for stable coexistence of grass, sheep, and wolves.
- e. For the grass we write $dG/dt = e(1 - \frac{G}{K}) - fGS$, where K reflects the number of grid points in which grass can grow. For sheep we can now write either $dG/dt = aGS - bSW$ or $dG/dt = aS - e\frac{SW}{G}$ depending on whether we put the dependence on grass in reproduction or death.
- f. To get rid of the grass equation we make a quasi steady state assumption for the grass. Thus we assume $dG/dt = e(1 - \frac{G}{K}) - fGS = 0$. This results in the following equation for grass $G = \frac{e}{e/K + fS}$, showing that the amount of grass is a declining function of the number of sheep. Let us fill this in for the first variant of the new dS/dt equation:

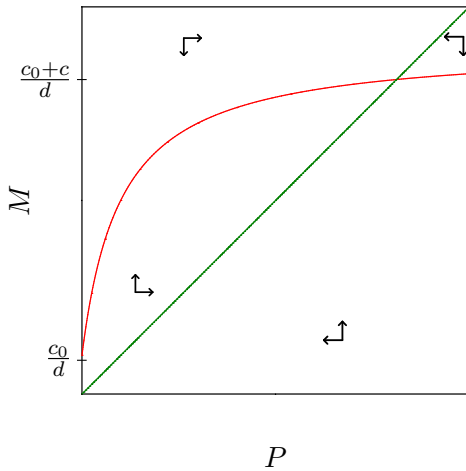
$$\frac{dS}{dt} = \frac{aeS}{e/K + fS} - bSW$$

This results in the sheep nullcline $W = \frac{ae/b}{e/K + fS}$. or $S = 0$ this nullcline intersects the y axis at $W = \frac{ae/b}{e/K} = \frac{aK}{b}$. For $S \rightarrow \infty$ W goes to zero in a hyperbolically decreasing fashion. The new nullclines are shown in the figure, right panel. Because the sheep nullcline is now decreasing, we have sheep having a negative feedback on themselves while wolves still have zero feedback on themselves, causing the equilibrium to be stable. Thus, by adding grass which has a space determined carrying capacity, sheep in essence also have a carrying capacity and are no longer able to grow exponentially, resulting in a stabilization of the equilibrium. However, since the IBM is stochastic in nature, rather than sheep and wolves staying at constant numbers, there will be fluctuations.

Question 7.1. Michaelis Menten



- a. From the conservation equation one obtains that the concentration of freely available enzyme is given by $E = E_0 - C$. From the reaction scheme one derives for the complex $dC/dt = k_1ES - (k_{-1} + k_2)C$, which, after substituting the conservation equation into this equation, becomes $dC/dt = k_1(E_0 - C)S - (k_{-1} + k_2)C$. For the formation of product one simply writes $dP/dt = k_2C$.
- b. To solve $dC/dt = 0$ we first collect all the terms containing C and rewrite as: $dC/dt = k_1E_0S - (k_1S + k_{-1} + k_2)C$. Because $dC/dt = 0$ we obtain $k_1E_0S = (k_1S + k_{-1} + k_2)C$, or $C = \frac{k_1E_0S}{k_1S + k_{-1} + k_2} = \frac{E_0S}{K_m + S}$, where $K_m = \frac{k_{-1} + k_2}{k_1}$.
- c. By defining K_m the simplification was already done above. This means the the product equation can now be written as $dP/dt = \frac{k_2E_0S}{K_m + S}$
- d. See the sketch.
- e. The beautiful trick of adding $dC/dt = 0$ to dS/dt readily simplifies the substrate equation into $dS/dt = -k_2C$. Filling in the quasi steady state expression for C gives $dS/dt = -\frac{k_2E_0S}{K_m + S}$

Question 7.2. Positive feedback

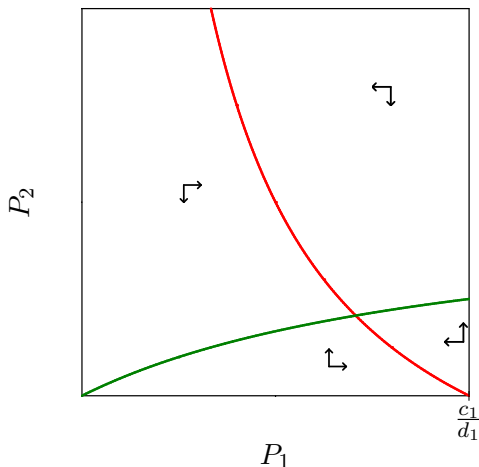
We now multiply the transcription rate with an increasing non-dimensional function $0 \leq P/(h + P) < 1$ to obtain:

$$\frac{dM}{dt} = \frac{cP}{h + P} - dM \quad \text{and} \quad \frac{dP}{dt} = lM - \delta P.$$

Since transcription can only start in this model if there already is some transcription factor, P , which needs to have been produced by prior transcription it is more natural to add a basal transcription rate c_0 that does not require any P :

$$\frac{dM}{dt} = c_0 + \frac{cP}{h + P} - dM \quad \text{and} \quad \frac{dP}{dt} = lM - \delta P.$$

- The $dM/dt = 0$ nullcline now is $M = \frac{c_0}{d} + \frac{(c/d)P}{h+P}$ which is an increasing saturation function. The $dP/dt = 0$ nullcline remains the same line $P = (l/\delta)M$. See the sketch.
- There is only one steady state and the vector field shows that it is stable. Yes, the system will approach the steady state and hence remains bounded despite this positive feedback.
- Setting $dM/dt = 0$ and solving the quasi steady state of M gives $M = \frac{c_0}{d} + \frac{(c/d)P}{h+P}$. Substituting this expression for M into the protein equation gives $dP/dt = c'_0 + \frac{c'P}{h+P} - \delta P$, where $c'_0 = lc_0/d$ and $c' = lc/d$.

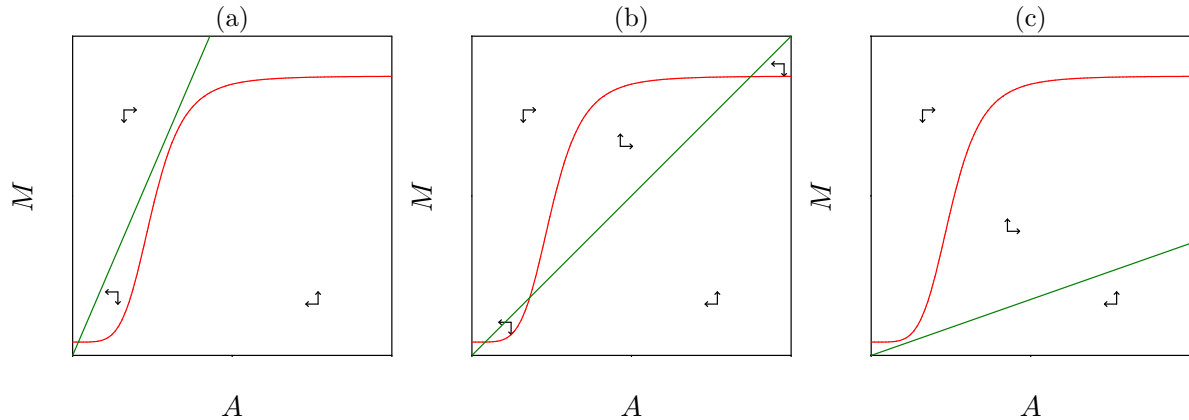
Question 7.3. Gene network

- At a protein concentration $P_1 = h_1$ the production of the transcription factor is half maximal (i.e., $c_2/2$).
- In the absence of P_2 we obtain $dP_1/dt = c_1 - d_1P_1$, and setting that to zero the steady state is $\bar{P}_1 = c_1/d_1$.
- In the absence of P_1 we obtain $dP_2/dt = -d_2P_2$. Hence the only steady state is $\bar{P}_2 = 0$.

- See the sketch. The $dP_2/dt = 0$ nullcline is the Hill function $P_2 = (c_2/d_2)P_1/(h_1 + P_1)$, which goes through the origin and has a horizontal asymptote $P_2 \rightarrow c_2/d_2$ when $P_1 \rightarrow \infty$. The $dP_1/dt = 0$ nullcline is the function $P_2 = h_2(\frac{c_1}{d_1P_1} - 1)$, which has $P_2 \rightarrow -h_2$ as a horizontal asymptote, and the vertical axis ($P_1 = 0$) as a vertical asymptote. In the upper right corner where both P_1 and P_2 are large, the negative decay terms dominate over the saturated translation terms, meaning that $dP_1/dt < 0$ and $dP_2/dt < 0$. The remainder of the vector field is constructed by flipping the arrows at the nullclines. The non-trivial steady state is stable because the vector field points towards it in all sectors.
- Trajectories will (monotonically) approach the non-trivial steady state.

Question 7.4. Lac-operon

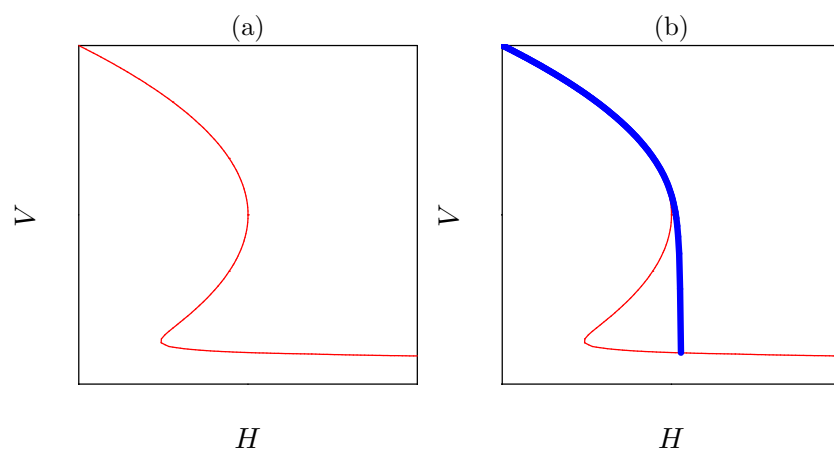
A possible good answer has the following sketches:



- a. The mRNA equation of the model is not affected by this and the allolactose equation becomes $dA/dt = ML - \delta A$. Thus the mRNA nullcline remains the sigmoid line derived in Fig. 7.3, and the allolactose nullcline becomes the straight line through the origin $M = (\delta/L)A$. There are three possibilities; see Panels (a-c).
- b. Left panel: stable node; Middle panel: two stable nodes, and one saddle point. Right panel: stable node (sorry: not visible).
- c. The quasi steady expression of the mRNA was already calculated in Eq. (7.5) when we computed the $dM/dt = 0$ nullcline. Substituting that expression for M into the allolactose equation one obtains $dA/dt = \frac{c_0 L}{d} + \frac{(c/d)LA^n}{1+A^n} - \delta A$
- d. Increasing the concentration of extracellular lactose, L , reduces the slope, δ/L , of the $dA/dt = 0$ nullcline. Since the simplified model has the same sequence of alternate steady states when the slope of the allolactose nullcline is reduced (see the three Panels), β -galactosidase is not required for the hysteresis, according to this simplified model.

Question 7.5. Sahel

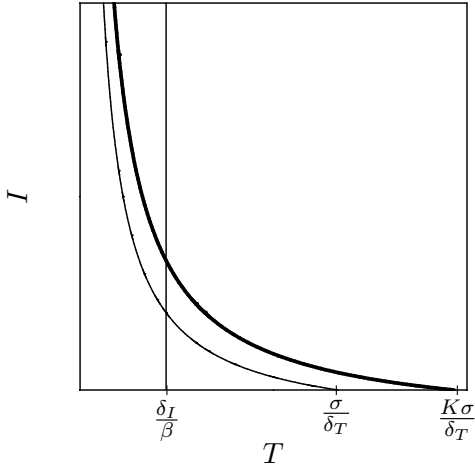
A possible good answer has the following sketches:



- a. This dV/dt equation is identical to the one used in the Noy-Meir construction and by simply rotating the $dV/dt = 0$ nullcline to have the vegetation, V , on the vertical axis and the herd size, H , on the horizontal axis, one obtains the steady state vegetation depicted in Panel (a).
- b. A trajectory following the upper branch until the saddle-node bifurcation is depicted in Panel (b). No the vegetation will not recover: due to the hysteresis the vegetation will stay at the lower branch when H is decreased (i.e., when cows are sold). The vegetation will only recover when the left saddle-node bifurcation is passed.

- c. Two: at a low value of H the lowest steady state merges with the saddle point, and at a high value of H the upper equilibrium merges with it.

Question 8.1. CD4⁺ T cells



- a. An immuno-stimulatory treatment should increase the production σ of the CD4⁺ T cells (or decrease the death rate δ). Let us increase the production by a factor $K > 1$:

$$\frac{dT}{dt} = K\sigma - \delta_T T - \beta T I .$$

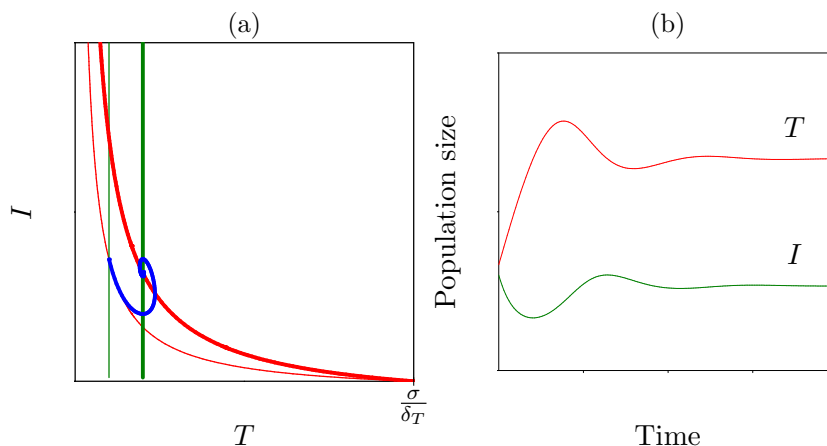
The equation for the infected cells stays the same, i.e.,

$$\frac{dI}{dt} = \beta T I - \delta_I I .$$

- b. We base our expectation on the nullclines shown in Panel (a), where the heavy curved line denotes the $dT/dt = 0$ nullcline during treatment and the light curved line the $dT/dt = 0$ nullcline before treatment. The vertical line is the $dI/dt = 0$ nullcline, which is not affected by the treatment. Because that nullcline is vertical, the new steady state lies at the same CD4⁺ T cell count, and the only result of the treatment is that the viral load goes up. Note that we would have obtained similar results when we had implemented the immuno-stimulatory treatment by a decrease of the death rate, δ_T , because the heavy line would again have intersected the horizontal axis at a value larger than σ/δ_T . This result is therefore generic.
- c. One should reduce (!) CD4⁺ T cell production, i.e., perform an immunosuppressive treatment that results in $K < 1$. This model even "predicts" that the infection will be cured when one reduces K so much that $K\sigma/\delta_T = \delta_I/\beta$. This possible benefit of reducing CD4 T cell production in patients who are ultimately dying from a lack of CD4⁺ T cells is a good example of "to think the unthinkable".
- d. The CD4 T cell count should not suffer from such a form of immunosuppression because the steady state remains located at $T = \delta_i/\beta$ as long as the virus is present.

Question 8.2. Rebound

A possible good answer has the following sketches:



- See the sketch in Panel (a): light nullclines denote the situation before treatment, and heavy nullclines are valid during treatment. Decreasing β moves the $dI/dt = 0$ nullcline to the right (because it is located at $T = \delta_I/\beta$), and curves the $dT/dt = 0$ nullcline upwards (because it is given by $I = \frac{\sigma}{\beta T} - \frac{\delta_T}{\beta}$).
- See the phase space in Panel (a). The trajectory starts in the pre-treatment equilibrium. When treatment is administered the local vector field in that point is pointing to the right and down. This means that the virus load goes down, and the target cells expand. When the trajectory intersects the new $dI/dt = 0$ nullcline, there are so many target cells that the viral load rebounds. Ultimately the new steady state is approached, which is located at a very similar viral load, and an increased CD4 T cell count.
- See the sketch in Panel (b): the target cells first recover, which then allows the infected cells to increase.
- No, this model demonstrates that a viral rebound can happen in the complete absence of drug resistance. It is the increase of the target cells that compensates for the suppression by the treatment, allowing the infected cells to rebound.

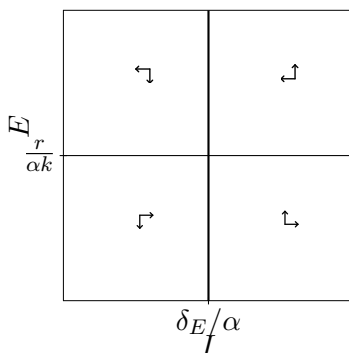
Question 8.3. Immune control

- Because the steady state expression of I in Eq. (8.2), i.e., $\bar{I} = \delta_E/\alpha$, does not contain the β parameter, the number of infected cells should ultimately return to the pretreatment level.
- Yes, target cell levels go up because β is present in the denominator of the expression for \bar{T} in Eq. (8.2). A negative effect is that the immune response is expected to decline, because \bar{E} increases in a saturated manner with β (see Eq. (8.3)).
- An immune escape mutant will become limited by target cell availability. Solving Eq. (8.1) from the simplest to the most difficult equation yields:

$$\bar{V} = \frac{p\bar{I}}{\delta_V}, \quad \bar{T} = \frac{\delta_I}{\beta'}, \quad \text{and} \quad \bar{I} = \frac{\sigma}{\beta'\bar{T}} - \frac{\delta_T}{\beta'} \quad \text{where} \quad \beta' = p\beta/\delta_V.$$

This equilibrium corresponds to the horizontal part of the graphs in Fig. 8.2, and has a higher viral load than any of the immune controlled steady states.

Question 8.4. Ogg *et al.*, 1998



- Setting $dV/dt = 0$ gives $V = (p/\delta_V)I$. Substitution into the equation for the infected cells yields $dI/dt = rI - \alpha kEI$, where $r = p\beta/\delta_V - \delta_I$. The equation for the immune effector cells remains the same.
- See the sketch. The heavy line is the $dE/dt = 0$ nullcline; the light one is the $dI/dt = 0$ nullcline.
- From $dE/dt = \alpha EI - \delta_E E$ one solves that $I = \delta_E/\alpha$, and from $dI/dt = rI - \alpha kEI = 0$ one solves that $E = r/(\alpha k)$.
- Because both expressions are inversely related to α , they should be positively correlated when α varies between patients.

Question 8.5. Competitive exclusion

- Because E_1 cancels from $dE_1/dt = 0$, it can only be solved from $dI/dt = 0$.
- The steady state of the infected cells: $\bar{I} = \delta_E/\alpha_1$.
- Also the steady state of the infected cells: $\bar{I} = \delta_E/\alpha_2$.
- No, \bar{I} cannot have two different values at the steady state of the whole system.
- Substituting $I = \delta_E/\alpha_1$ into $dE_2/dt = \alpha_2 E_2 I - \delta_E E_2$ gives

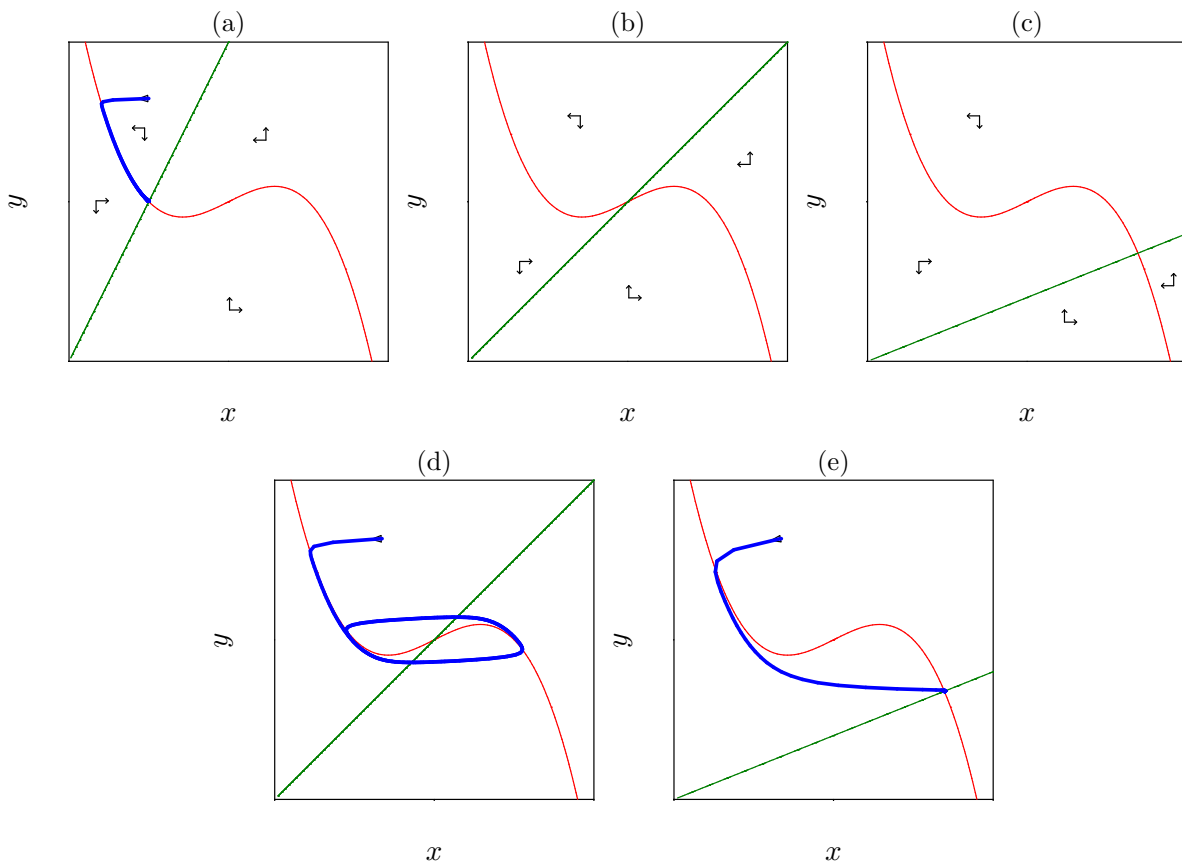
$$\frac{dE_2}{dt} = \alpha_2(\delta_E/\alpha_1)E_2 - \delta_E E_2 = \delta_E E_2 (\alpha_2/\alpha_1 - 1).$$

Since we agreed that $\alpha_2 < \alpha_1$ we obtain that $dE_2/dt < 0$. Thus, the second immune response declines when $dE_1/dt = 0$.

- f. The virus will then become controlled by the second response, i.e., the number of infected cells will increase from $\bar{I} = \delta_E/\alpha_1$ to $\bar{I} = \delta_E/\alpha_2$.

Question 9.1. Time scales

A possible good answer has the following sketches:



- a. For the stability of the steady state we see from the vectorfield that both x and y have a negative feedback on themselves, indicating that the equilibrium is stable. Since the dynamics of x is much faster than that of y change of y will occur on the nullcline and hence we obtain a trajectory like the one depicted in Panel (a).
- b. For the production of Y we can write based on this reaction: $dy/dt = kSx$. Thus, the ax term of the model corresponds to the kSx term here and hence $a = kS$. So a decrease in S means a decrease in a .
- c. Because the $dy/dt = 0$ nullcline is given by $y = (a/b)x$ its slope is proportional to a and hence its slope will decrease as a decreases. The $dx/dt = 0$ nullcline is independent of a .
- d. The two possibilities are depicted in Panels (b) and (c).
- e. In panel b we see that x has a positive and y has a negative feedback on to themselves. Thus, normally we would not be able to determine whether the positive or negative feedback is dominant and hence would not be able to tell whether the equilibrium is stable. However, in this case we know that the dynamics of x is much faster than the dynamics of y , thus the destabilizing influence of the positive feedback of x on itself will overrule the stabilizing influence of the negative feedback of y on itself and the equilibrium will be unstable. In panel

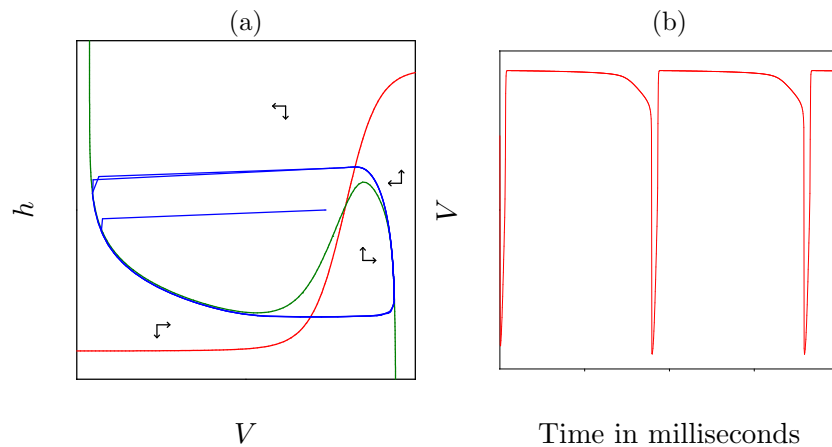
c bpth x and y have a negative feedback on themselves and the equilibrium is hence stable. The trajectories are depicted in Panels (d) and (e).

Question 9.2. Inhibition

The h_∞ line gives for every voltage the equilibrium value of h . The $dh/dt = 0$ nullcline is the set of h and V values where $dh/dt = 0$. That is the same.

Question 9.3. Hodgkin Huxley

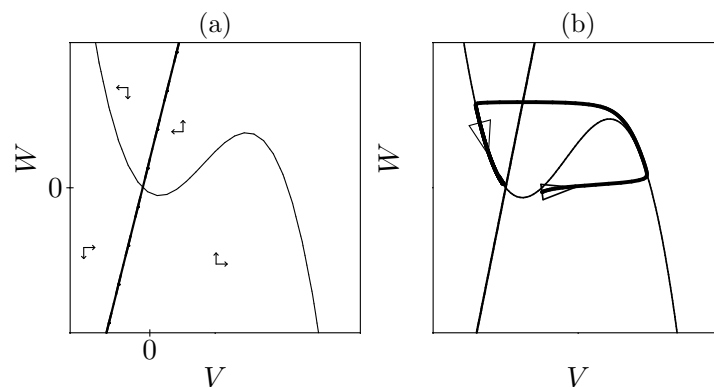
A possible good answer has the following sketches:



- The vector field is indicated in the phase space in Panel (a). We see that V has a positive and h a negative feedback on itself. Given that the dynamics of V are much faster than those of h the destabilizing influence of V dominates and hence the equilibrium is unstable.
- See the sketch in Panel (a).
- See the sketch in Panel (b).
- A neuron firing spontaneously

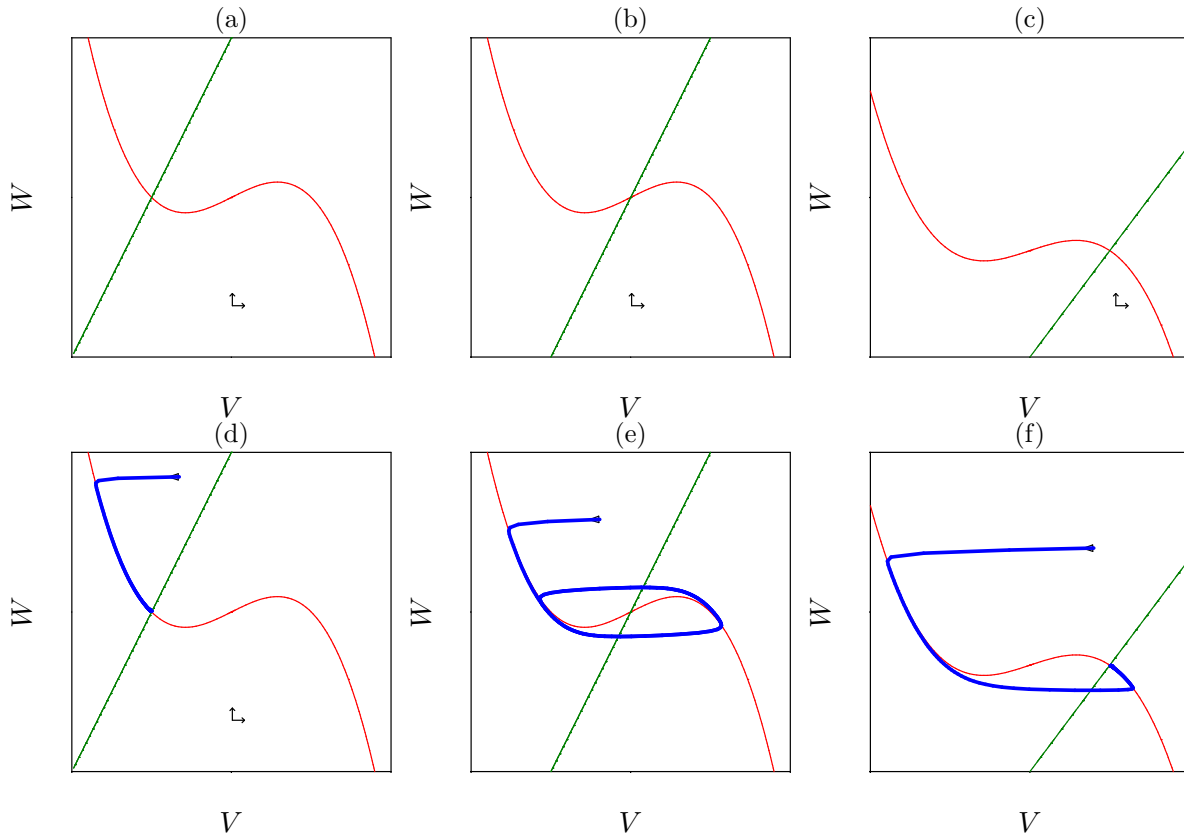
Question 9.4. FitzHugh-Nagumo model

A possible good answer has the following sketches:



- See the sketch in Panel (a).
- Because both V and W have a negative feedback on themselves the equilibrium is stable.
- See the sketch in Panel (b).

- d. Yes, very much.
 e. Yes, although it is not mechanistic, the model is attractively simple, and has very similar behavior.
 f. Due to the external input the V nullcline is shifted upward and may result in any of the three below situations:



- For $a = 0.5$, $b = 1$, $\epsilon = 0.01$ we get for $i = 0$ the phase space of Panels (a) and (d). For $i = 0.5$ we get those of Panels (b) and (e), and for $i = 1$ one gets those of Panels (c) and (f).
 g. In Panels a,d and Panels c,f we have a stable equilibrium because both V and W have a negative feedback on themselves. In Panels b,e V has a positive and W has a negative feedback on themselves. Since the dynamics of V are much faster than that of W the destabilizing influence of V is dominant and the equilibrium is unstable.
 h. See Panels (d)–(f).

Question 10.1. Diffusion

The answer should be something like the following:

During diffusion, substances move down their concentration gradient, giving rise to fluxes between neighboring points in space. Thus the flux between points $i-1$ and i is proportional to the concentration gradient between these points, where the gradient is formed by the concentration difference between these points divided over the physical distance between these points: $\frac{c_i - c_{i-1}}{\Delta x}$, then similarly the flux between points i and $i+1$ is proportional to $\frac{c_{i+1} - c_i}{\Delta x}$. Now the net change of concentration in a point i , depends on the net effect of these two fluxes, which is the difference between these fluxes divided over the physical distance over which these fluxes occur: $\frac{\frac{c_{i-1} - c_i}{\Delta x} - \frac{c_i - c_{i+1}}{\Delta x}}{\Delta x}$. So a single flux is a gradient and hence a single derivative to space, and a concentration change is a flux difference and hence a second derivative to space.

Question 10.2. Rabbit populations

- As the populations are large you can use continuous, so differential equations. As the populations are completely separated you can describe them with two independent ODE's.
- Again, populations are large, but now some rabbits are able to cross through the forest to join the other population, so the populations are no longer independent and should be described with a single PDE in which a slow diffusion models the migration between populations.
- Given that the population is tiny and 0.01 rabbits do not naturally occur, we need to use a discrete model, a CA. This also has the advantage that we can explicitly model space, putting in the forest between the populations and a small chance that rabbits go into the forest.

Question 10.3. Game of Life

For the first pattern the next two steps will be (it twinkles!)

```

.....      .....
...x...      .....
...x...      ..xxx..
...x...      .....
.....      .....

```

For the second pattern the next two steps will be (it is an equilibrium!)

```

.....      .....
.....      .....
..xx..      ..xx..
..xx..      ..xx..
.....      .....

```

Question 10.4. Majority Voting and plants in the desert

With Majority Voting, a region with more 0's than 1's will grow into a larger patch with all 0's whereas a region with more 1's than 0's it will grow into a patch with all 1's. So, a small local initial majority for 0 or 1 will be increased in space and time. Plants in a desert have trouble holding on to water in the soil, and more plants close together do a better job at this. Thus if initially more plants are together this will be able to grow out into a bushy patch with many plants, if initially only few plants are together they will die out.

Question 11.1. Fibrillation

- An infarct causes cells to die, producing scar tissue that does not conduct the excitation wave and thus acts like an obstacle. Obstacles break waves. A broken wave has a free end that curls up to form a spiral. The spiral may break into multiple spirals causing fibrillation
- The electrical shock causes all heart tissue still in rest to become excited simultaneously, and subsequently become refractory simultaneously. As a consequence, spiral waves have no unexcited, rest state tissue left to which they can propagate.
- Spirals take over control from the sinus node because they are faster. We can take over



control from the spirals by stimulating the heart even faster: overdrive pacing. As a consequence the spiral will die out, and if we stop with the overdrive pacing the sinus node can take over again.

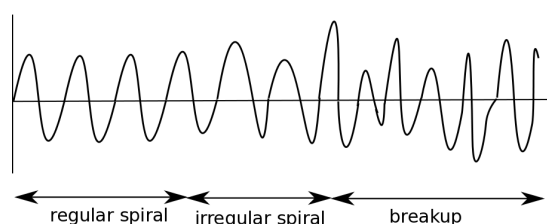


Question 11.2. Epidemic

- Everybody in the village was recently infected and hence is immune/refractory so the wave can not move into and through the village and comes to a halt.
- Yes, same as with defibrillation through electrical shock: everybody is excited and refractory at same time so disease has nowhere to go.
- Not. As long as it is only a few individuals, the wave will not find enough individuals it can infect to spread.
- It will no longer work: they will keep importing the disease.

Question 11.3. Spiral formation

- At a free end each excited point needs to excite more neighbours, as a consequence a delay in wavepropagation occurs, causing the free end to lag behind, this causes curvature to increase, causing a further delay, etcetera.
- If the tissue is smaller the chances are higher that the first turn of the spiral causes the free wave end to run into the boundary causing the spiral to exterminate itself. So for larger tissue the chances are higher that a wvebreak leads to a persistent spiral.
- Increasing the size of the spiral has the same effect as decreasing the size of the tissue. It makes the chance smaller that the initial turn of the spiral fits in the tissue and hence that the spiral wave will persist
- In the picture you see faster but quite regular activity as a spiral wave arises and than



irregular activity as the spiral wave breaks into multiple spirals.

Question 11.4. Fire spread

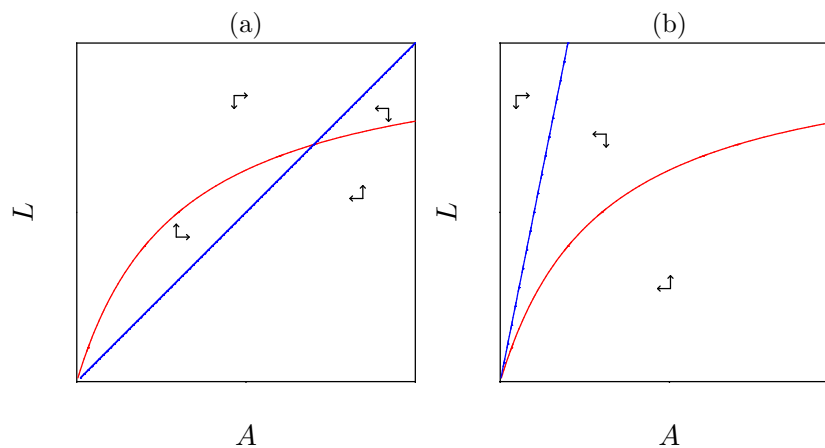
- The major observation you can make here is that as the average density of the vegetation decreases the spread of the fire becomes more and more irregular and blocks earlier and earlier. The reasons for this are simple: to spread the fire needs to jump from tree to tree, so if a tree is far from other trees the fire will burn that tree but not be able to move further locally causing a break in the wavefront of the fire. If the average density is low there will be many of such lone trees and the fire as a whole will come to a halt.
- There are several observations that can be made here. First, if the ignition rate is set lower and fewer fires are started per timestep, individual fires will be able to burn a larger part of the vegetation before running into a part of the vegetation that has recently been burned and has not recovered sufficiently to burn again. Second and related to the first, the path that a fire follows is strongly determined by previous fires and more so as more recovery time is needed.

Question 11.5. Evolution of Virulence and Contagiousness

If a virus would be very virulent and infected hosts all die, hosts may die out leaving the virus nowhere to go but also die out. If a virus would be ultra-contagious the virus wave would spread very fast, causing it to run into its own refractory back and then also die out.

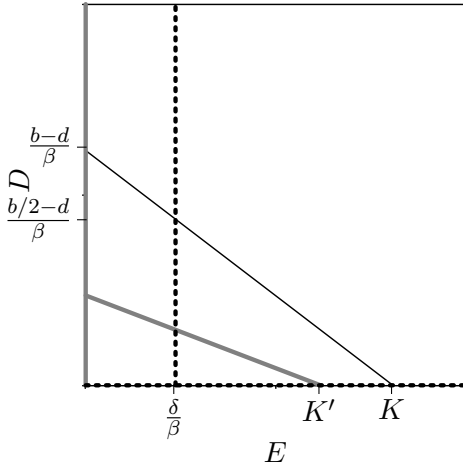
Question 13.1. Larvae and adults

A possible good answer has the following sketches:



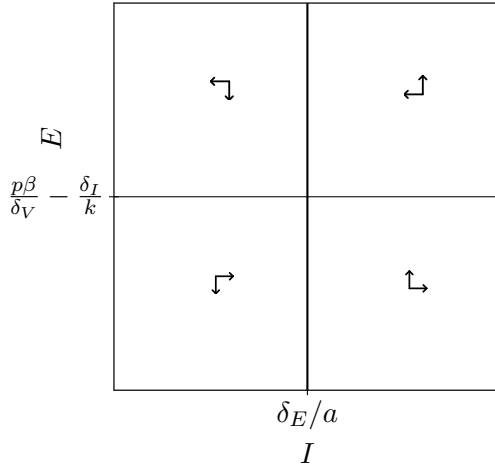
- Nullclines: $L = \frac{aA}{c+b+(b/k)A}$ and $L = (d/c)A$. See the sketch in Panel (a) and (b).
- See the arrows.
- The vector field shows that the non-trivial steady state is a stable node.
- The vector field shows that the steady state is stable.
- Do the quasi steady state assumption $dL/dt = 0$ and substitute into dA/dt . This yields $dA/dt = \frac{acA}{c+b+(b/k)A} - dA$.

Question 13.2. Eider down



- From $b = d(1 + cE)$ one solves $\bar{E} = K = (b/d - 1)/c$.
- For the ducks $R_0 = b/d$ and for the infection $R_0 = \beta K/\delta$.
- $K = (R_0 - 1)/c$.
- $K' = (R_0/2 - 1)/c$.
- Now \bar{E} has to be solved from $dD/dt = 0$: $\bar{E} = \delta/\beta$.
- Nothing: f is not part of the \bar{E} expression in **e**.
- This is basically a Lotka-Volterra model with an explicit parameter for the death of the eiders. The steady state of the eiders, \bar{E} , is determined by the $dD/dt = 0$ nullcline.

Question 13.3. Immunity



- The dT/dt equation disappears and dI/dt becomes:

$$\frac{dI}{dt} = \beta V - \delta_I I - kEI$$

- Substitute $V = (p/\delta_V)I$:

$$\frac{dI}{dt} = (p\beta/\delta_V)I - \delta_I I - kEI$$

- The $dI/dt = 0$ nullcline is $I = 0$ or $E = [(p\beta/\delta_V) - \delta_I]/k$, and the $dE/dt = 0$ nullcline is $E = 0$ or $I = \delta_E/a$. See the sketch.
- $I = E = 0$: uninfected individual. Non-trivial point: infected individual.

Bibliography

- Adler, F. R. (1997) , *Modeling the Dynamics of Life. Calculus and Probability for Life Scientists*, Pacific Grove: Brooks/Cole
- Agnes, F., Rosado, M. M., and Freitas, A. A. (1997) , *Eur. J. Immunol.* **27**, 1801
- Alon, U. (2007) , *An introduction to systems biology. Design principles of biological circuits*, Boca Raton, USA: Chapman & Hall/CRC
- Anderson, R. M. and May, R. M. (1991) , *Infectious diseases of humans. Dynamics and Control*, Oxford: Oxford U.P.
- Angly, F. E., Felts, B., Breitbart, M., Salamon, P., Edwards, R. A., Carlson, C., Chan, A. M., Haynes, M., Kelley, S., Liu, H., Mahaffy, J. M., Mueller, J. E., Nulton, J., Olson, R., Parsons, R., Rayhawk, S., Suttle, C. A., and Rohwer, F. (2006) , *PLoS. Biol.* **4**(11), e368
- Bonhoeffer, S., Coffin, J. M., and Nowak, M. A. (1997) , *J. Virol.* **71**, 3275
- Bonhoeffer, S., Funk, G. A., Gunthard, H. F., Fischer, M., and Muller, V. (2003) , *Trends Microbiol.* **11**(11), 499
- Borghans, J. A. M., De Boer, R. J., and Segel, L. A. (1996) , *Bull. Math. Biol.* **58**, 43
- Breitbart, M., Salamon, P., Andresen, B., Mahaffy, J. M., Segall, A. M., Mead, D., Azam, F., and Rohwer, F. (2002) , *Proc. Natl. Acad. Sci. U.S.A.* **99**(22), 14250
- Campbell, N. A. and Reece (2002) , *Biology, sixth edition*, Redwood city CA: Benjamin/Cummings
- Campbell, N. A. and Reece, J. B. (2008) , *Biology, Eighth edition*, San Francisco, CA: Pearson/BenjaminCummings
- Case, T. J. (2000) , *An Illustrated guide to Theoretical Ecology*, Oxford: Oxford U.P.
- Cornejo, O. E., Rozen, D. E., May, R. M., and Levin, B. R. (2009) , *Proc. Biol. Sci.* **276**(1659), 999
- De Boer, R. J. (2004) , *Modeling Population Dynamics: a Graphical approach*, EBook: <http://theory.bio.uu.nl/rdb/books/mpd.pdf>
- De Boer, R. J. (2012) , *PLoS. Comput. Biol.* **8**(7), e1002593
- De Boer, R. J., Freitas, A. A., and Perelson, A. S. (2001) , *J. theor. Biol.* **212**, 333
- De Boer, R. J., Ribeiro, R. M., and Perelson, A. S. (2010) , *PLoS. Comput. Biol.* **6**(9), e1000906
- De Jong, M. D., Veenstra, J., Stilianakis, N. I., Schuurman, R., Lange, J. M., De Boer, R. J., and Boucher, C. A. (1996) , *Proc. Natl. Acad. Sci. U.S.A.* **93**, 5501

- Edelstein-Keshet, L. (1988) , *Mathematical Models in Biology.*, New York: Random House
- Fitzhugh, R. (1960) , *J. Gen. Physiol.* **43**, 867
- Golding, I. and Cox, E. C. (2006) , *Curr. Biol.* **16(10)**, R371
- Golding, I., Paulsson, J., Zawilski, S. M., and Cox, E. C. (2005) , *Cell* **123(6)**, 1025
- Griffith, J. S. (1968) , *J. theor. Biol.* **20(2)**, 209
- Hastings, A. (1997) , *Population biology: concepts and models*, New York: Springer
- Hemelrijk, C. and Hildenbrandt, H. (2011) , *PLoS One* **6**, e2247
- HilleRisLambers, R., Rietkerk, M., Van den Bosch, F., Prins, H. H. T., and De Kroon, H. (2001) , *Ecology* **82**, 50
- Ho, D. D., Neumann, A. U., Perelson, A. S., Chen, W., Leonard, J. M., and Markowitz, M. (1995) , *Nature* **373**, 123
- Hodgkin, A. L. and Huxley, A. F. (1952) , *J. Physiol.* **117**, 500, Reprinted in *Bull. Math. Biol.* 1990, 52, 25–71
- Holland, J. J., De la Torre, J. C., Clarke, D. K., and Duarte, E. (1991) , *J. Virol.* **65**, 2960
- Holling, C. S. (1959) , *Can. Entomol.* **91**, 293
- Jacob, F. and Monod, J. (1961) , *J. Mol. Biol.* **3**, 318
- Kaunzinger, C. M. K. and Morin, P. J. (1998) , *Nature* **395**, 495
- Keener, J. and Sneyd, J. (1998) , *A mathematical introduction to medical physiology*, New York: Springer
- Lipsitch, M., Cohen, T., Cooper, B., Robins, J. M., Ma, S., James, L., Gopalakrishna, G., Chew, S. K., Tan, C. C., Samore, M. H., Fisman, D., and Murray, M. (2003) , *Science* **300**, 1966
- May, R. M. (1974) , *Stability and complexity in model ecosystems*, Vol. 6 of *Monographs in population biology*, Princeton, New Jersey: Princeton University Press, 2 edition
- May, R. M. (1977) , *Nature* **269**, 471
- May, R. M. (2004) , *Science* **303(5659)**, 790
- McAllister, C. D., LeBrasseur, R. J., and Parsons, T. R. (1972) , *Science* **175**, 562
- Mellors, J. W., Rinaldo, Jr, C. R., Gupta, P., White, R. M., Todd, J. A., and Kingsley, L. A. (1996) , *Science* **272**, 1167
- Müller, V., Marée, A. F., and De Boer, R. J. (2001) , *Proc. R. Soc. Lond. B. Biol. Sci.* **268**, 235
- Neumann, A. U., Lam, N. P., Dahari, H., Gretch, D. R., Wiley, T. E., Layden, T. J., and Perelson, A. S. (1998) , *Science* **282**, 103
- Novick, A. and Weiner, M. (1957) , *Proc. Natl. Acad. Sci. U.S.A.* **43(7)**, 553
- Novitsky, V., Gilbert, P., Peter, T., McLane, M. F., Gaolekwe, S., Rybak, N., Thior, I., Ndung'u, T., Marlink, R., Lee, T. H., and Essex, M. (2003) , *J. Virol.* **77(2)**, 882

- Nowak, M. A. and Bangham, C. R. (1996) , *Science* **272**, 74
- Nowak, M. A. and May, R. M. (2000) , *Virus dynamics. Mathematical principles of immunology and virology*, Oxford: Oxford U.P.
- Noy-Meir, I. (1975) , *J. Ecology* **63**, 459
- Ogg, G. S., Jin, X., Bonhoeffer, S., Dunbar, P. R., Nowak, M. A., Monard, S., Segal, J. P., Cao, Y., Rowland-Jones, S. L., Cerundolo, V., Hurley, A., Markowitz, M., Ho, D. D., Nixon, D. F., and McMichael, A. J. (1998) , *Science* **279**, 2103
- Ozbudak, E. M., Thattai, M., Lim, H. N., Shraiman, B. I., and Van Oudenaarden, A. (2004) , *Nature* **427(6976)**, 737
- Perelson, A. S., Neumann, A. U., Markowitz, M., Leonard, J. M., and Ho, D. D. (1996) , *Science* **271**, 1582
- Persson, A., Hansson, L. A., Bronmark, C., Lundberg, P., Pettersson, L. B., Greenberg, L., Nilsson, P. A., Nystrom, P., Romare, P., and Tranvik, L. (2001) , *Am. Nat.* **157**, 654
- Raj, A., Peskin, C. S., Tranchina, D., Vargas, D. Y., and Tyagi, S. (2006) , *PLoS. Biol.* **4(10)**, e309
- Rietkerk, M. and Van de Koppel, J. (1997) , *Oikos* **79**, 69
- Rosenzweig, M. L. (1971) , *Science* **171**, 385
- Scheffer, M., Carpenter, A., Foley, J. A., Folke, C., and Walker, B. (2001) , *Nature* **413**, 591
- Segel, L. A. (1988) , *Bull. Math. Biol.* **50**, 579
- Van Hoek, M. J. and Hogeweg, P. (2006) , *Biophys. J.* **91(8)**, 2833
- Wei, X., Ghosh, S. K., Taylor, M. E., Johnson, V. A., Emini, E. A., Deutsch, P., Lifson, J. D., Bonhoeffer, S., Nowak, M. A., Hahn, B. H., et al. (1995) , *Nature* **373**, 117
- Yodzis, P. (1989) , *Introduction to Theoretical Ecology*, New York: Harper & Row
- Zobl, H., Lang, W., and Georgii, A. (1975) , *Eur. J. Cancer* **11(3)**, 159